TÉCNICO LISBOA

Coverage and Efficiency Performance Evaluation of LTE in Urban Scenarios

Rui André de Almeida Pires

Dissertation submitted for obtaining the degree of
Master in Electrical and Computer Engineering

Jury

Supervisor:	Prof. Luís Manuel de Jesus Sousa Correia
Co-Supervisor:	Mr. Marco Serrazina
President:	Prof. Fernando Duarte Nunes
Members:	Prof. António José Castelo Branco Rodrigues

October 2012

To Marta

“To talk well and eloquently is a very great art, but that an equally great one is to know the right moment to stop.”

Wolfgang A. Mozart (1756-1791)

Acknowledgements

First of all, I would like to thank Prof. Luís Correia for both guidance and kindness during the development of this master's thesis, who proved to be not only a good supervisor but also an inspiring person, sharing his knowledge and giving advice as my transition from the academic world to the professional one took place. I would also like to thank him for the opportunity of developing my thesis in collaboration with Vodafone, which turned out to be a valuable experience, and for being part of the GROW, where I learned more about other telecommunication topics as well as presentation skills.

I would like to thank Vodafone Portugal and all the professionals that were involved in my thesis, with special emphasis to Mrs. Diana Caiado, Mr. Carlos Caseiro, Mr. Marco Serrazina and Mr. Ricardo Batista, who dedicated their time and effort to my work.

To my colleagues and friends from college, a very special thanks for following me in this journey, giving their friendship and support: Carlos Silva, Gonçalo André, Flépis, Marco Seabra, Gonçalo Aguiar, Duarte Dias, Ricardo Crisógono, Délcio Caseiro, Pedro Cruz, Guilherme Coelho, Pedro Alvarez and Pedro Vieira.

To my friend Jónatas Gaspar, a huge appreciation and gratitude for all the moments that we have shared together.

At last, but not the least, to my family, specially my Father, Mother and Brother, and to the love of my life, Marta.

Abstract

The main purpose of this thesis was to study LTE performance in terms of coverage and capacity, quantifying its key performance indicators in urban scenarios regarding low and high load cases. This purpose was achieved through the development of a suitable simulator for LTE DL, implementing a real urban cellular network and real users density applied to the city of Lisbon, using typical urban distributions of users along the pedestrian, vehicular and indoor scenarios. Regarding low load scenarios, measurements were also performed in order to collect data to confront with the simulated results. The low and high load results show that the users throughput gap between these two scenarios reach a factor of 15, the average throughputs being around 45 and 3 Mbit/s, respectively. The increase in the number of users, which will share the available resources among them, along with the increasing interference, as spectrum reuse takes place in order to achieve high data rates in each sector, degrades the overall QoS. The low load scenarios focus and explore users throughputs regarding the high peak data rates that characterise LTE in an almost empty network, while the high load ones aim to characterise the behaviour of the system in a resources constringe situation.

Keywords

LTE, performance, interference, capacity, urban scenarios, Lisbon.

Resumo

O principal objectivo desta tese foi o estudo de desempenho do LTE em termos de cobertura e capacidade, quantificando os seus principais índices chave de desempenho em cenários urbanos, tendo em conta baixa e elevada carga na rede. Este objectivo foi conseguido através do desenvolvimento de um simulador adequado para a ligação descendente do LTE, tendo-se implementado uma rede celular urbana real com densidade e distribuição de utilizadores baseados em informação estatística relativa à cidade de Lisboa, utilizando uma distribuição típica de utilizadores nos cenários pedonal, automóvel e interior. Relativamente aos cenários de baixa carga na rede, foram feitas medidas com o intuito de recolher informação para ser confrontada com os resultados das simulações. Os resultados de baixa e elevada carga mostraram que o débito binário dos utilizadores varia até um fator de 15, tendo este mesmo parâmetro registado os valores médios de 45 e 3 Mbit/s, respectivamente. O aumento do número de utilizadores, que terão de partilhar os recursos rádio disponíveis entre eles, bem como o aumento da interferência, à medida que a reutilização de espectro ocorre para permitir débitos elevados em cada sector, degradam em geral a qualidade de serviço. Os cenários de baixa carga focam-se e exploram os elevados débitos de utilizadores que caracterizam o LTE numa rede praticamente vazia enquanto que os cenários de elevada carga pretendem caracterizar o comportamento do sistema numa situação de constrangimento de recursos.

Palavras-chave

LTE, desempenho, interferência, capacidade, cenários urbanos, Lisboa.

Table of Contents

List of Figures

List of Tables

List of Acronyms

3GPP	3rd Generation Partnership Project
4G	4th Generation
AMBR	Aggregated Maximum Bit Rate
AMC	Adaptive Modulation and Coding
ANACOM	Autoridade Nacional de Comunicações
ARP	Allocation and Retention Priority
BER	Bit Error Ratio
BLER	Block Error Rate
BS	Base Station
CA	Carrier Aggregation
CP	Cyclic Prefix
CQI	Channel Quality Indicator
CS	Circuit Switch
DFT	Discrete Fourier Transform
DL	Downlink
EDGE	Enhanced Data rates for GSM Evolution
EESM	Exponential Effective SINR Mapping
eNB	Evolved NodeB
EPA	Extended Pedestrian A
EPC	Evolved Packet Core
EPS	Evolved Packet System
ETU	Extended Typical Urban
EVA	Extended Vehicular A
E-ARFCN	E-UTRA Absolute Radio Frequency Channel Number
E-UTRA	Evolved UTRA
E-UTRAN	Evolved UTRAN
FDD	Frequency-Division Duplex
FEC	Forward Error Correction
FFR	Fractional Frequency Reuse
FRS	Frequency Reuse Scheme
FST1	Frame Structure Type 1
FST2	Frame Structure Type 2

FTP	File Transport Protocol
GBR	Guaranteed Bit Rate
GBSB	Geometrically Based Single Bounce
GPRS	General Packet Radio Service
GSM	Global System for Mobile Communications
HLR	Home Location Register
HSDPA	High Speed Downlink Packet Access
HSPA	High Speed Packet Access
HSPA+	High Speed Packet Access Evolution
HSUPA	High Speed Uplink Packet Access
ICI	Inter-Cell Interference
ICIC	ICI Coordination
IDFT	Inverse Discrete Fourier Transform
IM	Interference Margin
IMS	IP Multimedia Subsystem
IMT	International Mobile Telecommunications
IP	Internet Protocol
ISI	Inter Symbol Interference
ITU	International Telecommunications Union
ITU-R	ITU Radiocommunication Sector
LoS	Line of Sight
LTE	Long Term Evolution
LTE-A	LTE Advanced
MAC	Medium Access Control
MBR	Maximum Bit Rate
MIMO	Multiple Input Multiple Output
MME	Mobility Management Entity
MT	Mobile Terminal
NLoS	Non Line of Sight
OFDM	Orthogonal Frequency-Division Multiplexing
OFDMA	Orthogonal Frequency-Division Multiple Access
OSI	Open Systems Interconnection
PAR	Peak to Average Power Ratio
PBCH	Physical Broadcast Channel
PCEF	Policy Control Enforcement Function
PCRF	Policy Control and Charging Rules Function
PDCCH	Physical Downlink Control Channel
PDCP	Packet Data Convergence Protocol
PDN	Packet Data Network
PDSCH	Physical Downlink Shared Channel

PF	Proportional Fair
PFR	Partial Frequency Reuse
PRACH	Physical Random Access Channel
PS	Packet Switch
PUCCH	Physical Uplink Control Channel
PUSCH	Physical Uplink Shared Channel
P-GW	PDN Gateway
QAM	Quadrature Amplitude Modulation
QCI	QoS Class Identifier
QoS	Quality of Service
QPSK	Quadrature Phase-Shift Keying
RAN	Radio Access Network
RE	Resource Element
RB	Resource Block
RLC	Radio Link Control
RMG	Relative MIMO Gain
RN	Relay Node
RR	Round Robin
RRC	Radio Resource Control
RRM	Radio Resource Management
RS	Reference Signal
RSRP	RS Reference Power
RTT	Round Trip Time
SAE	System Architecture Evolution
SC-FDMA	Single Carrier Frequency-Division Multiple Access
SF	Slow Fading
SFR	Soft Frequency Reuse
SINR	Signal to Interference plus Noise Ratio
SISO	Single Input Single Output
SMS	Short Message Service
SNR	Signal-to-Noise Ratio
S-GW	Serving Gateway
TDD	Time-Division Duplex
TDM	Time-Division Multiplex
TMN	Telecomunicações Móveis Nacionais
TTI	Transmission Time Interval
UE	User Equipment
UL	Uplink
UMTS	Universal Mobile Telecommunications System
UTRA	UMTS Terrestrial Radio Access

UTRAN	UMTS Terrestrial Radio Access Network
VoIP	Voice over IP
WCDMA	Wideband Code Division Multiple Access

List of Symbols

δ	General Sigmoid function
Δf	Radio channel bandwidth
λ	Wavelength
μ	Mean value
ρ_N	SNR
ρ_{IN}	SINR
σ	Standard deviation
ϕ	Angle of incidence of the signal in the buildings, in the horizontal plane
a_{pd}	Average power decay
B_{RB}	Bandwidth of an RB
d	Distance between the BS and the MT
$d_{\max user}$	Distance of the user further away from the serving BS
f	Carrier frequency
F_N	Noise figure
g	Statistical RMG
$G_{M/S}$	RMG
G_r	Gain of the receiving antenna
G_t	Gain of the transmitting antenna
h_b	BS height
h_m	MT height
H_B	Buildings height
I	Interference power
I_i	Interference power coming from transmitter i
k_a	Increase of pathloss for the BS antennas below the rooftops of the adjacent buildings
k_d	Control of the dependence of the multi-screen diffraction loss versus distance
k_f	Control of the dependence of the multi-screen diffraction loss versus frequency
L_0	Free space propagation pathloss
L_{bsh}	Loss due to the height difference between the rooftop and the antennas
L_c	Cable losses

L_{ori}	Street orientation loss
L_p	Path loss
$L_{p,environment}$	Environment losses
$L_{p,COST\ 231\ WI}$	COST 231 Walfisch-Ikegami pathloss
L_{rm}	Loss between the BS and the last rooftop
L_{rt}	Loss between the last rooftop and the MT
L_u	User losses
M_{SF}	Slow fading margin
N_{bs}	Number of bits per symbol
N_I	Number of interfering signals reaching the receiver
N_R	Number of receive antennas
N_{RB}	Number of RBs
$N_{sub/RB}$	Number of subcarriers per RB
$N_{sym/sub}$	Number of symbols per sub-carrier
N_T	Number of transmit antennas
$N_{u\ BS}$	Number of users in the BS
N_Z	Number of samples
P_r	Power available at the receiving antenna
$P_{r,min}$	Power sensitivity at the receiving antenna
P_{RX}	Receiver input power
P_t	Power fed to the antenna
$P_t^{\ DL}$	Power fed to the antenna in DL
$P_r^{\ UL}$	Power fed to the antenna in UL
P_{TX}	Transmission output power
R	Maximum cell radius
R_b	Data rate
$R_{b,BS}$	Throughput of the BS
$R_{b\ user_i}$	Data rate for user i
$R_{b,peak}$	Peak data rate
R_{b,RB_c}	Data rate of the RB obtained for the central frequency band carrier
R_{b,RB_i}	Data rate of the RB i, calculated for the respective attributed frequency
$R_{b,user}$	User data rate
R_{BS}	BS radius
s	Slope
T_{RB}	Time period of an RB
w_B	Buildings separation distance
w_S	Street width
$\bar{Z}$	Average value of population Z

Z_i	Sample i

List of Software

C++ Builder 6	C++ Integrated Development Environment software
Map Basic	Programming software and language to create additional tools and functionalities for the MapInfo
MapInfo	Geographic Information System software
Microsoft Excel	Calculation and Graphing software
Microsoft Word	Text editor software
TEMS Discovery	Network diagnostics and post processing tool
TEMS Investigation	Wireless network testing, troubleshooting and optimisation tool

Chapter 1

Introduction

This chapter introduces the subject of this dissertation, and presents the contextual and motivational perspective that leaded to this thesis. Furthermore, it establishes the scope of this work and describes the contents that together compose the work's structure.

1.1 Overview

The number of mobile subscribers has increased tremendously in recent years, and so has the number of people that perform more and more mobile voice and data communications rather than fix ones, anywhere, anytime, expecting to experience performances similar to the fixed services. In fact, data communications are the biggest challenge regarding wireless networks, because of the higher demand from an increasing number of users that require connectivity from their mobile devices. Following this demand, cellular systems and mobile technologies have constantly been evolving and standards-developing organisations, such as Third Generation Partnership Project (3GPP), played an important role in the adoption of the latest generation of mobile communication systems: Long Term Evolution (LTE) [HoTo09].

Second-generation mobile networks, such as Global System for Mobile Communications (GSM), were originally designed for carrying voice traffic, the data capability having been added later. Indeed, data usage was increasing, but traffic volume was clearly dominated by voice traffic. The introduction of third generation networks with High Speed Downlink Packet Access (HSDPA) boosted the data traffic in such a way that it changed mobile networks from voice to packet data dominated networks [HoTo09]. Applications, such as web browsing, file sharing, streaming services that distribute both audio and video contents, mobile TV, interactive games, social networks and real-time applications that require constant synchronisation, are pushing operators to develop higher data rates and capacity and lower latency networks. The traffic growth in Figure 1.1 shows that in 2012 data traffic is predicted to double the previous year and keeps an exponential growth over the next four years.

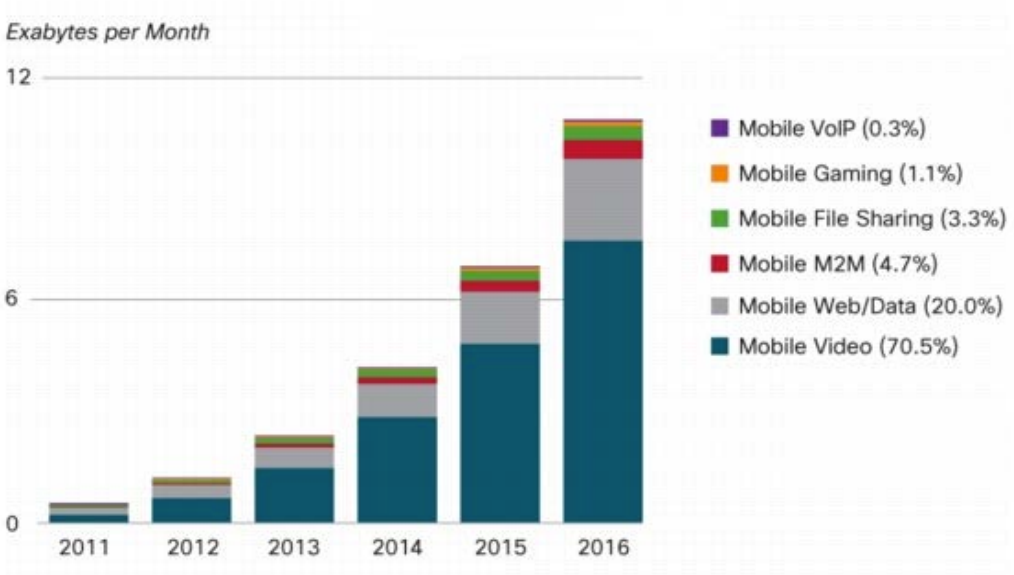

Figure 1.1. Global mobile data traffic forecast per service (extracted from [Cisc12]).

In spite of this huge data growth, the respective price charged to users per data size is falling almost as rapidly as its flow is growing, as one can see from Figure 1.2, along with the increase in the number of mobile-connected devices, such as laptops, smartphones and tablets, which is predicted to exceed the world's population this year of 2012 [Cisc12] and whose associated sales are illustrated in Figure

1.3. In addition, users that have more than one mobile device are generally not willing to subscribe another data plan to the operators, as they already pay for one, regularly laptop or smartphone, which makes users to prefer Wi-Fi when available, and pushes operators again in the direction of offering special data price plans per subscriber instead of per device [Wire11]. Thus, the overall data traffic growth creates a challenge for mobile operators, to provide more and more higher capacity systems for lower revenues, which requires more cost-efficient investments.

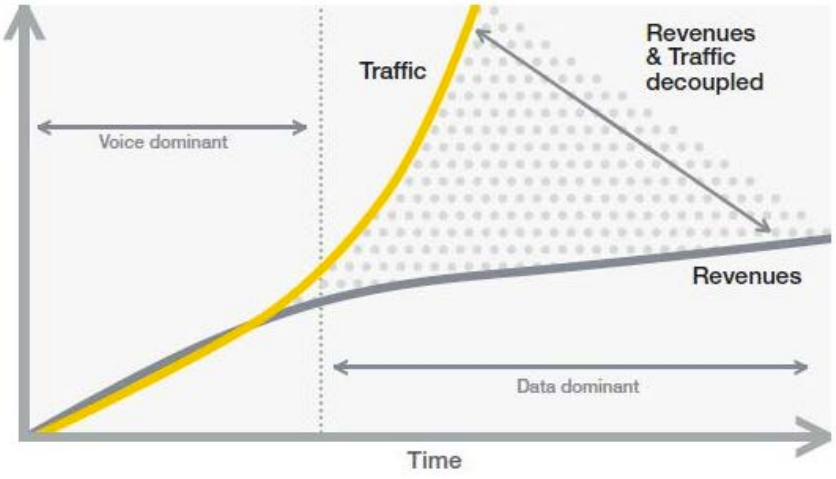

Figure 1.2. Traffic and respective revenue trend for mobile communications (extracted from [Wire11]).

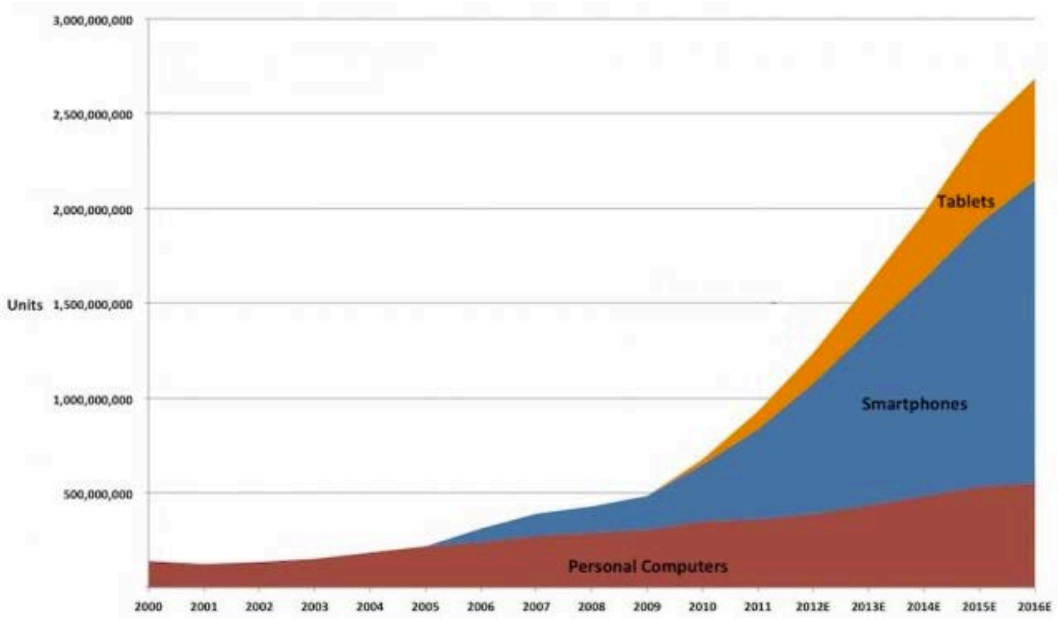

Figure 1.3. Global mobile-connected devices sales (extracted from [Busi12]).

3GPP technologies before LTE, i.e., GSM/Enhanced Data rates for GSM Evolution (EDGE) and Universal Mobile Telecommunications System (UMTS)/High Speed Packet Access (HSPA) were serving nearly 90% of the global mobile subscribers in 2008, with operators benefiting from a large and open 3GPP ecosystem and economics of scale for low cost mobile devices. Historically, regarding data rates, EDGE was defined in 3GPP in 1997 and UMTS at the end of 1999, both of them having had their first commercial deployment during 2002, as illustrated in Figure 1.4 (Wideband Code

Division Multiple Access (WCDMA) as UMTS). The HSDPA and High Speed Uplink Packet Access (HSUPA) standards were completed in March 2002 and December 2004, respectively, and the commercial deployments occurred in 2005 and 2007. The first phase of HSPA Evolution (HSPA+) was completed in June 2007 and the deployments started during 2009. The LTE standard was approved at the end of 2008 and the commercial deployments were initiated in December 2009, in the Scandinavian Capitals Stockholm and Oslo, the LTE Advanced (LTE-A) having been defined in the release 10 in March 2011.

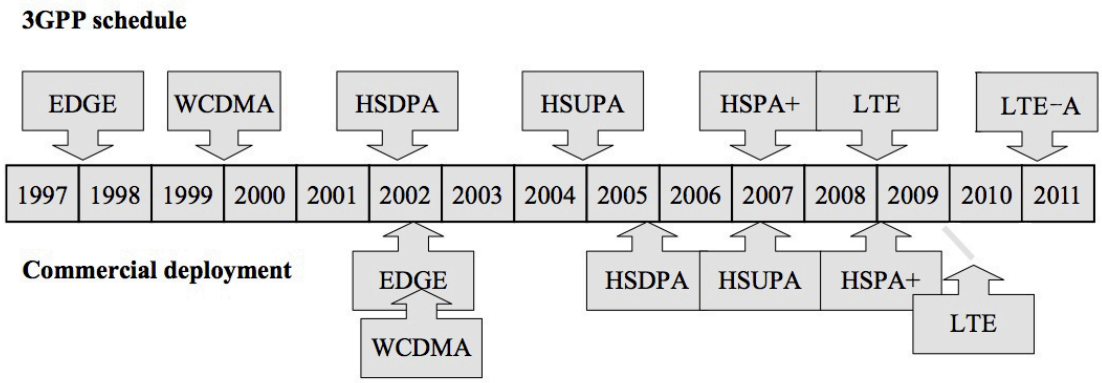

Figure 1.4. Schedule of 3GPP standard and their commercial deployments (adapted from [HoTo09]).

The evolution of peak data rates associated to 3GPP technologies is illustrated in Figure 1.5, and one can see that in a period of 8 years the peak data rates has grown more than 300 times, considering EDGE and LTE 2×2, as this configuration it the most popular as far as operators and users devices are concerned, LTE peak data rates provide users with high throughputs, even compared to the major offer by wired ADSL and fibre data rates.

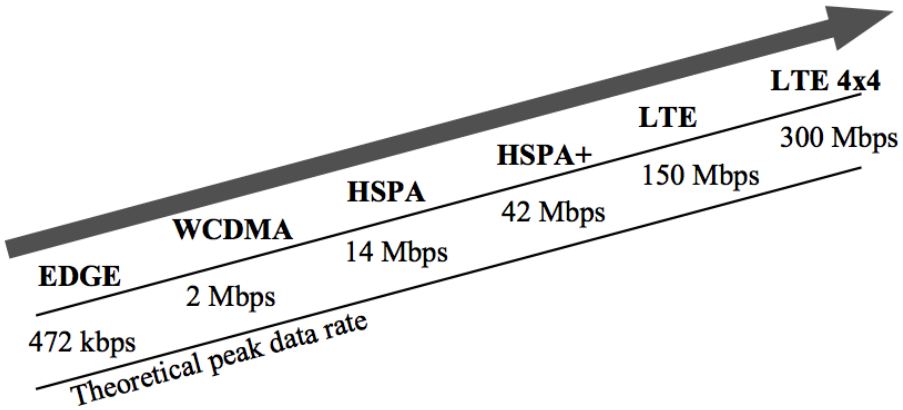

Figure 1.5. Peak data rate evolution of 3GPP technologies (extracted from [HoTo09]).

The first 3GPP release to specify LTE is Release 8, which specifies data rates up to 300 Mbit/s in Downlink (DL) and 75 Mbit/s in Uplink (UL), with a low latency and flat radio architecture, and all-IP (Internet Protocol) network with no backwards compatibility with UMTS. Release 9 includes some more features that were postponed from Release 8, namely overall architecture enhancements and interoperability with UMTS. Release 10 specifies additional LTE capabilities in the form of LTE-A by using Carrier Aggregation (CA) and enhanced DL Multiple Input Multiple Output (MIMO), which allows

the system to achieve the International Mobile Telecommunications (IMT) Advanced 4G requirements, such as the 1 Gbit/s peak data rate, UL MIMO, enhanced Inter-Cell Interference Coordination (ICIC) and relaying, as well as backwards compatibility with Release 8, as one could expect.

As a packet switch domain optimised system, LTE was required to support IP Multimedia Subsystem (IMS) and further evolved 3GPP packet core, because as the data rates increase, latency becomes a more limiting fact in order to achieve improvements. Security and mobility between earlier systems such as GSM and UMTS were also defined, as well as higher spectral efficiency and mobile terminal power efficiency. Also, one of the key factors taken into account was cost, to ensure that the new system could facilitate lower investments and operating costs compared to earlier systems [HoTo09].

1.2 Motivation and Contents

LTE is a technology with great potential as far as data rates, spectral efficiency and system latency are concerned, even though overall performance evaluations over real heterogeneous networks are yet to be performed. Moreover, urban scenarios are expected to be the most challenging areas, due to the fact that most of the subscribers are placed indoors, which adds a higher attenuation in the radio link between the Mobile Terminal (MT) and the Base Station (BS). Also, one can expect cell areas to be smaller than in rural environments, because cities have usually capacity limited cells, leading to an increase of the overlapping coverage area between neighbouring cells, creating interference that can be a much more performance-limiting factor than noise in these scenarios.

The main scope of this thesis is to study LTE performance by means of capacity, throughput, coverage and radio interface quality in urban scenarios, applying to the specific case of the city of Lisbon. These objectives were accomplished through the development of a model and the respective implementation in a simulator, and through measurements done in Lisbon. The main results of the model are the key performance indicators regarding LTE performance for the reference scenario in high and low loaded networks, the latter results being compared with the measurements, since they were done in similar conditions.

This thesis was done in collaboration with Vodafone Portugal, through the motivations that operators have focused on the initial deployment of LTE and the inherent optimisation work involved at this stage, which helped this work to put together academic and professional concerns. Vodafone also supplied the Lisbon network, as well as the necessary equipment to perform measurements and analyse the obtained data.

The main output of this thesis is the developed model on LTE network in an urban scenario, which recreates the city of Lisbon being composed of many BSs and inhabited by users that require a at given instance services from the network, in a given position from the serving BS and with a given associated throughput. Users compete for resources in capacity limited cells and Quality of Service (QoS), as well as scheduling algorithms take place to impose both fairness and equity in the access to

them.

This work is composed of 5 chapters, including the present one, and a group of annexes. Chapter 2 mainly introduces LTE and LTE-A network architecture and radio interface, performance specifications and associated QoS criteria redefined towards LTE. Basic aspects of modulation, spectrum organisation, frame structure and interference are presented, and at the end, the state of the art is addressed, with the latest work developed related to the present thesis.

Chapter 3 presents all the information regarding the developed models used to implement the simulator. Propagation and algorithm aspects are defined and models explained. Then, the simulator overview is given, concerning its architecture and full potential, being presented all the parameters that can be configured. Afterwards, the simulator assessment and assertiveness is presented.

In Chapter 4, the scenarios and measurements description are done at first. In the next section, measurements and results from low load scenarios are presented, compared and discussed. Then, more extensive simulation results regarding high load scenarios are presented and discussed as well. Along the results discussion, some conclusions and comments are presented.

Chapter 5 summarises the work in this thesis, pointing out the most important results and conclusions and addressing future work.

At the end, a group of annexes containing auxiliary information and additional results are included. Annex A addresses the frequency bands assignment auction performed by Autoridade Nacional de Comunicações (ANACOM) regarding spectrum licensing for LTE in Portugal. Annex B contents are about the link budget used in the calculations regarding signal propagation between the MT and the BS. Annex C describes the suitable propagation model for urban scenarios that was used in this work. Annex D contains additional results that were not included in Chapter 4. Annex E shows the user manual, explaining how one can configure and use the developed simulator. Annex F addresses the SINR and associated data rate models. Annex G presents the MIMO model used in the present work. Annex H describes the antennas radiation pattern with both horizontal and vertical patterns. Finally Annex I describes with more detail the distribution of BSs and users along the city area in the simulations graphic interface, and Annex J presents geographic data about the measurement campaign.

Chapter 2

Fundamental Concepts and State of the Art

This chapter provides an overview of LTE, describing the essential aspects that are relevant in this thesis and extending contents to LTE-A. Firstly, Section 2.1 presents the architecture design. Secondly, Section 2.2 addresses the physical features of the Radio Interface. Then, overall performance is assessed in Section 2.3. Services and applications are discussed in Section 2.4 and the state of art is presented afterwards in Section 2.5.

2.1 Network Architecture

LTE and LTE-A Network Architecture is presented in this section, the main contents being based on [SeTB09] and [3GPP11a].

LTE and LTE-A present the same flat architecture optimised for packet switched services, aimed to provide seamless Internet Protocol connectivity between the User Equipment (UE) and the Packet Data Network (PDN). The System Architecture Evolution (SAE) standardisation work resulted on a new overall system, named Evolved Packet System (EPS), being composed of Evolved UMTS Terrestrial Radio Access Network (E-UTRAN) and Evolved Packet Core (EPC), which consist of Radio Access and Core networks, respectively. These components are represented in Figure 2.1.

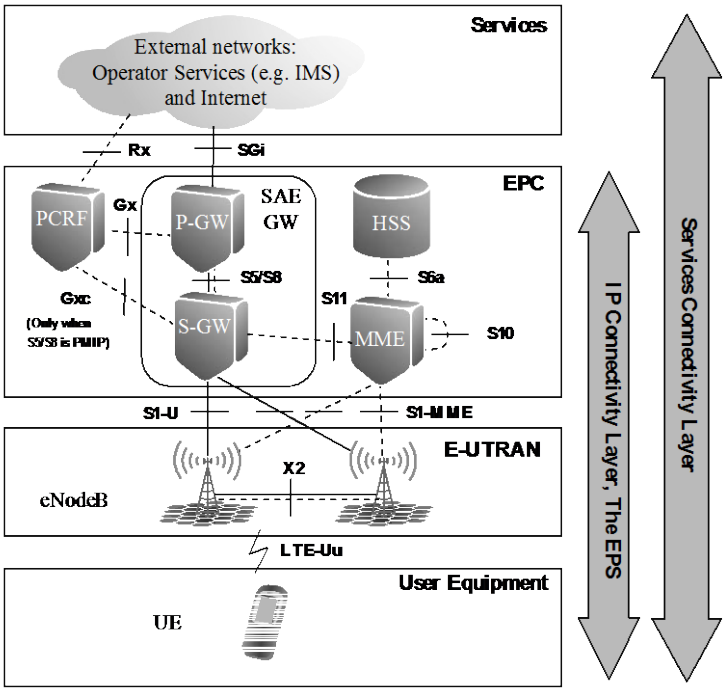

Figure 2.1. EPS architecture (extracted from [HoTo09]).

The EPC is responsible for the overall control of the UE and establishment of the bearers, and its main logical nodes and correspondent functions are:

- PDN Gateway (P-GW). The P-GW is responsible for IP address allocation to the UE, QoS enforcement and flow-based charging;
- Serving Gateway (S-GW). The S-GW acts like a local mobility anchor for the data bearers when the UE moves between evolved NodeB (eNB), i.e., for the purposes of handover, as well as when connections with other 3GPP technologies are required, such as General Packet Radio Service (GPRS) and UMTS;
- Mobility Management Entity (MME). The MME consists of the logical node that deals with all

the signalling and control between the UE and the EPC;

- Policy Control and Charging Rules Function (PCRF). The PCRF is responsible for policy control decision-making, as well as for controlling the flow-based charging functionalities in the Policy Control Enforcement Function (PCEF), which resides in the P-GW. It also provides the QoS authorisation (QoS class identifiers and bitrates) that decides how data flows are treated in the PCEF, taking the respective user's subscription profile into account.
- Home Location Register (HLR). HLR contains users' SAE subscription data, such as the EPS-subscribed QoS profile and access restrictions for roaming.

The E-UTRAN consists of a network of several eNBs that are inter-connected with each other through an X2 interface, and connected to the EPC through an S1 interface, as illustrated in Figure 2.2. Note that eNB corresponds to a BS in the 3GPP LTE terms. The E-UTRAN is responsible for all radio-related functions, which can be grouped into:

- Radio Resource Management (RRM), which covers all functions related to the radio bearers, such as radio bearer control, radio admission control, radio mobility control, scheduling and dynamic allocation of resources to UEs in both DL and UL. Regarding the RRM, X2 interface is important for eNBs to trade information related for example with users' handover and interference avoidance;
- Header compression, ensuring efficient use of the radio interface by compressing the IP packet headers;
- Security, using encrypted data over the radio interface;
- Connectivity to the EPC, consisting of signalling towards the MME and bearer path towards the S-GW.

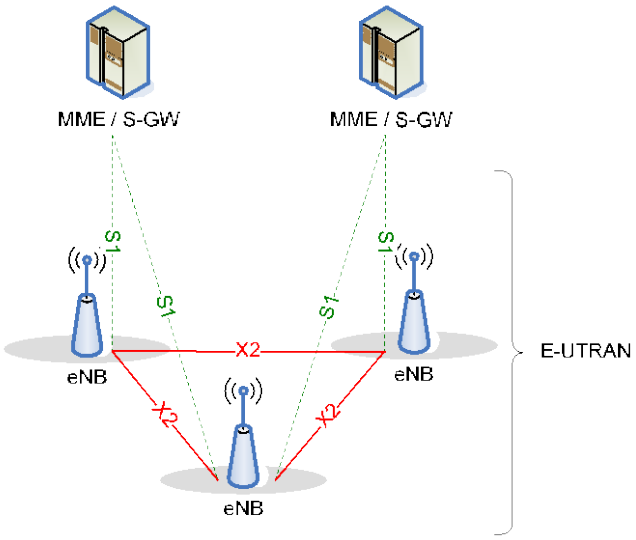

Figure 2.2. E-UTRAN architecture (extracted from [3GPP11a]).

2.2 Radio Interface

The LTE and LTE-A Radio Interface characteristics are presented in this section, mainly extracted from [SeTB09] e [HoTo09].

3GPP has specified 17 Frequency Division Duplex (FDD) and 8 Time Division Duplex (TDD) Evolved UMTS Radio Access (E-UTRA) operating bands [3GPP11b], which covers the two main bands from 700 to 900 MHz, and from 2500 to 2600 MHz, and still the bands of 1400 MHz, 1700 MHz and 2100 MHz. ANACOM, the Portuguese Telecommunications Authority, has chosen the bands around 450 MHz, 800 MHz, 900 MHz, 1800 MHz, 2100 MHz and 2600 MHz for the operating frequency band licenses auction, being the results of the auction [ANAC11] presented in Annex A.

Orthogonal Frequency-Division Multiple Access (OFDMA) and Single Carrier Frequency-Division Multiple Access (SC-FDMA) are the multiple access schemes specified for LTE DL and UL, respectively. OFDMA has been chosen for LTE due to the good performance in frequency selective fading channels, low complexity of base-band receiver, good spectral efficiency, handling of multiple bandwidths, frequency domain scheduling and compatibility with advanced receiver and antenna technologies, e.g., MIMO. The OFDMA orthogonality principle is the sampling instant of a desired sub-carrier to correspond to the neighbouring sub-carriers zero value, and the transmission bandwidth to be composed by many narrow sub-carriers spaced by 15 kHz, which eliminates Intra Cell or Adjacent Channel Interference.

3GPP specifies 2 radio frame structures, Frame Structure Type 1 (FST1) applicable to FDD and Frame Structure Type 2 (FST2) applicable to TDD [3GPP10]. This thesis only focuses on FST1, since it uses FDD, which is the most implemented division duplex. Concerning the physical layer, physical channels correspond to a set of resource elements carrying information:

- Physical Downlink Shared Channel (PDSCH), which is the main downlink physical channel used for unicast data transmission, also used for paging information transmission;
- Physical Broadcast Channel (PBCH), which carries part of the system information required by UE in order to access the network;
- Physical Downlink Control Channel (PDCCH), which carries scheduling assignments and other control information;
- Physical Uplink Shared Channel (PUSCH), which is the main physical uplink channel used for unicast data transmission, being the uplink counterpart of the PDSCH;
- Physical Uplink Control Channel (PUCCH), which is the uplink counterpart of the PDCCH;
- Physical Random Access Channel (PRACH), which is used for random access;

There are also other sets of Resource Elements (RE) that do not carry information, which are the synchronisation signals, used only on DL, and the reference signal used for channel estimation. DL physical channels mapping is shown in Figure 2.3.

In the transmitter, a cyclic extension called Cyclic Prefix (CP) is added to the beginning of each Orthogonal Frequency-Division Multiplexing (OFDM) symbol, by copying part of the symbol at the end

rather than existing a guard interval with no transmission at all. The CP avoids Inter Symbol Interference (ISI) and is large enough to ensure that it exceeds the delay spread, assuming different lengths. Regarding the multiple access of OFDMA, in the frequency domain users can be allocated to any of the sub-carriers, but due to the resulting overhead, this allocation is done with the finest granularity of a Resource Block (RB), consisting of a group of 12 sub-carriers, that together occupy 180 kHz, the minimum bandwidth allocation possible. This dynamical allocation of resources is known as frequency-domain schedule or frequency-domain diversity. In the time domain, an RB corresponds to a 0.5 ms slot and 2 slots correspond to a sub-frame with a 1 ms duration. Finally, a frame is a group of 10 sub-frames, i.e., 20 slots. The smallest unit of resource constitutes the Resource Element (RE), which consists of one sub-carrier with the duration of one OFDM symbol. As an RB groups 12 sub-carriers, each one carrying 6 or 7 OFDM symbols, depending on the CP length, it corresponds to 84 REs, in case of normal CP length thus 7 symbols per sub-carrier, and 72 RE, in case of extended CP length thus 6 symbols per sub-carrier. The range of bandwidth varies from 1.4 MHz to 20 MHz for LTE Releases 8 and 9, corresponding to 6 RBs and 100 RBs, respectively, and the maximum bandwidth allocation is extended to 100 MHz with LTE-A Release 10, corresponding to 500 RBs, as shown in Table 2.1. The practical implementation of OFDMA is based on Discrete Fourier Transform (DFT) and Inverse Fourier Transform (IDFT) to switch between the time and frequency domains.

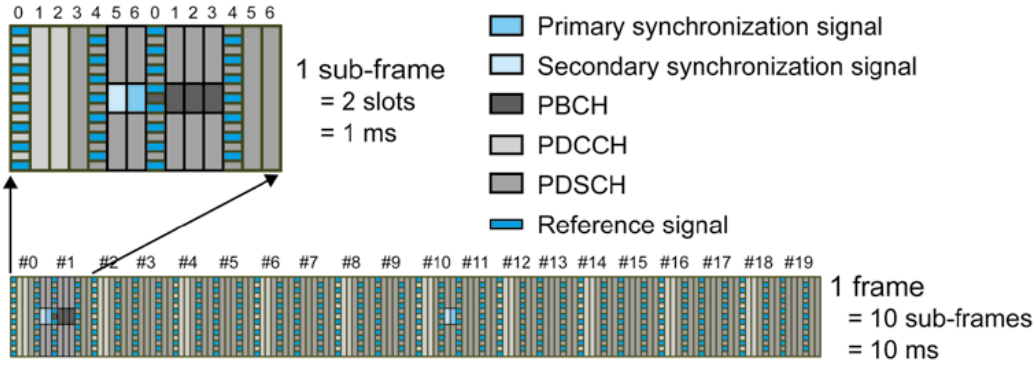

Figure 2.3. Frame and sub-frame downlink mapping with normal CP length (extracted from [Agil09]).

In spite of the OFDMA advantages referred previously, there are some challenges to OFDMA, the most important being the high Peak to Average Power Ratio (PAR) of the transmitted signal, which requires a high linearity response in the transmitter. These types of amplifiers have low power conversion efficiency, therefore, are not suitable for the UL connection due to battery issues, resulting in the choice of SC-FDMA for LTE UL connections instead of OFDMA.

Table 2.1. Correspondence between the allocated bandwidth and RB (based on [DaPS11]).

Bandwidth [MHz]	1.4	3	5	10	15	20	40	60	80	100
Number of RB	6	15	25	50	75	100	200	300	400	500

SC-FDMA takes a contiguous number of RBs and uses them in transmission with one single carrier in central frequency, with typically Quadrature Phase-Shift Keying (QPSK) and Quadrature Amplitude Modulation (QAM), symbols being sent on a sequence in time. The CP is also used periodically in order to prevent ISI, but it is added after a block of symbols instead of each symbol, as the symbol rate takes now higher values than in OFDMA. A certain user occupies a continuous part of the spectrum and the granularity usage time is 1 ms, the frequency gaps being of 180 kHz RB and the maximum bandwidth of 20 MHz. Although each user allocated frequency bands are contiguous, the band value itself might be expressed on RB or subcarrier bands as well as the structures of the slots, sub-frames and frames. It must be taken in account also that guard bands are also necessary, resulting in a transmission band smaller than the allocated one, e.g., 9 MHz of transmission band on a 10 MHz allocated one. Figure 2.4 shows a sequence of SC-FDMA symbols with bandwidth and bitrate variation.

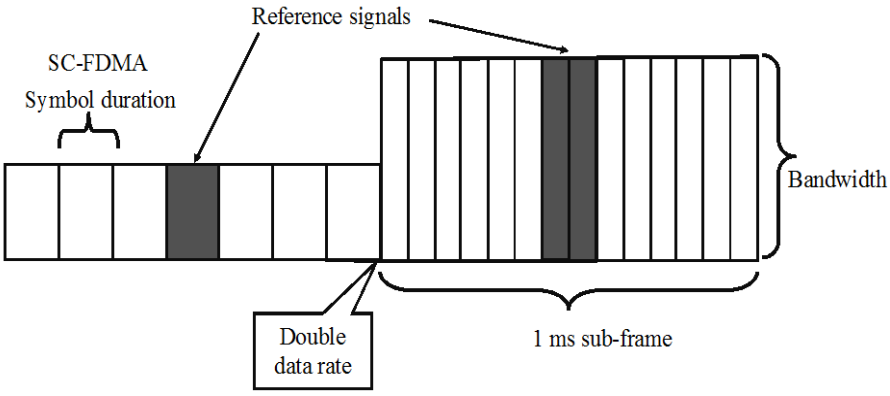

Figure 2.4. SC-FDMA symbols sequence (extracted from [HoTo09]).

Another fundamental enhancement used in LTE is MIMO. This technology relies on using 2 or more antennas in the transmitter and receiver in order to take advantage of spatial, pre-coding and transmit diversity. In spatial diversity, signals are sent from 2 or more different antennas with different data streams, and are received and separated at the receiver, and through signal processing peak data rates are increased by 2 or more, depending on the configuration. In pre-coding, the signals transmitted from the antennas are weighted in order to maximize the received Signal-to-Noise Ratio (SNR). Finally, transmit diversity consists of sending the same exact signal from multiple antennas with some coding to exploit the gains from independent fading between the antennas. The reference symbols existent in the streams enable the receivers to separate the different antennas of which the streams came from.

In addition to the physical properties of LTE presented previously, LTE-A brought some new enhancements to the system, fulfilling 4G specifications, according to IMT Advanced, which constitutes the requirements of the International Telecommunications Union (ITU), more specifically ITU Radiocommunications Sector (ITU-R), a new Radio Access Network (RAN) named Advanced E-UTRA being introduced. Backwards compatibility is guaranteed, meaning that an earlier-release LTE terminal shall always be available to a carrier supporting this new 3GPP Release 10 [3GPP11A].

The major target improvements on the system are:

- Peak data rates of 100 Mbit/s for high mobility and 1 Gbit/s for low mobility;
- Peak spectrum efficiency of 30 bps/Hz and 15 bps/Hz and minimum peak spectral efficiencies of 15 bit/s/Hz and 6.75 bit/s/Hz, for DL and UL respectively;
- CA, allowing a bandwidth allocation between 40 MHz and 100 MHz;
- Extended MIMO configurations of 8×8 and 4×4 for DL and UL, respectively;
- Support for relaying.

The most outstanding aspect of LTE-A is CA. It allows a terminal to transmit or receive in parallel up to 5 LTE carriers, each one with a bandwidth up to 20 MHz, aggregating at most 100 MHz [DaPS11]. The CA can occur with the carrier in the same frequency band or not, being classified as Intra or Inter-band aggregation, respectively. In addition, in intra-band aggregation, the component carrier can be contiguous or non-contiguous. The possibility to aggregate non-adjacent component carriers allows for exploitation of the fragment spectrum as a single wideband by the operators. Another improvement, relative to cell planning is relaying, also known as multihop, which consists on retransmitting information from the BS to other nodes, called Relay Nodes, in order to raise both coverage and capacity on a certain area, by providing end users with a stronger power signal. This overcomes the high attenuation due to larger distances or obstacles, such as buildings in situations of NLoS, without installing more BSs that have higher installation costs, require more capacity from the fixed access network, and can lower neighbor BSs capacity due to additional interference. It also improves spectral efficiency, since it only uses the same radio channel instead of more channels with extra BSs, avoiding also Inter-Cell Interference (ICI).

When dealing with sub-carriers or RB distribution among users in DL on at a given instance, the spectrum can be divided by localised and distributed OFDMA, the subcarriers of a certain user being contiguous or spread along the bandwidth, as shows Figure 2.5. The benefit of distributed OFDMA compared to the localised one is the possibility of additional frequency diversity, as even a low-rate distributed OFDMA signal can be spread over a potentially very large overall transmission bandwidth. Nevertheless, not only it consumes more RBs, but also is more sensitive to frequency shift errors and has higher requirements on power control.

Even though, a mixture of the two approaches can be expected, in the sense that CA that is implemented in 3GPP Release 10 will be able to group either contiguous or separate bands, each one up to 20 MHz for a single user.

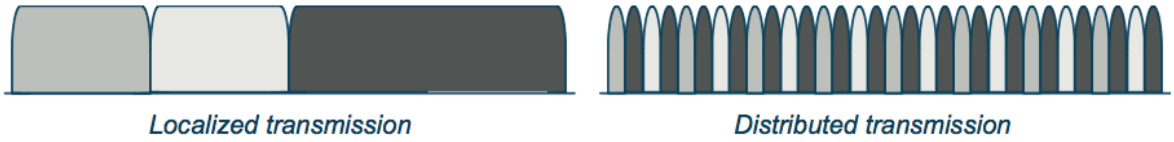

Figure 2.5. Localised and distributed OFDMA transmission.

2.3 Performance Analysis

This section addresses the performance of LTE and its main contents, being based on [HoTo09] and [DaPS11].

The first LTE performance assessment is about peak data rates. The main factors that affect data rates or throughputs are:

- Bandwidth or number of RB instantaneously allocated.
- Number of symbols per sub-frame.
- Modulation scheme order.
- Channel encoding rate.
- Number of transmit antennas with MIMO operation.
- Control and signaling overhead.

The values of bandwidth and RBs for LTE Releases 8 and 9 vary between 1.4 and 20 MHz, and between 6 and 100 RBs, as one can see from Table 2.1. The main modulations schemes used in LTE are QPSK, 16QAM e 64QAM, which corresponded to bit rates of 2, 4 and 8 bit/s respectively, considering an encoding channel rate of 1. MIMO possible configurations are 4×4, 2×2 or no MIMO at all, i.e., SISO, corresponding up to quadrupling, doubling or maintaining the number of bits per symbol. Taking into account the control and reference signal overheads, such as Physical Downlink Control Channel, DL and UL reference signals, and synchronisation signals, which represent an overhead usually between 13% and 30% [HoTo09], one can use (3.3) to calculate the peak data rates for the various combinations of modulation, coding rate, MIMO configuration and RB or bandwidth, presented in Table 2.2 for DL and in for Table 2.3 UL.

The DL peak data rates range between 0.8 and 89.7 Mbit/s with SISO, and reaches 325.1 Mbit/s with 4×4 MIMO. UL peak data rates take lower vales, using no MIMO at all, and range between 0.9 and 86.4 Mbit/s. In fact, these values exceed the initial target ones, which are 100 Mbit/s for DL and 50 Mbit/s for UL. Although the peak data rates take appreciable high values, they can only be achieved under very good channel conditions. Indeed, the practical data rate is limited by both interference and noise in the network, as Shannon's expression can demonstrate, and also by redundancy expressed by the coding rate due to Forward Error Correction (FEC), as well as by signaling and control data.

In order to determine which modulation scheme, coding rate and number of symbols per sub-frame that allow the calculation of the achievable throughput, first one has to estimate the Signal-to-Interference plus Noise Ratio (SINR). There are both periodic reports through the PUCCH and aperiodic through the PUSCH to estimate the radio link condition. Figure 2.6 shows the minimum SNR that is required for the modulations and coding schemes combinations for a given BLER, highlighted for a BLER of 10%, which is the highest reference value to consider in a radio link. The combination of modulation schemes and code rate as a function of the SINR that provides the highest spectral efficiency is presented in Annex F, where achievable data rates are presented for each scenario and modulation and coding rate.

Table 2.2. DL peak data rates (extracted from [HoTo09]).

Modulation and coding	MIMO usage	Bit/symbol	DL peak data rates [Mbit/s]					
			Number of RB / Bandwidth [MHz]					
			6 / 1.4	15 / 3	25 / 5	50 / 10	75 / 15	100 / 20
QPSK ½	SISO	1.0	0.8	2.2	3.7	7.4	11.2	14.9
16QAM ½	SISO	2.0	1.5	4.4	7.4	14.9	22.4	29.9
16QAM ¾	SISO	3.0	2.3	6.6	11.1	22.3	33.6	44.8
64QAM ¾	SISO	4.5	3.5	9.9	16.6	33.5	50.4	67.2
64QAM 1/1	SISO	6.0	4.6	13.2	22.2	44.7	67.2	89.7
64QAM ¾	2×2 MIMO	9.0	6.6	18.9	31.9	64.3	96.7	129.1
64QAM 1/1	2×2 MIMO	12.0	8.8	25.3	42.5	85.7	128.9	172.1
64QAM 1/1	4×4 MIMO	24.0	16.6	47.7	80.3	161.9	243.5	325.1

Table 2.3. UL peak data rates (extracted from [HoTo09]).

Modulation and coding	MIMO usage	Bit/symbol	UL peak data rates [Mbit/s]					
			Number of RB / Bandwidth [MHz]					
			6 / 1.4	15 / 3	25 / 5	50 / 10	75 / 15	100 / 20
QPSK ½	SISO	1.0	0.9	2.2	3.6	7.2	10.8	14.4
16QAM ½	SISO	2.0	1.7	4.3	7.2	14.4	21.6	28.8
16QAM ¾	SISO	3.0	2.6	6.5	10.8	21.6	32.4	43.2
16QAM 1/1	SISO	4.0	3.5	8.6	14.4	28.8	43.2	57.6
64QAM ¾	SISO	4.5	3.9	9.7	16.2	32.4	48.6	64.8
64QAM 1/1	SISO	6.0	5.2	13.0	21.6	43.2	64.8	86.4

The actual radio signal quality is continuously transmitted over the radio interface by the Channel Quality Indicator (CQI) index, which takes an integer number between 1 and 15 and indicates the data rate supported by the cannel, taking into account the SINR and the MT's receiver. Taking into account the CQI value, one of the modulation schemes QPSK, 16QAM and 64QAM is chosen periodically as well as the amount of redundancy included, known as Adaptive Modulation and Coding (AMC). The corresponding bit rate per symbol is standardised by 3GPP, being shown in Table 2.4. The code rate presented is obtained as the number of information downlink bits divided by the number of physical channel bits on PDSCH. The condition that a CQI index has to verify is to be the highest CQI index number that guarantees the reception of transport blocks with respective error probability not

exceeding 10% [3GPP11g].

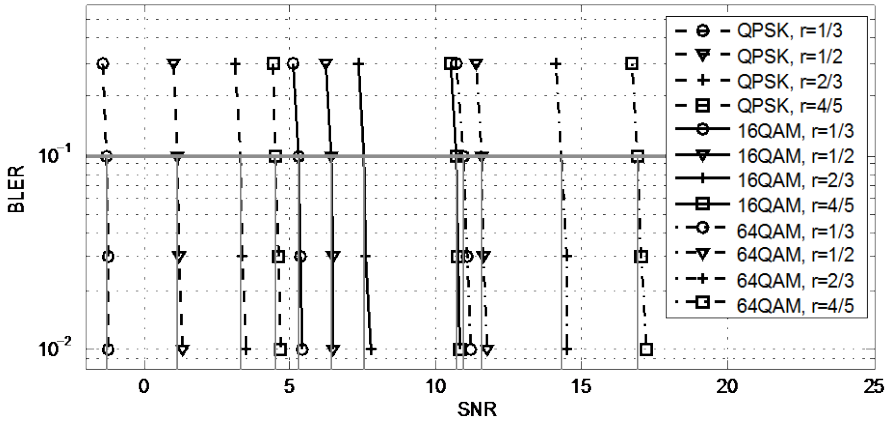

Figure 2.6. Typical BLER versus SNR for different modulation and coding schemes (extracted from [SeTB09]).

Table 2.4. CQI indexes (extracted from [3GPP11g]).

CQI index	Modulation scheme	Code rate × 1024	Efficiency
1	QPSK	78	0.1523
2	QPSK	120	0.2344
3	QPSK	193	0.3770
4	QPSK	308	0.6016
5	QPSK	449	0.8770
6	QPSK	602	1.1758
7	16QAM	378	1.4766
8	16QAM	490	1.9141
9	16QAM	616	2.4063
10	64QAM	466	2.7305
11	64QAM	567	3.3223
12	64QAM	666	3.9023
13	64QAM	772	4.5234
14	64QAM	873	5.1152
15	64QAM	948	5.5547

In LTE, the capacity can be associated to the number of available RBs at a given time, and to the number of users that can be assigned to them, in the sense that the sum of the instantaneously served users' throughputs defines the instantaneous load of the BS. Capacity can also be evaluated by the number of users that can be served simultaneously for a given service, so the maximum number of users that can access to the network at a given instant depends on the number of RBs that each user is using. Also, the number of RBs being used by each user depends on the required

throughput that varies along time and depends on the SINR of the user. In this manner, the higher number of RBs being allocated to each user, the lower the possible number of simultaneous users will be. The total throughput of the users will not only depend on the bandwidth but also on the SNR and others parameters as shown above. Nevertheless, a trade-off between the number of active users and the perceived QoS must be achieved.

Focusing on the idea that the LTE was designed to be a high speed packet switch optimised data system over the IP network layer, one main concern is the network latency, which can be defined as a measure of the time it takes for a packet to travel from a client to a server and back again, also known as Round Trip Time (RTT). In fact, there are many applications that do not require such a very high bitrate, but require very low latency such as voice, real time gaming and other interactive applications. ITU-R target was set to the value of 10 ms, but for one-way latency, defined as the one-way transit time between a packet being available at the IP layer in the user BS and the availability of this packet at the IP layer in the UE, this is achieved in 4 ms in LTE FDD. The average RTT including retransmission can be below 15 ms with pre-allocated resources, and around 20 ms including scheduling delay [HoTo09].

Another aspect to take into account designing cell network is interference, which starts having more importance when its power takes higher values than noise, a situation that happens due to BSs' coverage areas overlapping. Regarding SINR, ICI must be quantified for every user in a cell in order to calculate the maximum throughput under a certain Block Error Rate (BLER), because interference power is definitely a far more limiting factor than noise one [Øste11], especially for urban scenarios where BSs coverage area overlapping is bigger compared with rural ones. The most unfavourable situation in terms of interference is at the cell-edge, due to the reduced signal power from the connected BS and closer to the neighbour interfering BSs.

Interference can be divided into categories:

- Adjacent-channel or intra-cell interference: it is due to signals from adjacent channels extending into the band of the desired signal, which can be neglected if perfect orthogonality between sub-carriers is considered, as one can expect from LTE.
- Co-channel interference or ICI: it is due to the existence of signals of the same frequency reaching the same receiver, which is an inevitable fact in mobile telecommunications system with reuse of the same frequencies along the cells.

In LTE, ICI is the main cause of performance degradation, especially if a reuse factor of 1 is used, which is highly desirable in order to reach the target spectral efficiency gain [BQCR08] and meet the growing users demand in terms of bit rate, leading to a higher capacity of the network [RaYW09]. Therefore, this dense reuse of frequencies results in a strong ICI, which limits not only the system capacity but also the cell-edge throughput, which are the two factors that influence cell planning and interference mitigation algorithms.

Consequently, interference mitigation is a major aspect of LTE in order to reach the maximum performance on a real scenario, i.e., a real network with multiple and asymmetric tri-sectorised cells. According to [RaYW09], interference mitigation techniques can be categorised into three major

classes:

- Interference cancellation: the basic principle is the receiver signal processing to estimate interference and subtract it from the desired signal component;
- Interference averaging: it ensures UEs to access a range of channels rather a narrow set in a specific pattern so that the interference effect is averaged out for all UEs, such as the frequency hopping technique;
- Interference avoidance: it focuses on finding an optimal effective reuse factor often achieved through restrictions on frequency and power allocations to achieve network performance goals.

Interference avoidance can be implemented through static frequency reuse schemes that implement definitive restrictions on bandwidth and power, such as the division of the available bandwidth for the three sectors on part or the entire cell area, which achieve reduction on ICI with reduction on cell throughput. Consequently, an optimal partitioning depends on the distribution of the MTs, arrived traffic and channel dynamism, which can be the dynamic inter-cell coordination between sectors of the same BS and between different BSs through X2 connections, where RBs collisions are avoided by using different carriers. In [RaYW09], it is proposed and evaluated by extensive simulations a dynamic scheme for DL, which in comparison to the reference usage scheme, achieves at cell-edge of 171% and 266%, and total sector throughput gains of 7.2% and 3.9% respectively, when compared to the performance of reuse 1 scheme. For each RB, a utility matrix covering all three sectors of a BS is used, in order to get rid of restrictions on RB usage that maximize cell throughput, based on dominant received interference from four BS interferes. The implemented scheme involves the preparation of the utility matrix, using suitable heuristics and applying Hungarian assignment algorithm, and then a threshold-based strategy is used to determine which interferers are to be restricted.

Other factor that influences directly users' throughput and overall capacity is the scheduling scheme. Taking into account a cell for example, the number of resources that can be allocated to the users requesting connection to the cell is obviously limited, therefore, an algorithm or RB distribution must be defined, i.e., a criterion of capacity maximisation with reasonable fairness between users, along time and frequency domains. The most popular scheduling algorithms are:

- Maximum SINR;
- Round Robin (RR);
- Proportional Fair (PF).

In the Maximum SINR scheduling, the probability of resources being allocated to each user depends on the SINR of the respective radio link, users with high SINR having higher probabilities to get resources than users with low SINR. Assuming a single user DL TDM system, there is a maximisation of the available resources if the scheduled user at a given instance is the one who experiences best radio channel condition, as Figure 2.7-a) illustrates. This guarantees that the highest throughput is achieved for a certain BS transmit power, which is one of the requirements from the QoS point of view, along with latency and packet error rate. As the radio channel condition varies independently for all users in a cell, due to their different positioning and speed, at each instance there will probably be

users experiencing receiving signal at its high power appropriate to use the available resources. Guaranteeing the best links between users and BS, it maximises the obtained throughout and consequently the highest system capacity is achieved. This strategy is also known as multi-user diversity because the higher the number of users in the cell and the channel variation, the higher the multi-user gain. The problem of this algorithm is the lack of fairness, because users will also experience differences in slow fading and path loss, and it may happen that most of the time, some users will experience good channel condition while others will not, so that they will never be scheduled, degenerating into two groups of greedy and starving users.

RR scheduling provides users the same amount of resources, not taking the radio channel condition into account, in order to be as fair as possible, as Figure 2.7-b) shows, where the channel is attributed the same amount of time to each user. The two problems are that there is no maximisation of each user throughput and consequently of the overall capacity, and as users experience different instantaneous radio channel condition, some users would need more RBs than others to achieve the same bit rate so that one could say there is perfect fairness among users.

PF scheduling is a variation of the Maximum SINR that takes into account not also the radio channel condition but also the past scheduling, in order not to exclude users from scheduling, illustrated in Figure 2.7-c). Resources are assigned to the user with the relatively best radio-link conditions, i.e., a user scheduled is selected for transmission according not only to his SNR but also to the history of the recent attribution of resources. The average data rate is calculated over a certain period, which usually takes the value of 1 s, so that it is longer than the short-term variations and still not strongly noticeable by users.

On all scheduling schemes, resources are not scheduled purely on time-domain, but obviously also in frequency-domain, because the users scheduled may not occupy the full channel capacity and the unused resources are scheduled to another users. Also, scheduling algorithms are expected to satisfy the QCI parameters defined for each service describe on Table 2.6, in order to preserve the overall QoS of users.

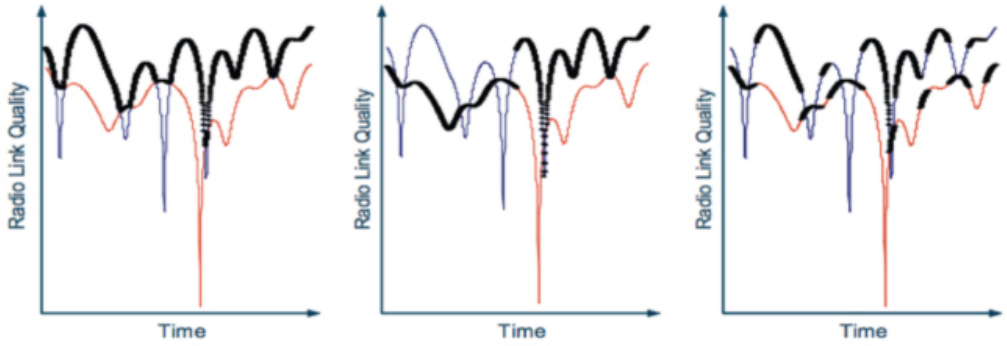

a) Maximum SINR b) Round Robin c) Proportional Fair

Figure 2.7. Maximum SINR, RR and PF scheduling schemes (extracted from [DaPS11]).

2.4 Services and Applications

The main goal of a mobile communication system is to provide wireless links between users, transporting relevant information in order to provide them the services they need. The oldest and most popular service is obviously the voice service, which is assured by every mobile phone available. This service has the particular characteristic of being predictable on its demanding performance from the network: the bit rate of voice is specified and well known and does not vary along time. Consequently, the main concern of the operators for most of the cases relies on the capacity aspect in order to provide at a given time interval, access to the voice service to all their clients requiring a phone call at the referred time interval, the delay being the factor that can mostly affect the quality of the phone call.

Nevertheless, there is obviously another type of services that is becoming more and more challenging for the mobile communication systems, which is the data. Data services are a huge group of services that are very popular, such as Short Message Service (SMS), email, videoconference, web browsing, interactive and real time applications, video streaming and File Transport Protocol (FTP). They not only may be very demanding on the bit rate, delay and duration, but also are growing very fast, with a tremendous traffic volume. In addiction, they consist of several applications that are very different from each other, in the sense that to guarantee a good QoS, many quality requirements have to be monitored according to the specific service. These services are the ones that are pushing both operators and mobile equipment manufacturers to go further on their development: operators strive to provide customers services anywhere and anytime, and manufacturers strive to produce the best equipment that allow customers to enhance their services usage, that have evolved from simple mobile phones to very powerful capable devices, known as smartphones, which are very data-focused.

To face these challenges, parameters have to be defined, and performance has to be quantified, resulting on the creation of several classes of services. For the previous 3GPP mobile communication system UMTS, 3GPP has specified four QoS classes, also referred to as traffic classes, based on their QoS requirements [3GPP11e]. The four different QoS classes are conversational, streaming, interactive and background. There are many factors that characterise the classes, but the main distinguishing factor is the delay sensitiveness. Conversational and streaming are obviously the classes that are more performance dependent on delay, due to their real time service nature. Conversational services include voice, video-telephony and Voice over IP (VoIP), being supposed to respect the maximum delay margins that keep the conversation intelligible, such as an adequate end to end voice sound and video frame refreshment. Streaming includes audio and video streaming for music and mobile TV, for example. Interactive and background classes are meant to be used by traditional Internet applications, like web browsing, e-mail, FTP, etc. Due to less demanding delay requirements, interactive and background, compared to conversational and streaming, provide better Bit Error Ratio (BER) by means of channel coding and retransmission. The interactive class is mainly used in interactive applications while background is meant for background traffic such as background download, e-mail or background application, leading to a higher priority to interactive than background.

Table 2.5 summarizes the information about the 4 classes, describing the parameters that characterize the classes designed for UMTS.

Table 2.5. Services and applications according 3GPP (extracted from [3GPP11e]).

Service class	Conversational	Streaming	Interactive	Background
Real time	Yes	Yes	No	No
Symmetric	Yes	No	No	No
Guaranteed bit	Yes	Yes	No	No
Delay	Minimum fixed	Minimum	Moderate	High variable
Buffer	No	Yes	Yes	Yes
Bursty	No	No	Yes	Yes
Switching type	CS	CS	PS	PS
Example	Voice	Video streaming	Web browsing	SMS, e-mail

Performing the transition from UMTS to LTE, SAE was designed into a simplified bearer model with few layers, as described previously in Section 2.1, and a network resource management done by the inner network exclusively, having been specified only one signalling transaction from the network to the UE and all interim network elements. Regarding the data focused purpose of LTE and the enormous growth of traffic worldwide on mobile devices, 3GPP re-specified the QoS standards to keep up with performance requested. [3GPP11f] QoS parameters were also reduced in their number but were optimised. LTE's specified QoS parameters are [HoTo09]:

- QoS Class Identifier (QCI). It is an index that identifies a set of locally configured values for the three QoS attributes: priority, delay and loss rate. QCI is signalled instead of the values of these parameters, ten pre-configured classes having been defined (although this thesis only presents nine). Operators within their network can create additional classes;
- Allocation and Retention Priority (ARP). ARP indicates the priority of the bearer compared to others bearers, providing admission control information in bearer set-up and in congestion situations if bearers need to be dropped;
- Maximum Bit Rate (MBR). MBR Identifies the maximum bit rate for the bearer;
- Guaranteed Bit rate (GBR). GBR identifies the bit rate that will be guaranteed to the bearer;
- Aggregated Maximum Bit Rate (AMBR). As IP flows may be mapped on to the same bearer, AMBR indicates the total maximum bit rate a UE can have for all bearers in the same PDN.

The standard QCI classes and its respective parameters values are shown in Table 2.6. The QoS parameters are:

- Resource Type: indicates which classes will have GBR associated to them;
- Priority: is used to define the priority for the packet scheduling of the radio interface;
- Delay budget: helps the packet scheduler to maintain sufficient scheduling rate to meet the delay requirements for the bearer.
- Loss rate: helps to use appropriate Radio Link Control (RLC) settings, e.g., number of re-

transmissions.

Although LTE was designed and optimised for packet switch, it is expected that it will provide voice and video-call as well, so that both GBR and non-GBR services will share the same radio resources.

Table 2.6. Standardised QoS parameters for QCI (extracted from [3GPP11f] and [HoTo09]).

QCI	Resource Type	Priority	Packet Delay Budget [ms]	Packet Error Loss Ratio	Example Services
1	GBR	2	100	10^{-2}	Conversational Voice
2		4	150	10^{-3}	Conversational Video
3		3	50	10^{-3}	Real Time Gaming
4		5	300	10^{-6}	Non-Conversational Video (Buffered Streaming)
5	Non-GBR	1	100	10^{-6}	IMS Signalling
6		6	300	10^{-6}	Video (Buffered Streaming) TCP-based
7		7	100	10^{-3}	Voice Video (Live Streaming) Interactive Gaming
8		8	300	10^{-6}	Video (Buffered Streaming) TCP-based
9		9			

As most of GBR services have a higher priority than non-GBR ones, as shown previously on Table 2.6, the available resources are first distributed among users requiring GBR services and the remaining resources are distributed within non-GBR ones. Nevertheless, the usage of GBR with high bit rates caused by low SINR, e.g., user at cell edge, presents a high demand of radio resources, therefore, the GBR allocation must be limited.

2.5 State of the Art

Relaying techniques are tested on a real scenario, using numeric results from models in [ScZW08]. The authors study coverage and capacity on the island of Jersey, USA, on three situations: one BS only, one BS with four Relay Nodes (RNs) and one BS with four RNs plus a ring of nine RNs. It is

shown that the two tiers of relay, compared to the BS only scenario, increase coverage by a factor of 2.08 and capacity and spectral efficiency by a factor of 1.33. This is a good and low cost enhancement to the existing BS exploring improvements of the original BS performance.

In [KhPr08], a performance evaluation of frequency hopping schemes in UL is addressed to explore frequency diversity gains through simulations for 16QAM 4/5 in typical urban channel mode. Localised and Distributed frequency hopping modes are compared and their frequency hopping schemes are presented: Inter-Transmission Time Interval (TTI) Frequency Hopping and Intra-TTI Frequency Hopping. Regarding the ideal channel estimation, from the performance point of view, Localised SC—FDMA provided the best results of all, which varied between 0.3 and 0.7 dB.

The impact of control channels limitations on VoIP capacity are studied in [PPAH10], where the authors perform fully dynamic simulative analysis on DL and UL constraints, which are PDCCH and PUCCH capacity, that has impact on the number of multiplexed users by TTI and Control Channel Indicator resolution. Therefore, different packet scheduling schemes and CQI reporting resolution are addressed. Semi-persistent packet scheduling present a 40% to 67% improvement VoIP capacity gain with over dynamic packet scheduling without packet bundling, and provide a more efficient use of the scarce PDCCH resources in higher number of multiplexed user per TTI and in PDSCH.

Interference Margins (IM) for OFDMA cellular networks are analysed in [HPYW10], and are one of the key inputs to LTE cellular networks planning, as its relevance is paramount in link budget calculation accuracy, IM being introduced as using the general expression of SINR based on Exponential Effective SINR Mapping (EESM) method, considering the frequency reuse factor and verified by Monte Carlo simulations. The authors demonstrate that there are less interfered subcarriers by co-channel interference with a lower load factor, and that IM decreases significantly with the reuse factor. Also with improvements on performance dealing with interference on the link budget calculation, it allows to relax the requirements in order to improve coverage radius.

In [SHWH], the authors introduce a deterministic approach for the simulation and performance evaluation of LTE networks in urban and indoor scenarios, together with to measurement campaigns that confirm their model's high accuracy. Received power, delay spread, channel capacity along the receiver trajectories are first addressed, considering the outdoors scenario taking into account a 3D ray tracing propagation model, and then peak data rates are calculated in indoor scenario with different antenna configurations. This paper is important as it takes a real urban scenario and calculates performance of antenna configuration, because this type of environment faces a lot of uncertainty on the propagation path of the signal, as well as high data rates are expected to take the most out of LTE performance, which obviously require a good SNR.

In [RaYW09], co-channel interference mitigation techniques are studied to obtain dense spectrum reuse on a real scenario, in order to achieve the high peak data rates of LTE using dynamic inter-cell coordination facilitated through X2 interface. The authors propose a scheme that is evaluated through extensive simulations and compared to a number of popular reference schemes and provides both higher overall cell and cell-edge users throughput, combining an efficient distribution of resources with fairness among users along the cell radius. Results show two proposed schemes that, compared to

Reuse-1, achieve 171% and 266% higher cell-edge users throughput and 7% and 3.9 higher sector users throughput.

Chapter 3

Performance Models and Simulation

This chapter provides an overview of the developed and implemented model, in order to assess LTE performance by means of users throughput, and cells load and coverage, considering realistic radio channels conditions as well as reasonable RRM strategies to guarantee QoS and fairness between users. In Section 3.1, the implemented model is described as far as radio channel and radio resource distribution characteristics are concerned. In Section 3.2, implementation is described in order to obtain the simulator of LTE performance. In Section 3.3, the simulator assessment and model's validation is performed.

3.1 Model Description

This section describes the radio interface models used in the implementation of the simulator, as well as the implemented algorithms of radio resources distribution, the basic telecommunications expressions being based on [Corr09] and the specific contents of LTE on [HoTo09].

3.1.1 SNR and SINR

In a first step, the calculation of SNR is done for each user, taking into account the average received signal power and the noise power at the receiver, where the frequency carrier used is the central frequency band of the entire bandwidth, since at this phase only an estimation is needed to calculate the necessary number of RB to satisfy the wanted throughput by the users, the SNR being calculated by (B.7).

The average signal power at the receiver is calculated by the link budget and the COST 231 Walfisch-Ikegami Model, presented in Annex B and Annex C, respectively, and is given by (B.1). In the calculation of the signal pathloss, there are two additional attenuation terms that represent the user environment, such as vehicular and indoor penetration margin, and the Slow Fading (SF) margin as shows (B.6). The noise power at the receiver can be calculated by (B.8).

The calculation of the SINR is done after the users throughput reduction, which is performed when the BSs capacity is exceeded, i.e., the required number of RBs for a given sector is higher than the available one, and after the distribution of the wanted RBs along the frequency band. As the reuse of the same RBs frequency carriers originate interference, the RBs frequency attribution is done randomly across the frequency band, respecting the restrictions from the FRSs in order to avoid allocating RBs in the same position, as it is not considered pro-activity in detecting collisions between neighbour BSs and even between sectors of the same BS.

Consequently, for each RB attributed and for each BS in the network, the SINR in the receiver is calculated by (B.9), taking now into account the accurate frequency carrier being used, as well as the interference power coming from neighbouring sectors, which is calculated for each source in the same way as the received signal power, with the exception of the origin of the interfering transmission.

The interference power at the receiver can be calculated by (3.1), as the sum of the interfering signals that reach the receiver that have power equal or greater than the noise power and use the same frequency carrier, and each one of the interfering powers at the receiver can be calculated by (B.1).

$$I_{[\mathrm{mW}]} = \sum_{i=1}^{N_I} I_{i\,[\mathrm{mW}]} \tag{3.1}$$

where:

- I_i is the interference power coming from transmitter i;
- N_I is the number of interfering signals reaching the receiver.

Interference power can be originated by others sector of the same BS or by neighbour BSs, as shown in Figure 3.1.

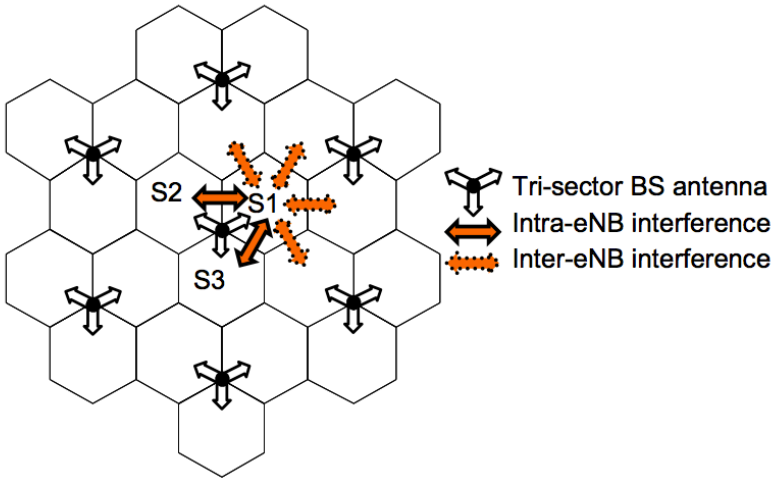

Figure 3.1. Intra-eNB and Inter-eNB interference.

3.1.2 Throughput

The first calculation of the users throughput, which is an approximation, since the RBs carrier frequency is not known at this stage neither is the interference power, is done by calculating the throughput of an RB with the central frequency of the entire radio channel bandwidth, and using its value for the other RBs:

$$R_{b\,[\text{Mbit/s}]} = N_{RB} R_{b,RB_c\,[\text{Mbit/s}]} \tag{3.2}$$

where:

- N_{RB} is the number of RBs allocated to the user;
- R_{b,RB_c} is the data rate of the RB obtained for the central frequency band carrier.

One can calculate an RB throughput by the following expression:

$$R_{b\,[\text{bit/s}]} = \frac{B_{RB\,[\text{Hz}]}\, N_{sub/RB}\, N_{sym/sub\,[\text{symbol/Hz}]}\, N_{bs\,[\text{bit/symbol}]}}{T_{RB\,[\text{s}]}} \tag{3.3}$$

where:

- B_{RB} is the bandwidth of a RB, which takes the value 180 kHz;
- $N_{sub/RB}$ is the number of subcarriers per RB;
- $N_{sym/sub}$ is the number symbols per subcarrier;
- N_{bs} is the number of bits per symbol;
- T_{RB} is the RB time period.

The mapping of the SNR is used in the calculation of the RBs throughput, which takes the highest value for the three possible modulation schemes QPSK, 16QAM and 64QAM, and is shown with detail in Annex F.

The interference power is calculated for every RB and so is the SINR, for each user, their RBs throughput being calculated accurately mapping the value of SINR instead of SNR, in order to obtain the real users throughput:

$$R_{b\,[\text{Mbit/s}]} = \sum_{i=1}^{N_{RB}} R_{b,RB_i\,[\text{Mbit/s}]} \tag{3.4}$$

where:

- R_{b,RB_i} is the data rate of the RB i, calculated for the respective attributed frequency.

At this stage, RBs throughput can differ from each other in the value for the same user, since the interference power can also take different values and so can the pathloss due to the different frequency carrier associated to each RB.

3.1.3 Capacity

Capacity is a more complex performance parameter to describe, in the sense that it can be evaluated by the number of users that can be served simultaneously by a BS, which depends on the service itself as well as the serving throughput of each user and on their radio condition due to the number of used RBs. Also, one can inspect the BS load by calculating the cell throughput, which is given by the sum of the instant throughputs for the active users in a cell:

$$R_{b,BS_{[\text{Mbit/s}]}} = \sum_{i=1}^{N_{u\,BS}} R_{b\,user_i\,[\text{Mbit/s}]} \tag{3.5}$$

where:

- $R_{b,BS}$ is the BS throughput;
- $N_{u\,BS}$ is the number of active users of the BS.

As shown in Chapter 2, instantaneous throughputs are influenced by the scheduling algorithms due to the radio channel condition and the priority defined for the users, especially for GBR users. Capacity evaluation relies on the instantaneous load required to the network on every BS, where the BS throughput is aimed to be as close as the maximum one, to allow the higher number of users and higher users throughput as possible. The number of used RBs is evaluated as well in the capacity analysis. Thus, one can evaluate capacity by the number of users per sector, and again this number depends on the required throughput and the respective radio channel condition. Assuming that SNR is a non-limiting factor and that each user requires the same throughput, one can define the number of users to be served by:

$$N_{served\ users/BS} = \left\lfloor \frac{R_{b,peak}}{R_{b,user}} \right\rfloor \tag{3.6}$$

where:

- $R_{b,peak}$ is the peak data rate;
- $R_{b,user}$ is the user data rate.

The limit of users per sector of a BS is actually the number of available RBs, since is the granularity used in the distribution of radio resources, so 100 is the maximum number of users per sector in case

of 20 MHz bandwidth, not taking into account the dedicated RBs to signalling and controlling.

3.1.4 Coverage

Concerning the calculations of coverage, one can use the link budget expression combined with an adequate environment propagation model for the path loss to determine the maximum cell or coverage radius as follows:

$$R_{[\text{km}]} = 10^{\frac{P_{t[\text{dBm}]} + G_{t[\text{dBi}]} - P_{r,min\ [d\text{Bm}]} + G_{r[\text{dBi}]} - L_{p[\text{dB}]}}{a_{pd}}} \tag{3.7}$$

where:

- P_t is the power fed to the antenna;
- G_t is the gain of the transmitting antenna;
- $P_{r,min}$ is the power sensitivity at the receiving antenna;
- G_r is the gain of the receiving antenna;
- L_p is the path loss;
- a_{pd} is the average power decay.

Even through, cell radius is obtained by (3.7) as the maximum distance of users from the BS, because this is probably the best characterisation possible for coverage concerns, due to the distance between neighbour BSs in a dense urban network that takes many times lower values than the coverage radii, especially for the lower frequency band of 800 MHz, this can be calculated by:

$$R_{BS\ [\text{km}]} = d_{\max user\ [\text{km}]} \tag{3.8}$$

where:

- $d_{\max user}$ is the distance of the user further away from the serving BS.

3.1.5 Frequency Reuse Schemes

The focus of this thesis is on static interference avoidance techniques and its influence on the performance of the overall capacity of the system. Two popular Frequency Reuse Schemes (FSR) are Reuse-1 and Reuse-3. Reuse-1, or Universal Frequency Reuse, consists of using the whole available bandwidth on each sector of the BS, as in Figure 3.2-a), where there is no distinction between sectors. Si represents the i^{th} sector of the cluster and there is no power control, as power remains constant for the whole bandwidth.

Reuse-3, which is represented in Figure 3.2-b), divides the whole bandwidth along in three equal parts, each for a sector of the cluster, and arranges the clusters joint position in order not to exist sectors using the same frequency band to be next to each other. As interference worst cases scenarios are usually users at cell-edge, when using the same RBs frequency as another neighbour user but belonging to the adjacent cell, this avoids them receiving identical interference power to the signal power they get from their sector. Nevertheless, this frequency scheme reduces by three times the maximum theoretical capacity of sectors and cluster, not using for example the whole bandwidth in

the cell centre where SINR takes higher values than at cell edge.

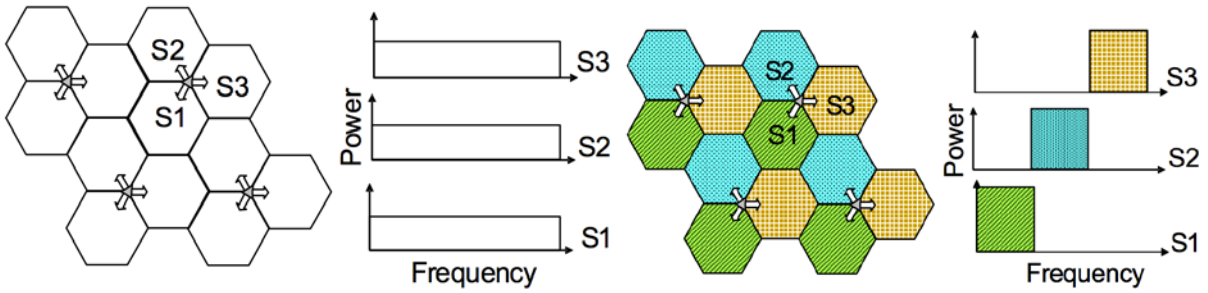

a) Reuse-1 b) Reuse-3

Figure 3.2. Basic FSR (extracted from [RaYW09]).

Again, the most problematic cases of interference are the ones at the cell or sector border, where UEs experience high interference from neighboring transmitters, both others UEs and BSs, in addition to low power signal or high path losses, due to larger distances between them and the BS's antennas. Consequently, these users have poor radio channel conditions, and do not contribute much as others to the total cell throughput. So, the objective of interference avoidance is to provide better services to cell-edge UEs without sacrificing cell-centre throughput.

ICI can be reduced significantly with the traditional frequency reuse strategy, so that the higher the cluster size, the greater the reduction in ICI. However this improvement can only be done with the reduction in cell throughput, due to the reduced use of the available radio bandwidth, so what has been considered in literature is a reuse partitioning in which cells-edge UEs are assigned resources with higher reuse factor compared to the UEs at the cell-centre, resulting in an effective reuse greater than 1 but not too high, such as 1.5, 2.0 and 2.5. These FRSs are named Fractional Frequency Reuse (FFR) schemes and variants have been adopted for LTE by 3GPP, such as Soft Frequency Reuse (SFR) and Partial Frequency Reuse (PFR), which are shown in Figure 3.3. Bear in mind that while this approach improves cell-edge UEs situation, there is a great potential to lose overall cell throughput, due to resource loss resulted from partitioning. An optimal partitioning depends on the distribution of the UEs, arrived traffic and channel dynamism, therefore, any static partitioning scheme is a highly sub-optimal solution.

The SFR scheme has reuse factor 1 in the cell-centre and equal or greater than 1 in the cell-edge, an example of it being shown in Figure 3.3-a), S1, S2 and S3 being the three sectors of a cell. The cell edge is usually 1/3 of the available spectrum and is orthogonal to neighbouring cells. The cell-edge subcarriers are called major subcarrier group, while the cell-centre frequency band is called minor subcarrier group, corresponding to the white and coloured bands in Figure 3.3-a). Cell-edge users are restricted to the major band, while cell-centre users have exclusive access to the minor band and can also have access to the major band, but with less priority. The total transmit power is set constant and each group is assigned a transmission power depending on desired effective reuse factor, which is determined by the power ratio of cell-centre to cell-edge groups. As Figure 3.3-a) illustrates, transmissions can use higher power on the major band compared to the minor one.

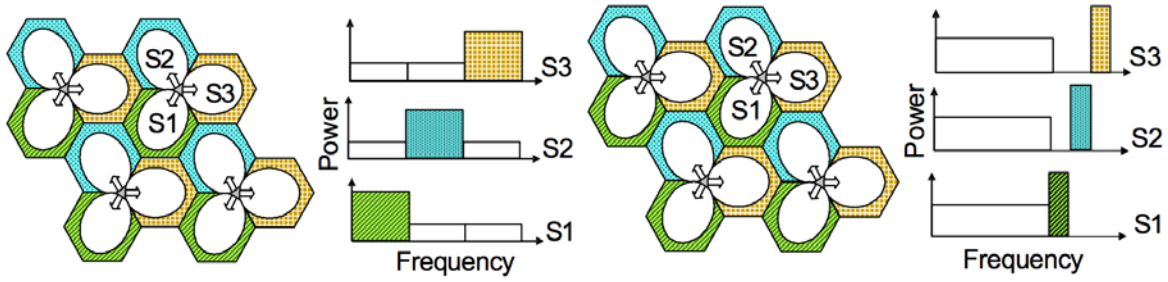

a) SFR b) PFR

Figure 3.3. FFR schemes (extracted from [RaYW09]).

The PFR scheme uses an effective reuse factor always bigger than 1. It shares the existence of an inner zone with an outer one on the sectors like SFR, but the cell-edge of each sector has a dedicated part of the spectrum, along with higher power if necessary, as Figure 3.3-b) shows.

The FRSs taken in this work are Reuse-1 (Universal), Reuse-3, SFR and PFR. The cell radius considered for the separation between the centre and the edge of the cell is the one obtained from simulations using reference scenario conditions. This is done in order to use a more realistic radius in the zone separation rather than using (3.7), which would results in centre-only cells.

The bandwidth restrictions from each scheme were implemented as follows:

- Reuse-1: the whole bandwidth is available in each sector of a cluster and there is no raised power;
- Reuse-3: only one third of the bandwidth is available per sector and sector i^{th} gets the i^{th} part of the bandwidth;
- SFR: two thirds of the bandwidth available in cell centre and another third is available in the cell edge. The i^{th} sector uses the i^{th} part for the edge and the rest for the centre;
- PFR: two thirds of the bandwidth available in the cell centre, counting from the lowest frequency carrier and a ninth is available in the cell edge. The i^{th} sector uses the two thirds of the bandwidth in cell centre and the i^{th} ninth of the bandwidth for cell edge.

3.1.6 Algorithms

The scheduling algorithms implemented in the simulator are Maximum SNR, RR and PF. As the nature of the simulation is a snapshot basis, and it has no time depth to explore the temporal distribution, they were implemented as follows:

- Maximum SNR: RBs are distributed among users with higher SNR, as Figure 3.4 shows;
- RR: RBs distribution is limited by a number of RBs that guarantees that every user can get a certain minimum number of RBs (in fact, this number can be lower if it is sufficient to fulfil the users wanted).
- PF: users are allocated a number of RBs that achieves the average service throughput, before reduction algorithms occur.

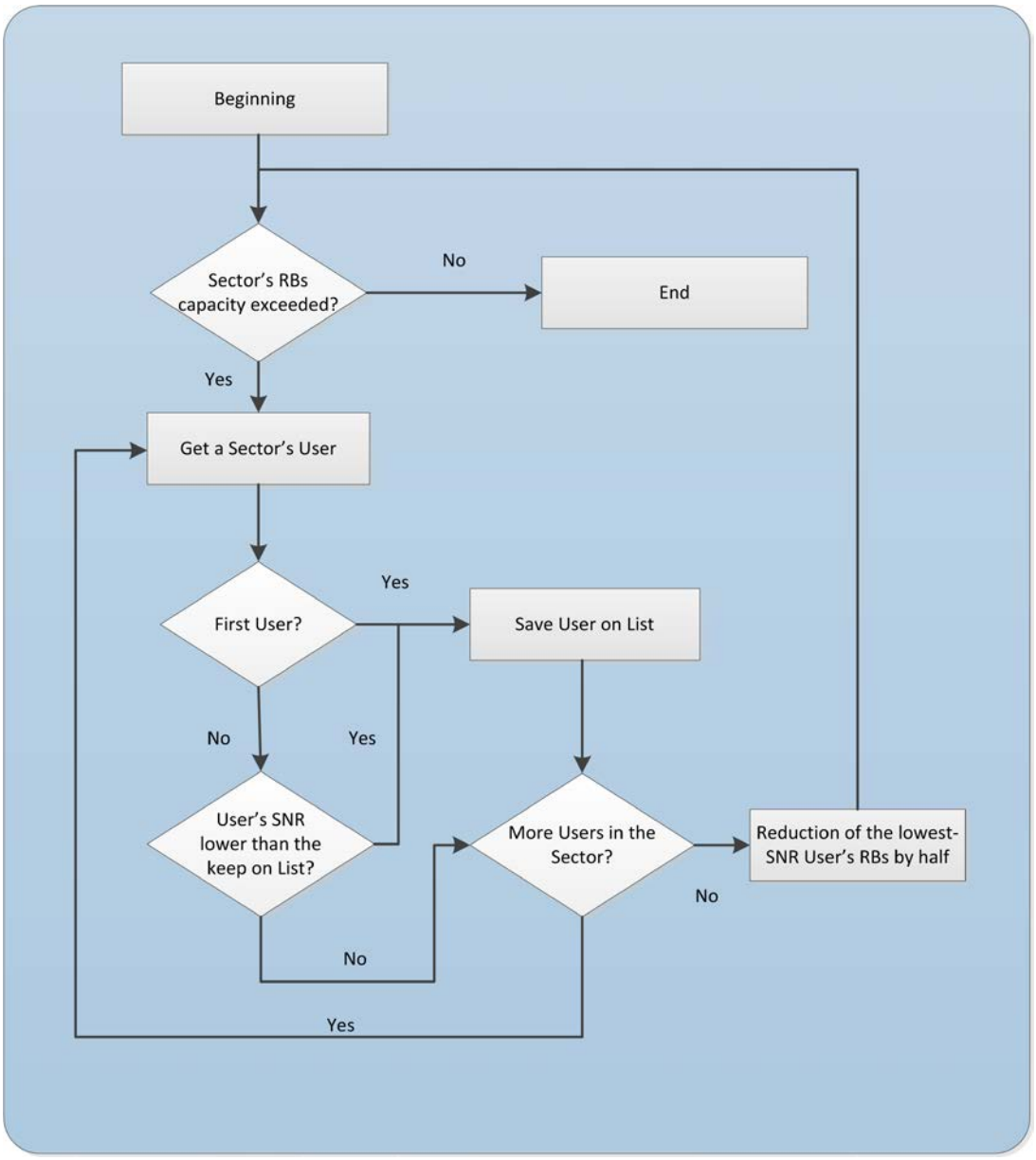

Figure 3.4. Maximum SNR scheduling algorithm.

The interference calculation algorithm is presented in Figure 3.5, showing how the radio channel condition for each RB is recalculated, taking the interference from neighbour cells into account, leading to users adjustment regarding throughput.

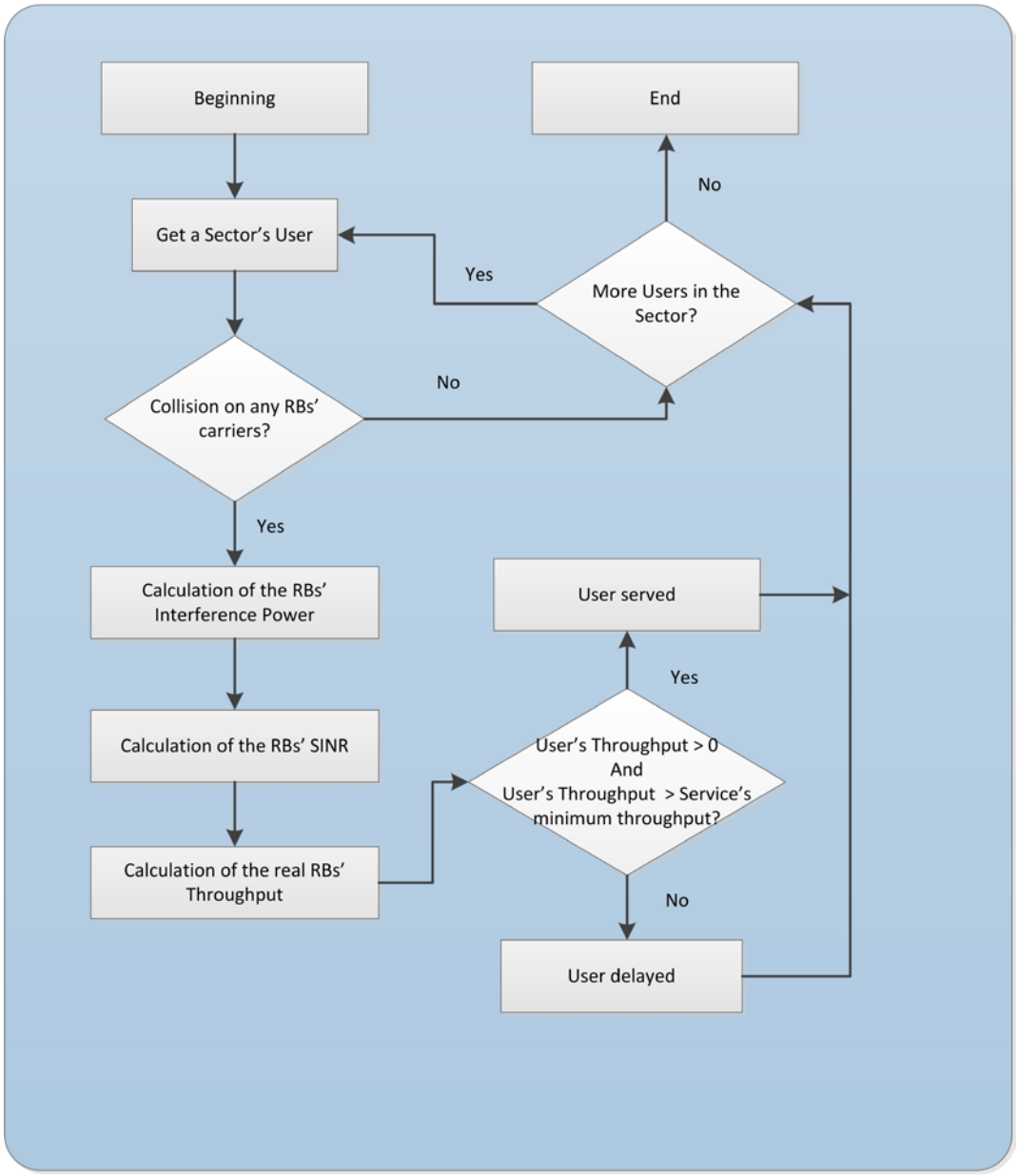

Figure 3.5. Interference calculation algorithm.

3.2 LTE Performance Simulator

In this section, the developed simulator as well as its fundamentals and implemented algorithms are presented.

3.2.1 Simulator Overview

This simulator aims to analyse the performance of LTE in DL, deployed over a dense urban UMTS cellular network. Several parts compose the developed simulator, the result being the work from

previous studies, namely the thesis in [Card06], [LaCo06], [Lope08], [Salv08], [SeCa04] and [Duar08] plus the modified modules developed in this thesis. Its main structure is presented in Figure 3.6, which highlights in red the modified modules in order to implement all the performance models described in Section 3.1. The simulator consists of three major modules:

- Users generation;
- Network deployment without load;
- LTE DL ICI analysis.

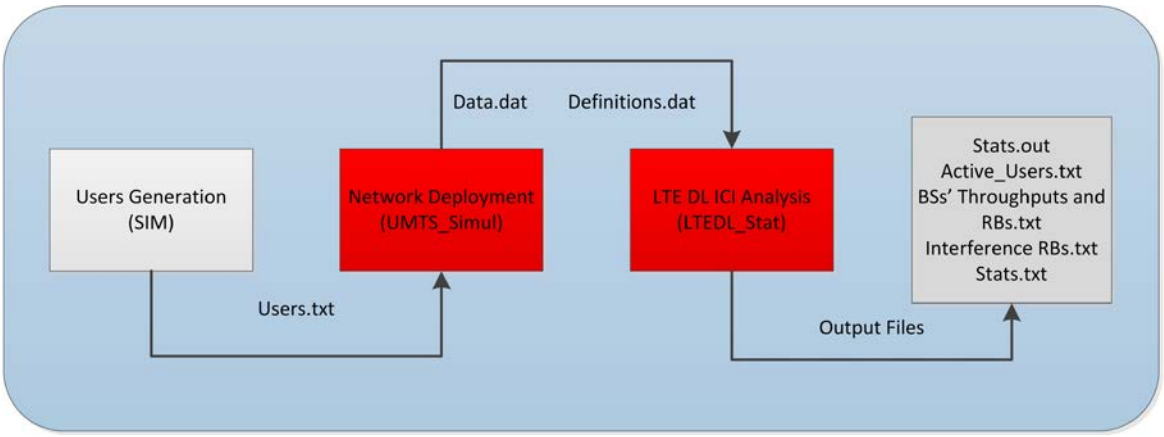

Figure 3.6. Modules that compose the simulator and the respective output files.

The users generation module is described in detail in [Lope08] and [Salv08], and creates a file with the information about the user and its location. Users are distributed randomly and services are also randomly distributed among users, according to a given service penetration percentage. The input data for the traffic distribution and the services penetration percentage, needed for users generation, as well as QoS priority number, are described in Section 4.1.

The network deployment module is described with detail in [LaCo06] and performs the task of placing the users from the output file created by the previous module in the network, distributing them along populated areas, after which the network is deployed. All users within the coverage area are the ones to be considered in the LTE DL module. This module was also subject to changes in this thesis, in the sense that it was improved through the Map Basic programming tool in order to configure the additional radio resources parameters, such as FRSs and respective cell data, as well as scheduling algorithms in the executable UMTS_Simul Map Info file that constitutes the Network Deployment module.

LTE DL ICI Analysis module is the one that implements the described algorithms in this thesis, being responsible for taking the information of users, BSs and radio configuration parameters, and reproduce on a snapshot basis the users access to the network, by requiring a given throughput from the respective serving BS to perform their DL service, and competing for the available RBs, which might not be enough for all the requested load. After the RBs distribution is complete, an ICI analysis takes place, where for every RB of each user, the real SINR is calculated in order to achieve the real throughput of each user. Then, output files are created with the users information about the served throughputs, SINR, distance from the BS, among others.

The functioning and instructions to perform simulation are described in Annex E, where the user's manual is presented in detail.

3.2.2 Simulator Algorithms / LTE DL ICI Analysis Implementation

The modules of LTE DL ICI were implemented to enable the analysis of the performance of LTE radio interface taking into account the ICI on the network. Using a snapshot approach, these two modules analyse the network capacity, through the sum of the instantaneous users throughputs, coverage through the average of the cells radius, and overall users served by the BS, through the QoS priority classes reduction when maximum capacity is not enough to provide the required services by users. Firstly, an analysis for all BSs is done, associating users to the closest one, and distributing the available RBs according to the wanted services and respective throughputs as well as according to the QCI when the required capacity exceeds the maximum capacity. Secondly, an analysis of ICI is performed, where, for all users, the BSs and respective sectors are obtained, whose interference power values are higher than noise at the receivers. Then, for the users of the signal provider BS, these interference powers are used to calculate their real SINR for each RB, which is used to map their RBs throughputs. Thirdly, the modules calculate appropriate statistics with the simulation results, such as average BS's capacity and cell radius, and average users' throughput. The workflow of the simulator is shown in Figure 3.7, where the algorithms functioning along the processes are identified.

There are many radio and strategy parameters that can be modified, as Figure E.4 shows, and were used in this thesis in order to tune settings for obtaining the LTE DL ICI simulation results as follows:

- Bandwidth
- Frequency band and operating frequency;
- MIMO configuration;
- FRS;
- Scheduling algorithm;
- DL transmission power;
- MT antenna gain;
- User and cable losses;
- Noise figure;
- Urban scenario characterisation for the propagation model;
- Services QoS priority;
- Services minimum and maximum data rate;
- Antennas' downtilt angle;
- ICI switch.

Other parameters, such as the number of users, their associated services and the services penetration values have to be chosen at the Users Generation module, creating users files to be loaded by the Network Deployment module.

Bandwidth, frequency band and MIMO configuration are the most important parameters for the LTE

performance evaluation. The bandwidth of the radio channel corresponds to the number of available RBs to distribute between users, and the data rates or capacity associated to each RB depends directly on the MIMO configuration, modulation and coding rate. The number of RBs associated to the bandwidth is presented in Table 2.1, and only LTE bandwidth configurations are used. The frequency band affects coverage and capacity through the pathloss of the received signals, as its variation between 800 and 2600 MHz frequency bands reaches 23 dB. On the one hand, this pathloss variation has a huge impact on both the cell radius that is diminished and the reduced SNR of users further from the cell centre, which makes it more difficult to use higher order modulation in order to obtain higher user data rates and higher cell capacity. On the other, it reduces the interference power reaching the neighbour BSs, the trade-off being one of the analysed results in Chapter 4.

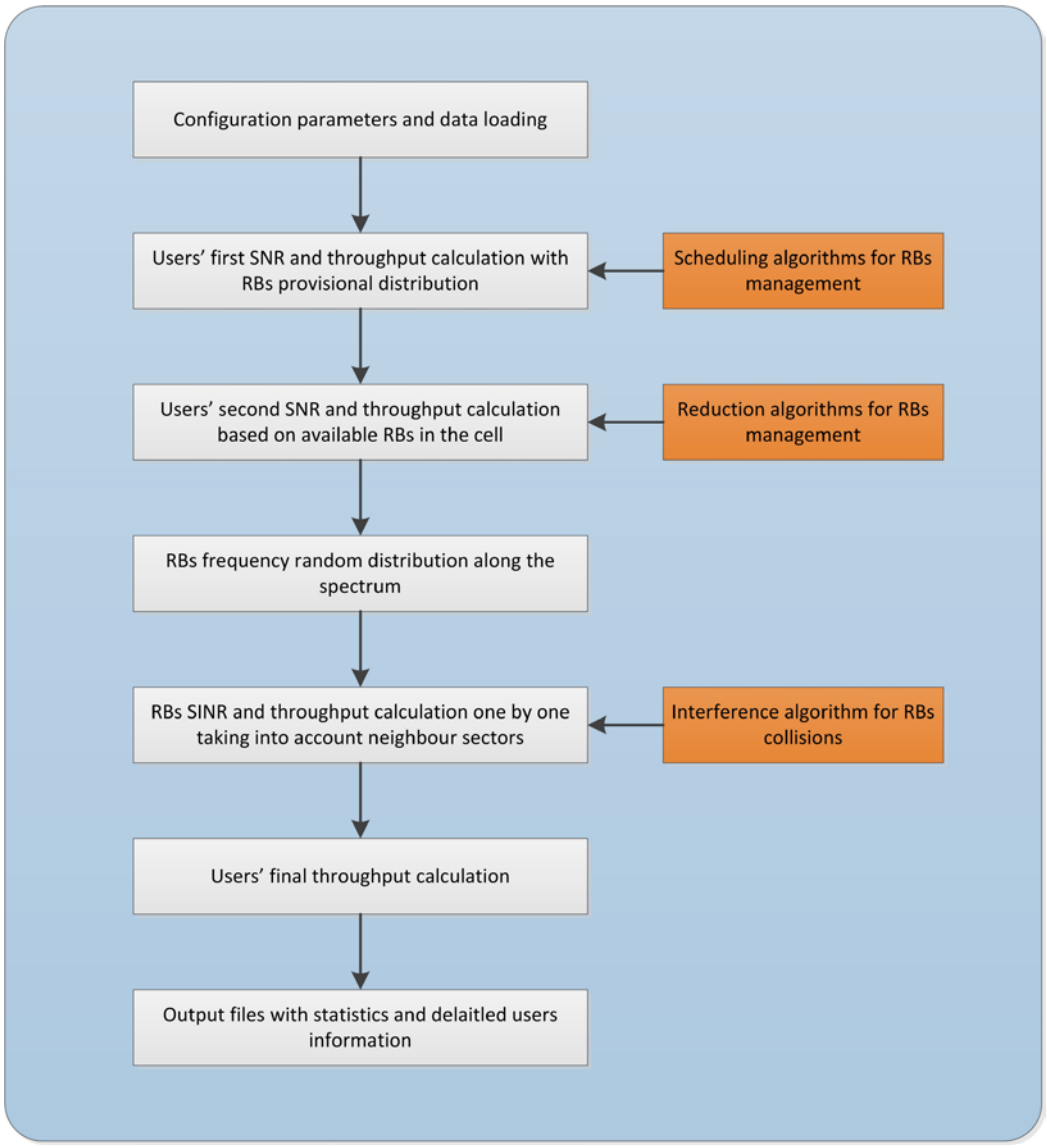

Figure 3.7. Simulator workflow.

A fixed percentage of 10% of the total RBs constitutes the dedicated RBs for Signalling and Controlling. In the throughput mapping, one OFDM symbol for DL and one SC-FDMA symbol per RB are discounted from the throughput, as they represent the reference signals, which constitutes an

overhead of 1/7 in the case of seven symbols per subcarrier. The expressions of throughput in order of the SINR were extracted from [Duar08], where SISO throughput was obtained from the available SIMO from 3GPP, in order to obtain the RB throughput for the MIMO configuration used in the simulation, the difference in the pathloss between SISO and SIMO being the diversity gain that SIMO has. The Relative MIMO Gain (RMG) is calculated by the RMG model developed in [KuCo07], and is shown in Annex G, according to the MIMO configuration and distance from each user to the BS. Although the RMG model was not developed for the conditions to be simulated in this work, it can be considered a good approximation, being detailed in [Duar08] and its implementation explained in [Bati08].

The FSR parameter allows the choice of the ICI avoidance schemes explained in Section 3.1, where for SFR and PFR the percentage of the radius that belongs to the cell centre and the raised power for the cell edge can be chosen. Again, for SFR and PRF, two areas of the cell are defined, centre and edge, for the distribution of the RBs along the cell, the unused cell edge RBs being available for the cell-centre. The cell radius considered here is the one obtained from simulation with reuse-1 FRS, which was chosen to be 200 m and obtained by simulations, which along with the suitable value of cell-edge radius divides the cell in such a way that approximately 1/3 of the users belong to the cell edge, regarding the same quantity of RBs is available to the part of the cell in SFR and PFR.

The reduction strategy allows the choice between the “throughput reduction”, where all users throughput is reduced by one RB, and “QoS Class reduction”, where for a specific service all users of that service are reduced one RB. The reduction strategies were based on [Duar08], and were improved to the tri-sectorisation of BSs, users of each sector being reduced only if the number of demanded RBs is higher than the available one (reuse-1 and reuse-3) or the number of demanded cell edge and/or cell centre RBs is higher than the available one (SFR and PFR). In this thesis, only the QoS Class reduction [Duar08] was used, being improved in the sense that the RBs reduction was changed to be reduce the users’ number of RBs by half instead of one, which avoid more starving users with less RBs compared with the draining users, as far as radio resources are concerned, the results having been proved by simulation.

Bearing in mind that for Reuse-1 and Reuse-3, RBs are freely assigned between users along the sector, but for SFR and PFR cell edge users are only allowed to use their cell edge RBs, while the cell centre users can use their dedicated cell centre RBs plus the remaining cell edge ones that were not occupied. The minimum and maximum services throughputs can be modified in the User Profile window, Figure E.5, and are respectively limited by the minimum data rates associated to the services and the maximum system throughput due to the bandwidth and MIMO configuration.

After the introduction of the users and BSs network data, the number of covered and uncovered users regarding the references services is calculated as well as the uncovered area of Lisbon. The following output files are created and are used in the LTE DL ICI analysis module:

- data.dat, which gathers the information of each BS such as their location on the network and respective covered users, distance, services requested, environment, among others.
- definitions.dat, which contains the radio interface and strategy parameters chosen in Figure

E.4, as well as the minimum and maximum services throughputs.

In the situation of overlapping BSs as far as coverage area is concerned, each user is connected to the closest BS. Although connecting users to BSs with more available RBs could be a better strategy regarding capacity, the network is not yet created, and being this simulation based upon a snapshot, approach, information about previous occupied resources is not available.

The next step is to calculate the throughput associated to the user distance from the BS and reference scenario and specific environment where the user is placed, taking into account the number of RBs being used and the SNR, which is calculated using the link budget and COST 231 Walfisch-Ikegami Model presented in Annex B and Annex C, respectively. Starting from one RB to the maximum number RBs of the available spectrum, the throughput is calculated until the requested throughput is achieved. For each configuration of SNR and number of RBs, three possible throughputs are calculated, each one corresponding to modulation schemes QPSK, 16QAM and 64QAM, the highest throughput being chosen. The requested throughput by each user is calculated randomly, and takes values between the minimum and maximum service throughput specified in the User Profile window, Figure E.5.

Concerning the calculation of the users served throughput, whether the situation is the initial RBs distribution, the reduction strategy or the ICI SINR readjustment, three cases can occur:

- the user is served with the requested throughput;
- the user is served with a throughput that is higher than the minimum service associated throughput, but lower than the required one, due to the maximum achieved capacity in the BS or due to the reduced SINR that limits higher data rates;
- the user is delayed (not served) because he would be served with a throughput lower than the minimum one of the requested service, due to the lack of available RBs, high user distance or high interference power from neighbour BSs.

The allocation of the used RBs by users is completely random, picking up any RB available along frequency, being the position in the frequency band marked so that it is possible to know between two different BSs if the RBs in usage are interference, i.e., are assigned to the same frequency. Then, interference power is calculated as the sum of the interfering signals reaching the affected MT with power no less that the receiver's noise power, for a given RB that the user was assigned. After the calculation of the interference power, RB's throughput is then calculated taking into account SINR rather than the SNR obtained previously for the estimation of the number of RBs, the users throughput resulting as the sum of the attributed RBs individual throughputs. As soon as capacity ICI adjustment is finished, output files are created, with all the information used in the results analysis.

3.2.3 Input and Output Parameters

To run the simulator, the following files need to be inserted in the simulator:

- Ant65deg.TAB, which is the BSs' antennas radiation pattern table;
- Kathrein Horizontal.txt and Kathrein Vertical.txt, which contain the horizontal and vertical

radiation pattern of the antennas;

- Dados_Lisboa.TAB, which contain information regarding the city of Lisbon and its districts;
- ZONAS_Lisboa.TAB, which contains the area characterisation;
- users.txt, which contains the position of users along the city of Lisbon, being the output of the Users generation SIM;
- Vodafone Network.TAB, which contains the location of the BSs in the network;
- Vodafone Centre Network.TAB and Vodafone Edge Network.TAB, which contains the location of the BSs of the centre and edge of the Lisbon's network, respectively.

The UMTS_Simul module then provides the following output to the LTE DL ICI analysis modules:

- definitions.dat, which contains the urban scenario characterisation, propagation information such as BSs and MTs transmission power, MIMO configuration, fading margins as well as losses along the propagation between the receiver and transmitter, operating frequency band and bandwidth, services characterisation and frequency reuse scheme identification.
- data.dat, which contains a list of all users and BSs location as well the distance between them. For each user, it is also indicated the user scenario and requested service.

After the simulation is complete, the LTE DL ICI analysis modules create many output files, one of which is used by UMTS_Simul to be present the results in the Map Info:

- stats.out, which include the results for the simulation, concerning the network analysis and services statistics, which is presented in the end of the simulation in MapInfo.

Other files are text files, which describe on each line the users and BSs that were active throughput the simulation:

- Stats.txt, which contains more statistics about the users and the radio interface and algorithm parameters;
- Active_Users.txt, which contains a list of the served users of the simulation along with the respective number of used RBs, interfered RBs, distance to serving BS, average RBs SNR and SINR, average signal and interference power at the user's MT, service performed and position along the cell, i.e., cell-centre or cell-edge;
- BSs throughputs and RBs.txt, which contain the list of the active BSs along with the number of used RBs, interfered RBs, served users and radius;

These output files contain information about the simulation, which was obtained either directly from the data kept in the inner data structures such as users distance and users average throughput and SNR. All other calculations, such as PDF and CDF and also standard deviation values, were done afterwards in Microsoft Excel.

3.3 Simulator Assessment and Model Evaluation

In this section, the simulator is assessed in order to guarantee the validity of the generated output and

to come up with the necessary number of simulations that ensure statistic relevance of the obtained results. To characterize the results, statistical parameters such as the average and standard deviation [Mora10] of several output data were analysed. The average value and standard deviation of the output results were calculated by (3.9) and (3.10), respectively.

$$\mu = \frac{\sum_{i=1}^{N_Z} Z_i}{N_Z} \tag{3.9}$$

where:

- Z_i is the value of sample i;
- N_Z is the number of samples.

$$\sigma = \sqrt{\frac{1}{N_Z}\sum_{i=1}^{N_Z}(Z_i - \bar{Z})^2} \tag{3.10}$$

where:

- $\bar{Z}$ is the average value of the population Z.

Bearing in mind that the simulator provides output that is generated on a multi-user basis located on an urban radio network with hundreds of BSs and thousands of users, it is expected that the minimal number of simulation to ensure statistical relevance does not take as high values as one can expect from isolated BS simulation. The parameters considered in this analysis are BSs throughput, users throughput, BSs radius of coverage and users' distance from the BS providing service, for the reference scenario with 7000 users in the city and a centre radius of 0.5 of the cell but vertical radiation pattern was not taken into account yet.

The number of simulations is based on the results presented in Figure 3.8, which shows that 5 simulations is a reasonable value to consider in order to obtain results, since an increase in the number of simulations would add no relevant impact on results, and also considering that a single simulation takes around half of an hour to complete. Also, one can see from Figure 3.9 that BSs and users throughput average value and standard deviation, which constitute the main performance indicators in this thesis, vary very little along the number of simulations. In addiction, a single simulation can take from 15 minutes to 2 hours, the latter being the most frequent one, because the simulator running time is highly growing with the number of users and BSs in the network, as well as its load.

To validate the implemented model, several tests and appropriate debugging were made regularly along its development, as well as a huge group of tests that were made in the end, to confirm that the simulator performs a good approach to the process of distributing the limited number of radio resources among users, with different radio channel condition and requesting different services, which are distributed along a very heterogeneous network of BSs in Lisbon. In Figure 3.10, one can see the that the higher the number of covered users in the network, the higher the number in served ones, as one could expect, until the saturation of radio resources is achieved, i.e., the increase of the number of users no longer means a higher number of served ones. In Figure 3.11, the variation of the cells radii is presented, which confirms the decrease of the radii with the increase of the frequency band used.

One could surely expect higher differences due to the pathloss, but one must bear in mind that the distance between neighbour BSs very often take lower values than the maximum radii that one could obtain from (3.7).

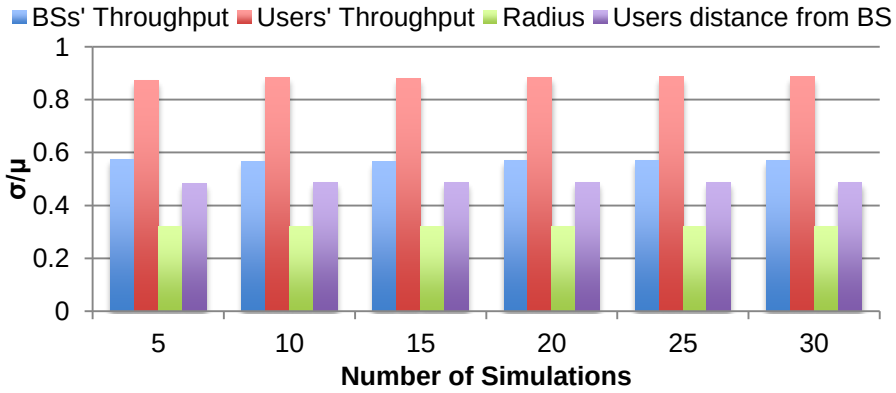

Figure 3.8. Standard deviation over average along the simulations.

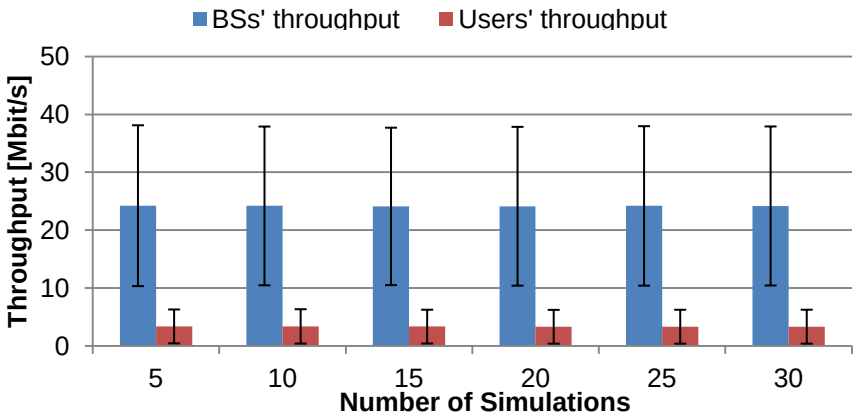

Figure 3.9. BSs and users throughput along the simulations.

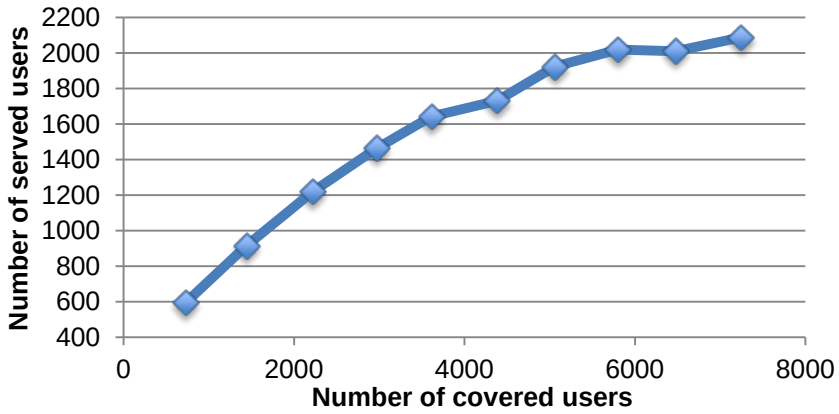

Figure 3.10. Number of served users along the number of covered users in the network.

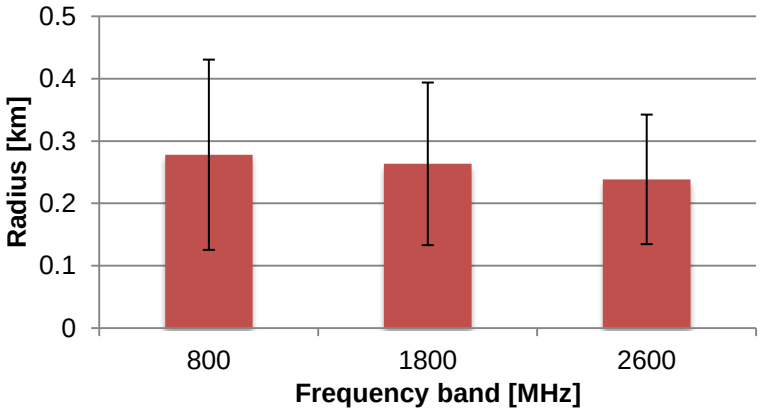

Figure 3.11. Average cell radius along the frequency band.

Chapter 4

Results Analysis

This chapter contains the scenarios descriptions used for low and high load simulations, and their results analysis. Firstly, a brief description of the parameters and environments used is done, and afterwards, low load scenarios results, which include measurements and simulations results, as well as the high load scenarios results, regarding the reference scenario performance and the network's behaviour towards the variation of the input data such as the radio parameters and number of users in the coverage area, are presented.

4.1 Scenarios Description

The reference scenario used in this thesis, over which the multi-user distribution is implemented, is the city of Lisbon, whose map is illustrated in Figure 4.1, divided into centre and outer zones because of its heterogeneity, as detailed in Annex I, where the density and distribution of users and BSs are characterised.

a) Map of Lisbon b) Centre of Lisbon

Figure 4.1. City of Lisbon.

Lisbon being mainly constituted by urban environment, the propagation model used to calculate pathloss is the COST 231 Walfisch-Ikegami one, and the respective parameters are shown in Table 4.1. Four different environments are considered by assigning additional pathloss to the user in order to characterize outdoors, vehicles and indoors with low and high losses, as one can see in Table 4.2. The MT considered for the reference scenario is a smartphone.

The reference scenario parameters regarding radio interface and algorithms are specified in Table 4.3. Transmission power was set to 46 dBm, the maximum reference power suggested by Vodafone for the 2600 MHz frequency band. The maximum bandwidth of 20 MHz was used, the exception being for the 800 MHz frequency band, where only 10 MHz are available. The downtilt angle of 8° was chosen, because it is the value that maximizes the whole networks throughput and serves users percentage, it is a highly sensitive parameter in the networks configuration, considering that the used antenna has a vertical half power beam width of 3.5°. Typical values of user and cable losses, noise figure, and slow fading margin from similar LTE simulations were used. A fixed percentage of 10% of the BSs' RBs is dedicated to signalling and controlling purposes, thus, not available for the users' services throughput. The antennas radiation pattern is illustrated in Figure H.1, where one can observe the horizontal pattern as well as the vertical one with downtilt angle of 0° and an offset of 90°.

Table 4.1. COST 231 Walfisch-Ikegami model parameters.

Propagation model parameter	Value
BS height (h_b) [m]	26
Buildings height (H_B) [m]	24
Streets width (w_s) [m]	24
Width between buildings' centres (w_B) [m]	48
Departing angle from the closest building (ϕ) [º]	90
MT height (h_m) [m]	1.80

Table 4.2. Additional user scenario loss and respective penetration.

User scenario	Additional loss [dB]		Users scenario penetration [%]
	Frequency band [MHz]		
	800	2600	
Pedestrian	0	0	30
Vehicular	3.65	11	15
Low indoor	3.65	11	20
High indoor	7.3	21	35

Regarding the reference scenario, two analyses were performed, trying to evaluate performance by the users' and operators' perspectives. One is done with few users in the network, which allows users to achieve the high peak data rates presented in Table 2.2 for the 2×2 MIMO case, which represents better the present situation at Lisbon, where the cells load is still very low, and compares best with the performed simulations. The second one is done with the network loaded, with much more users than the ones that can be served at an instant, where radio resources algorithms take place to share the bandwidth along the users and according to QoS criteria.

Services minimum and maximum throughputs are presented in Table 4.4 with the respective QoS priority and penetration. The throughputs could easily be assigned higher values, but due to the RBs number-based reduction algorithm functioning and the decrease of the SNR with the increase of the number of RBs due to noise power at the receiver, fairness in the resources distribution is more guaranteed with initial lower allocated throughputs, a fact that has been verified with simulations regarding different values for these throughputs. Users are specified in the city, as covered and served. That is related to the creation of users that are first placed around the area, 7000 for the reference scenario, from which the covered ones are selected to the input for the LTE simulator, and then only some of them will succeed in achieving resources and throughput.

Table 4.3. Configuration of the parameters used in the reference scenario.

Parameters	DL values
BS DL Transmission Power [dBm]	46
Frequency [MHz]	2640
MIMO Configuration	2×2
Bandwidth [MHz]	20
Modulation	QPSK, 16QAM, 64QAM
Maximum BS Antennas Gain [dBi]	18
Downtilt Angle [°]	8
User Losses [dB]	1
Cable Losses [dB]	3
Users Noise Figure [dB]	7
Slow Fading Margin [dB]	8.8
Frequency Reuse Scheme	Soft Frequency Reuse (0.7×radius and 0 dB cell border gain)
Scheduling Algorithm	Proportional Fair

Table 4.4. Smartphone services characterisation.

Smartphone MT Service	**QoS Priority**	**Penetration [%]**	**Minimum Throughput [Mbit/s]**	**Maximum Throughput [Mbit/s]**
Streaming	1	36	1.024	6
Chat	2	5.5	0.064	0.384
Web Browsing	3	25	1.024	20
FTP	4	9.5	1.024	21.5
Email	5	6	1.024	8
P2P	6	18	1.024	5

4.2 Low Load Scenarios Results Analysis

This section presents the measurements performed in outdoors environment in order to obtain results to compare with simulated ones, having been performed in Lisbon, mainly in the most important avenues. Data characterised by several parameters was collected, describing the radio channel condition and the obtainable throughput.

4.2.1 Measurements Scenarios

Measurements were made with equipment provided by Vodafone, such as the MT Huawei K5005 USB Stick shown in Figure 4.2, software and respective hardware key for the data register. Also a personal laptop was used to process and store the acquired data, as well as a car to perform the traced route along Lisbon. The equipment was placed around 1m above the floor level on a car sit, which was used to move along the desired places. The performed route is illustrated in Annex J, and was done in order to measure performance along the axial and urban environments, to explore some diversity between the urban structures, which varies from large avenues to narrow regular urban structures.

Figure 4.2. Vodafone LTE MT.

The average car speed was around 20 km/h and efforts have been made to move as slow as possible, due to the higher variations of radio channel condition imposed by the Doppler frequency shift caused by mobility and constantly moving position, changing rapidly the distance of the MT to the serving BS and the consequent handovers along sectors of the same cell and along different cells. This implies lower throughputs during the process, also because of being placed in the cell border and overlapping zone of the two neighbour cells associated to the handover process.

In addition, the used MT works with a 2×2 MIMO configuration, and is limited internally to a peak data rate of 100 Mbit/s. The majority of the LTE BSs is set to use the 2600MHz frequency band, which allows a bandwidth usage of 20MHz, but there are a few BSs using the 800MHz frequency band as one can see in Figure J.1, which only allows a bandwidth usage of 10MHz, i.e., half of the number of RBs compared to the other frequency band.

The measurement software was TEMS Investigation 11.1 [Asco12], which allows measuring and monitoring the radio channel condition of mobile networks, collecting the information and showing it on real time. TEMS Discovery was used afterwards for the graphic data workflow. During the capture of the radio signal, an enormous number of radio parameters are collected, the most relevant ones being chosen and analysed in this section, such as the throughput, number of RBs, radio channel condition parameters, and the MT speed.

The collected data from measurements was processed in order to eliminate erroneous information such as invalid or unachievable data rates or RBs usage, in order to keep the process of comparison between simulations and measurements results consistent.

In the simulations, radio parameters such as average user SNR and received signal power at the MT are considered for the whole used RBs, while in the measurements this information is collected by the RSs along the RBs, so that they are referenced as RS SNR and RS Received Power (RSRP). Also in the measurements, frequency carriers are identified by the E-UTRA Absolute Radio Frequency Channel Number (E-ARFCN) 2950 and 6300, corresponding to 2600 MHz and 800 MHz frequency band carriers.

As one can see from all the figures presented in Annex J, the long avenues of Lisbon mainly composed the route from the Downtown to Northern part of Lisbon, along with some neighbourhoods nearby, such as Estefânia, Arco do Cego, Campo Pequeno in the centre part of Lisbon, and Parque das Nações in the outer zone of Lisbon.

The results obtained from simulations were done with significant modifications regarding the reference scenario in order to approach the measurements environment, and therefore only 100 users performing FTP service were introduced in the network. The FRS used was Reuse-1 to avoid cell-position RBs distribution restraints, the maximum throughput associated to FTP service was set to 100 Mbit/s, and users intended throughput was set to this same value, the scheduling algorithm was set to Max-SNR to optimize throughput, the used pathloss model was the COST 231 Walfisch-Ikegami for LoS situation, because most of the route was axial along the larger avenues, and the vehicular margin was set to 11 dB for the 2600 MHz frequency band. Table 4.5 synthetizes the information of different parameters regarding the reference scenario presented in the next section.

Table 4.5. Low load scenarios parameters adjustment.

Parameter	DL value
Pathloss Model	COST 231 Walfisch-Ikegami LoS
Number of Users	100
Reference scenario margin for 2600 MHz [dB]	11 (vehicular)
Service	FTP with 100 Mbit/s maximum throughput
FSR	Reuse-1
Scheduling algorithm	Max-SNR

One must bear in mind the differences between the simulations and measurements environment: LTE's commercial network in Portugal is on only for a few months (since March 2012) and the number of subscribers is still very small, compared to GSM or UMTS, and so is the network load, which means that few users can be expected in each cell, improving the possibilities to achieve the highest data rates from the network, not only because of the majority of the RBs are available, but also because interference can be negligible. Also, there is a lower number of LTE active BSs at the moment than the network used in the simulations.

4.2.2 Low Load Scenarios Results Analysis

In this section, results obtained from data collected in the measurements, as well as in the simulations

tuned to approach the measurements environment, are analysed and compared, in order to characterize the key performance indicators for both situations. Additional results regarding the measurements can be seen in Annex J, where radio channel condition parameters, such as E-ARFCN, RSRP, RS SNR, CQI, number of RBs along with obtained throughput and MT speed is shown along the performed route.

Users throughput, illustrated in Figure 4.3, shows the obtained throughput from measurements and the global users throughput obtained by the group of covered users out of 100 FTP users placed in the city of Lisbon, in the case of simulations. One can observe that the throughputs are identical on average, with values around 45 Mbit/s, as well as the respective variation, which was already expected as the throughput ranges from low to high values, depending on the radio channel, mainly conditioned to the users distance from the serving BS and handover events. As in this scenario the lack of RBs was frequently not an issue, as shown below in Figure 4.6 and Figure 4.7.

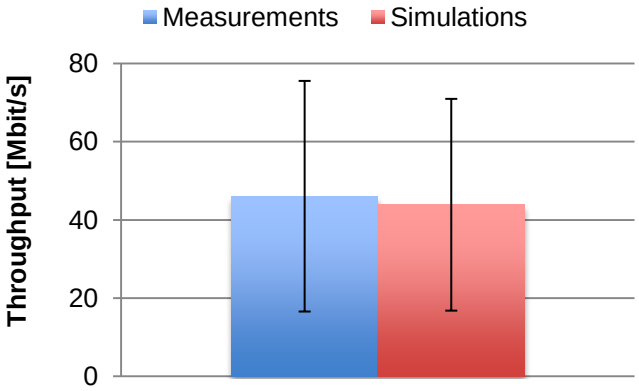

Figure 4.3. Users' throughput obtained in measurements and simulations.

In Figure 4.4, one can observe the results of the RSRP in the MT, whose average values differences between measurements and simulations are around 10 dB; the simulation scenario shows a higher RSRP, which can be explained by the use of the maximum reference transmission power at the BSs' antennas, 46 dBm, although the Vodafone BSs transmission power is unknown and probably variable between different BSs and sectors. RSRP values also vary significantly as one could expect, representing the varying position along the cell performed by the route in the case of the measurements, and by the different distance of users from the serving BSs due to their randomly attributed position. Also, there is probably a minority of the route performed in the measurements that placed the MT in NLoS situations, which adds additional pathloss, reducing average received power, which was not taken into account in these low load scenarios simulations.

Regarding RS SNR, illustrated in Figure 4.5, one can observe a higher SNR in the simulations scenario than in the measurements one, presenting also higher variations in this parameter; the difference between the average values reaches almost 5 dB, but both have high values in order to achieve high data rates. Again, a high BSs' transmission power and sometimes-lower pathloss can explain this higher value of SNR in the simulations scenario.

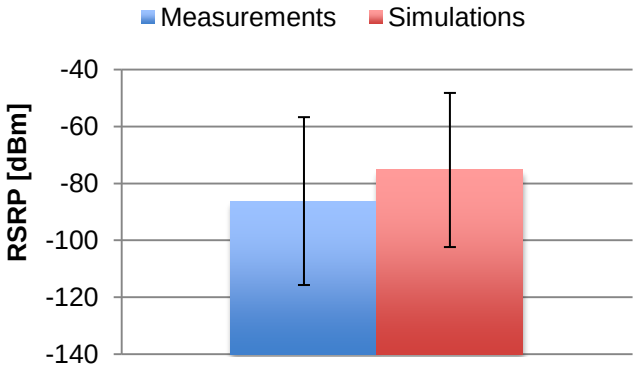

Figure 4.4. Received Signal Power obtained in measurements and simulations.

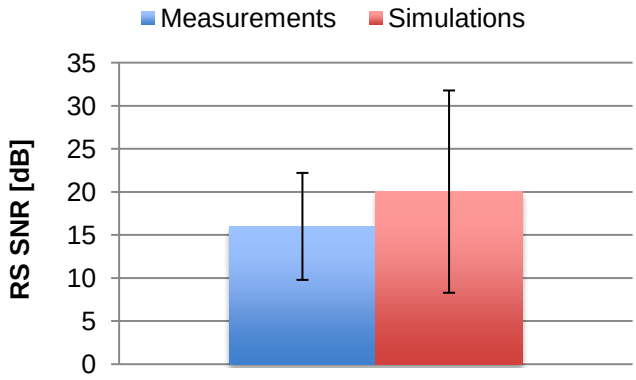

Figure 4.5. RS SNR obtained in measurements and simulations.

As one could expect from a recently implemented telecommunication system and low loaded network, the number of used RBs per user shown in Figure 4.6 is close to the maximum value of 100, the mean being around 80, which confirms the fact that users had the chance to take advantage of almost the whole 20 MHz bandwidth. In Figure 4.7, one can see the distribution of the number of used RBs per user in the measurements and simulations: for the former, around 15% of the time 50 RBs were used, and 70% of the time nearly 100 RBs were used in the radio link, while for the latter one can see that 90% of the users used 90 RBs, the maximum available, since 10% of the total number of RBs is dedicated to signalling and controlling, thus, not being available for users' throughput purposes.

Considering the correlation between throughput and RSRP illustrated in Figure 4.8, with an average relative deviation of 54% from the simulations to the measurements, one can see an increasing trend of the throughput along the RSRP as one could expect, because for the same level of noise power, the SNR increases with the RSRP and so does the obtained throughput, being noticeable the higher increase by the simulations curve than the measurements one. One can also see that there is a gap around 20 dB in the RSRP between the beginning of an achievable throughput, which can be explained by the dispersive RBs allocation in the measurement scenario and the exclusive 45 and 90 RBs allocation in the simulations.

In fact, the difference is the noise power interval between a single RB utilisation and 90 RBs, it being around 20 dB, therefore, for the same minimum SNR required for data transmission, with lower noise

power, the minimum signal power is also lower.

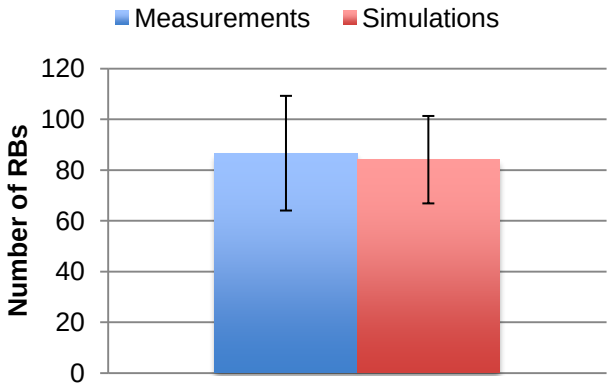

Figure 4.6. Number of RBs per user obtained in measurements and simulations.

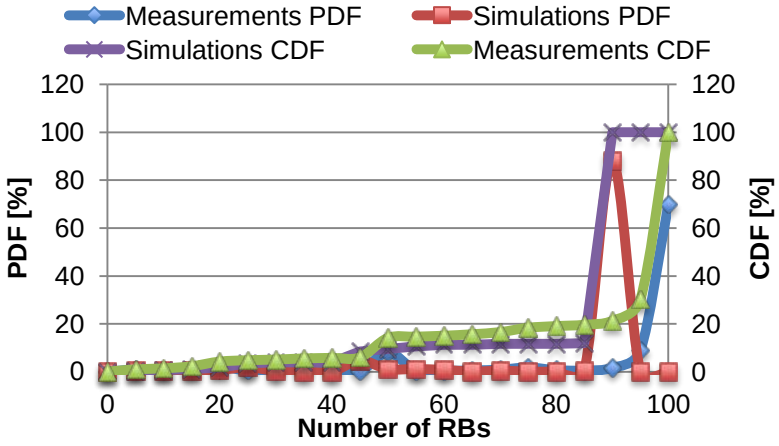

Figure 4.7. PDF and CDF of the number of RBs obtained for measurements and simulations.

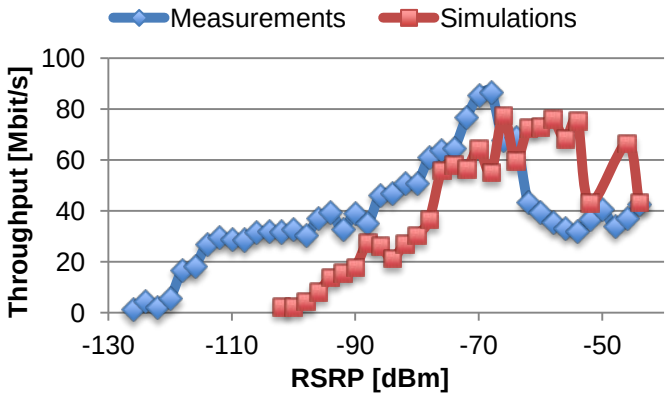

Figure 4.8. Throughput along the RSRP obtained in measurements and simulations.

Also, from -70 dBm to around -50 dBm, there is clearly a different behaviour in the measurements throughput; from Avenida da Liberdade, to Campo Pequeno, the widest streets zone routed, RBs usage was between 40 and 60 RBs during most of the time, as one can observe in Figure J.7, which limited the maximum throughput achieved at -70 dBm RSRP to around half of it, approximately from 80 Mbit/s to 40 Mbit/s. In fact, in a part of this route, the 800 MHz frequency band was used, as illustrated in Figure J.1, so that only 50 RBs were available, which obviously limits the maximum

achievable throughput. Regarding simulations throughput around -50 dBm, one can explain this fact also by the users that only had access to 45 RBs shown in Figure 4.7, probably because there were two users in the respective sectors and the 90 RBs were shared by them, resulting in a 45 RBs usage.

In Figure 4.9, one can observe not only a much higher correlation between the throughput and the RS SNR, but also a higher proximity between measurements and simulations, with an average relative deviation of 30% from the simulations to the measurements. As one could expect, the higher the SNR, the higher the obtained throughputs are in general. One can see that there are very small throughputs for the interval [-10, -2] dB in the measurements that are not present in the simulations, which can be explained as the signalling and controlling information performed between the MT and serving BS during the process of handover and in situations of connection loss. In the end of the graph, there are some higher down peaks of throughput, which again can be explained by the usage of a lower number of RBs.

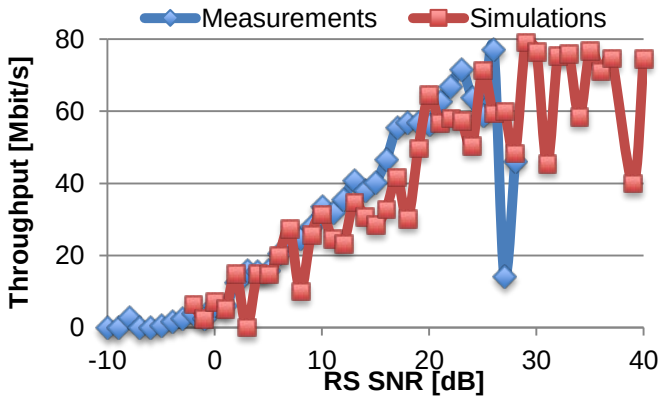

Figure 4.9. Throughput along RS SNR obtained for measurements and simulations.

4.3 High Load Scenarios Results Analysis

In this section, performance of the reference scenario is accessed and presented, as well as the influence of several radio and scheduling input parameters in the simulation, which are changed one by one in order to characterize the networks behaviour along them. BSs and users output parameters such as throughput, SNR and SINR and signal and interference power are used to characterize the obtained results.

4.3.1 Reference Scenario

One can group the network performance analysis by BSs and users. To start with, BSs throughput for the centre and edge of Lisbon is presented in Figure 4.10 and Figure 4.11. In the former, one can observe that the average BSs throughput takes very low values compared to the peak data rates, bearing in mind that each BS is tri-sectorised. In fact, only 10% of the BSs have higher throughputs

than 45 Mbit/s and 40 Mbit/s in the centre and edge of Lisbon, respectively. Also, one can observe that there is a trend for BSs in the centre of Lisbon to have higher throughputs than the ones in the edge, approximately almost 25% more on average. Comparing Figure 4.11-a) and Figure 4.11-b), it is noticeable that the PDF in the former is increasing until 20 Mbit/s and decreasing after that, while in the latter it is almost only decreasing with the throughput, and that the centre of Lisbon presents a higher number of BSs with higher throughputs.

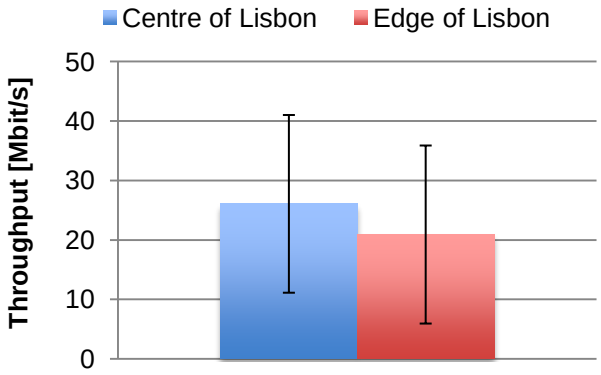

Figure 4.10. BSs' throughput.

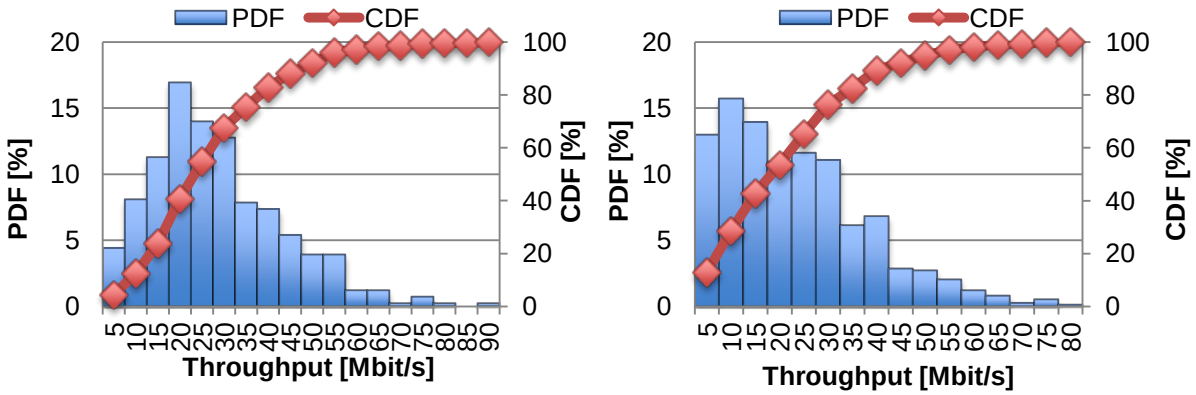

a) Centre of Lisbon

b) Edge of Lisbon

Figure 4.11. BSs' throughput PDF and CDF of the centre and edge of Lisbon.

Regarding the number of users per BS, the simulations results presented in Figure 4.12-a) suggest that it takes higher values on average in the centre of Lisbon compared to the outer zone, which suggests higher load in that part of the city in the situation of identical users throughput as illustrated below in Figure 4.14, where not only the users density is higher than the edge zone, but also the BSs density is. Considering the number of used RBs per BS illustrated in Figure 4.12-b), one can see that there is a trend for BSs from the centre of Lisbon to allocate more RBs than the edge. Even because of the high number of BSs in the network, on both analyses there is clearly a great variation of values compared to the difference between the centre and edge of Lisbon average ones.

Focusing on the cell radius illustrated in Figure 4.13, one can see that there is little variance between the centre and edge of Lisbon, taking into account that this parameter is obtained as the distance of the furthest user away from the serving BS, which turns out to be a given fact, since it is determined

not only by the link budget but also by the distance between neighbour cells, and thus the overlapping area between them. Nevertheless, one could expect the average cell radius from the outer zone to be higher, since the separation distance between BSs is higher in this zone.

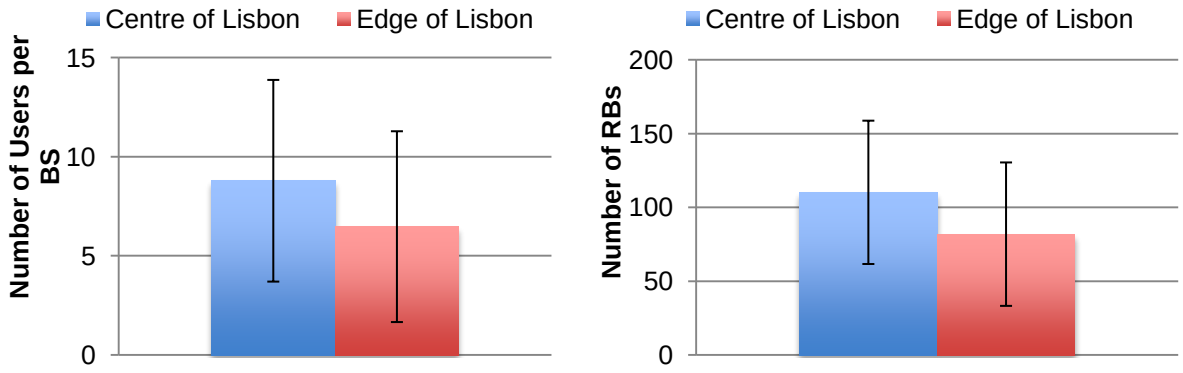

a) Number of users per BS

b) Number of used RBs per BS

Figure 4.12. BSs load regarding users and used RBs per BS.

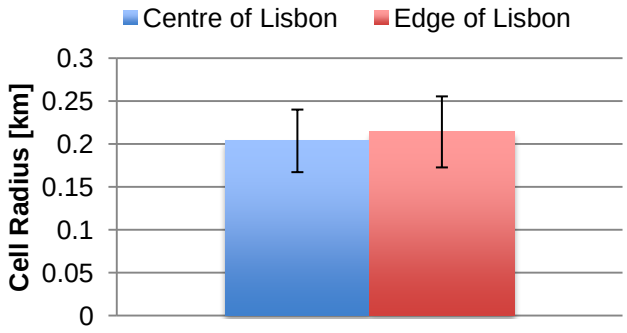

Figure 4.13. Cell radius in the centre and edge of Lisbon.

Considering the users performance indicators, one can see that in Figure 4.14 it is suggested that the users throughput varies little on average between the inner and outer zone of the city, while there is a stronger trend for users nearer the serving cell to achieve higher data rates compared to the ones further from it; nevertheless, the variation between users is huge considering the average values, suggesting the throughputs are highly variable, which is expectable from the randomly requested throughput along the respective services throughputs. Figure 4.15 shows that approximately only 15% of the served users experience throughputs higher than 5 Mbit/s, the most experienced throughput being 2 Mbit/s, and that the throughputs experienced were indeed very similar between the two regions of Lisbon.

From Figure 4.16-a), one can see that on average the users in the network use the same number of RBs wherever their service is requested. It is also noticeable large variations when allocating these resources, as one could expect considering the highly variable throughputs and radio condition shown above, due to different services required and distances to serving and interfering BSs.

In Figure 4.16-b), one can see that there is a trend for users in the edge of Lisbon to be slightly further away from the serving BS than the ones in the centre, which is easily explained by the lower BSs

density in that zone, as one can see in Annex I, so that higher-distance-from-serving-BS users are expected.

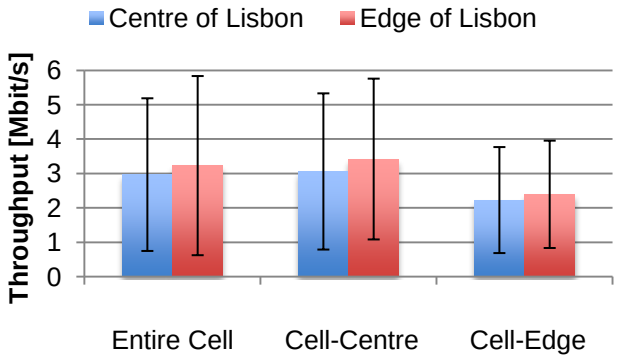

Figure 4.14. Users throughput throughout the cell.

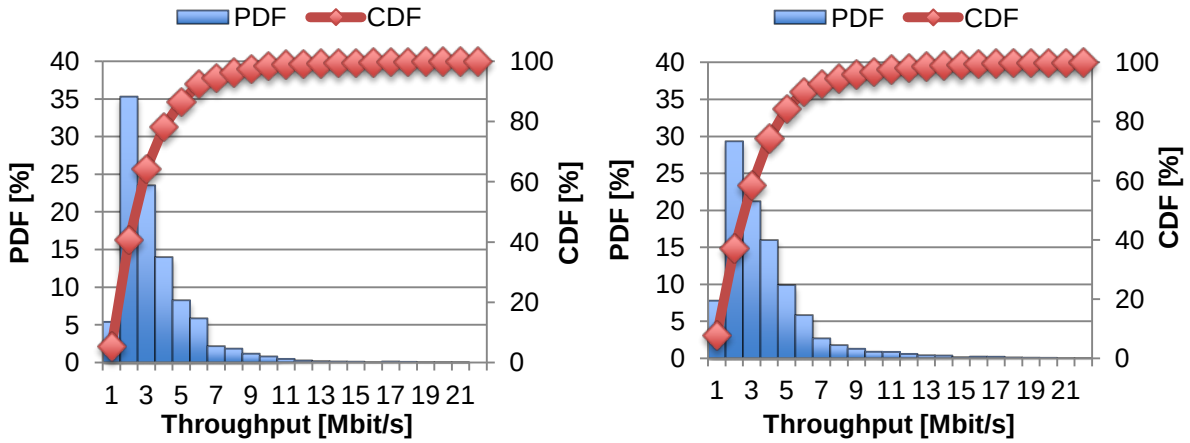

a) Centre of Lisbon b) Edge of Lisbon

Figure 4.15. Users throughput PDF and CDF of the centre and edge of Lisbon.

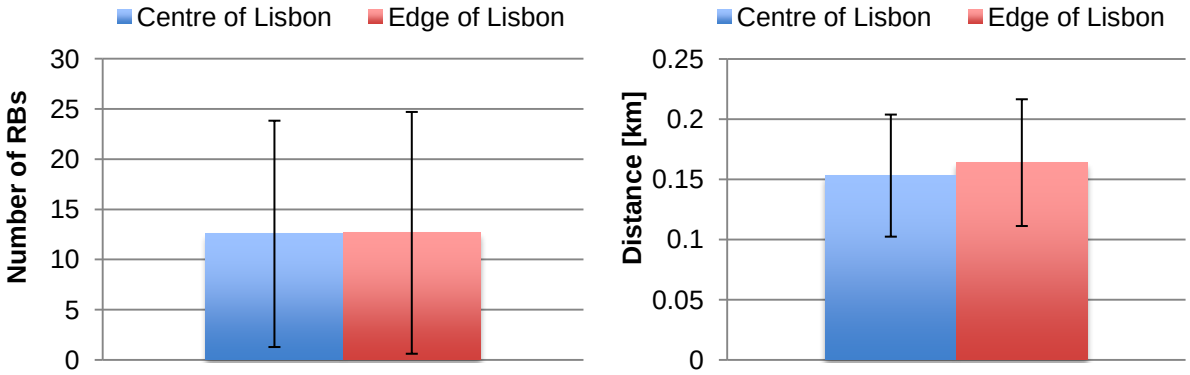

a) Number of used RBs per user b) Users' distance from serving BS

Figure 4.16. Number of used RBs per user and users distance form serving BS.

One can see from Figure 4.17 that SNR and SINR is highly variable for the users displaced throughout the network, which is reasonable considering the fact that the position of the users takes a random value according to higher or lower population statistics regarding the city districts, thus users closer

and further from the serving BS as well as from the interfering ones can be expected. One can also observe a trend of users in the edge of Lisbon to take higher SNR and SINR values than the ones in the centre of the city, the difference between SNR and SINR being slightly bigger for the users belonging to the centre of Lisbon. This fact can be explained as the higher density of BSs in the centre, which generates higher overlapping coverage areas and consequently more interference power at the MT.

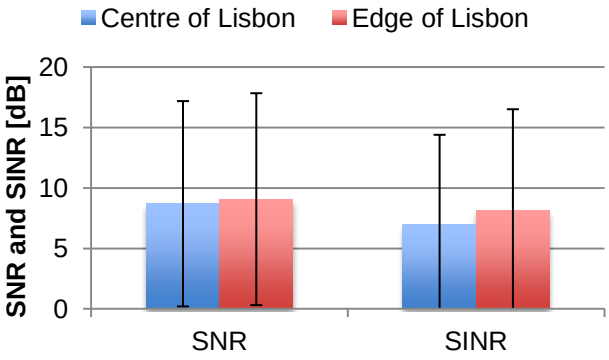

Figure 4.17. Users' SNR and SINR.

Comparing the results from Figure 4.18-a) and Figure 4.18-b), one can see the penetration of users with the respective SNR and SINR by the PDF and observe the higher degradation of the radio channel condition in the centre of Lisbon compared to the edge, as the SNR and SINR CDF curves are slightly further away from each other. Even neglecting the interference and focusing only on the SNR, one can observe that the majority of the users are the ones with lower SNR and that the number of users is decreasing along it.

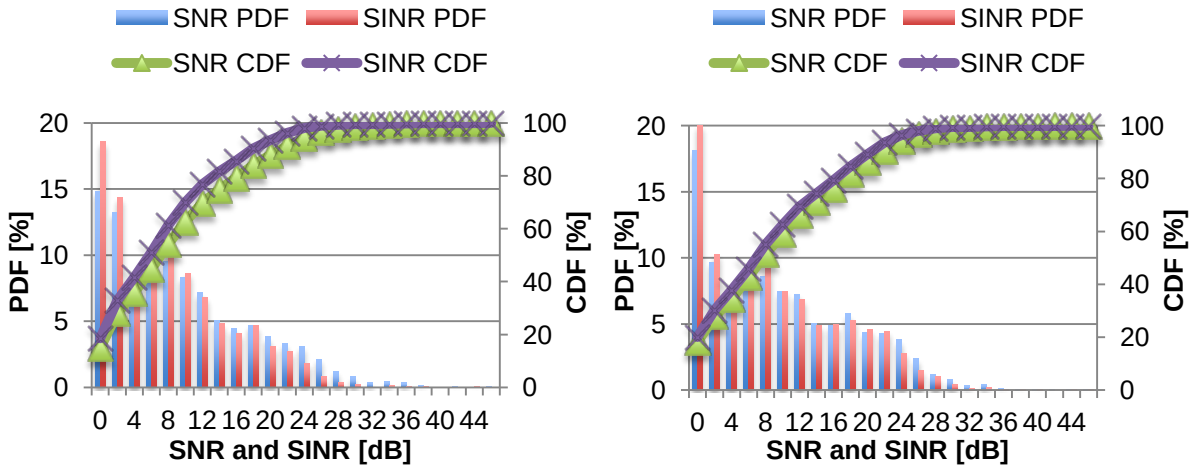

a) Centre of Lisbon

b) Edge of Lisbon

Figure 4.18. Users' SNR and SINR PDF and CDF in the centre and edge of Lisbon.

From the results presented in Figure 4.19, one can see that the ratio of served users over covered ones decreases in the edge of Lisbon compared to the centre from 29% to 23%. Also, one can see that globally, around 6500 out of 7000 users are covered, but only around 1600 were served with the

minimum throughputs that guarantee the required services properly.

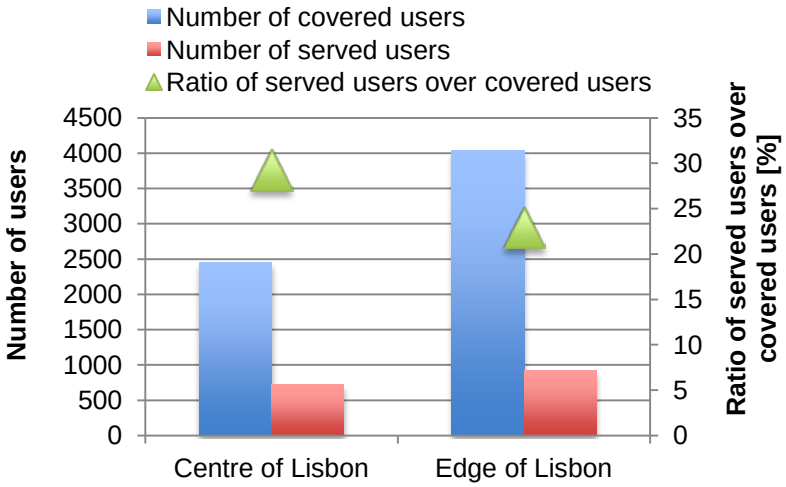

Figure 4.19. Number of served and covered users and its ratio for the centre and edge of Lisbon.

Still regarding the penetration of served users, in Figure 4.20 one can see the served users by service, where services such as streaming, chat, web browsing and P2P have a higher gap between users from the centre and edge, while other services such as FTP and email present a minor difference between users of the two areas.

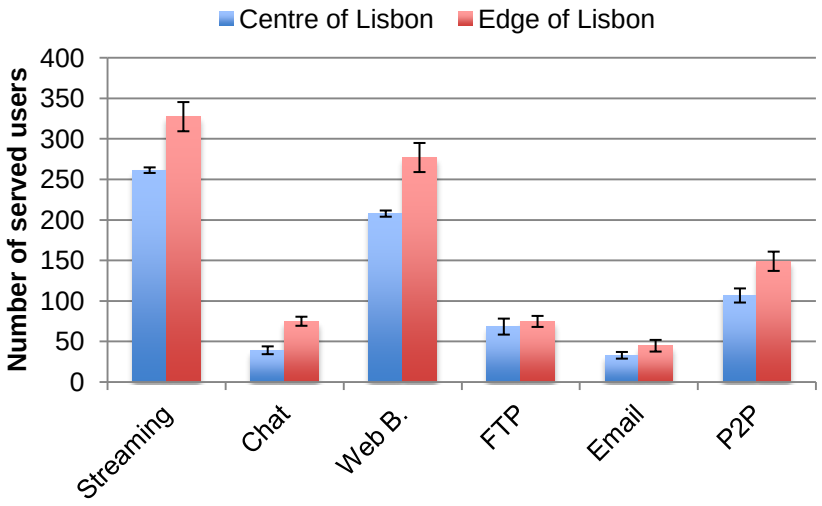

Figure 4.20.Number of served users per service.

Regarding the services provided to users and the associated QoS classes, one can observe the behaviour of the reduction algorithms in Figure 4.21; there are some services such as streaming that have a similar penetration, while there are services with high QoS priority index that have higher offered penetration such as chat and web browsing, and services with lower QoS priority index with lower penetration such as FTP, Email and P2P; this is expected, since this criteria is applied when the number of required RBs exceeds the available one and since reduction starts by the services with lower priority.

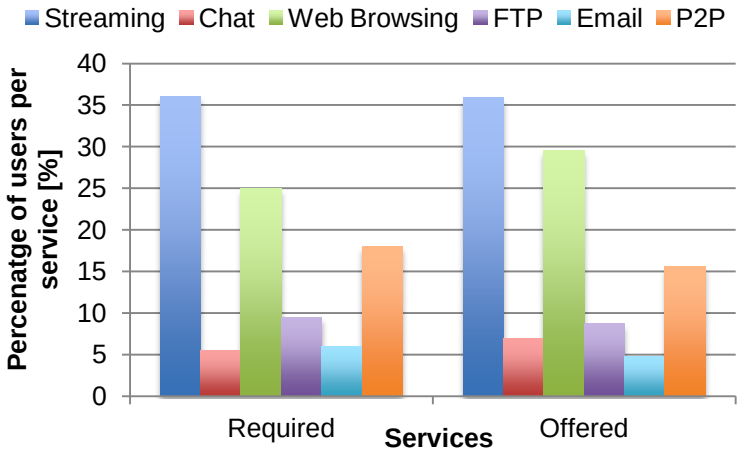

Figure 4.21. Services' penetration required and offered in the network.

4.3.2 Bandwidth

In terms of available bandwidth, 10 and 20 MHz bandwidths, corresponding to 50 RBs and 100 RBs respectively, were the two tested configurations, being the maximum available bandwidths for the 800 and 2600 MHz frequency bands, respectively.

One has to take into account that the reduction to half of the available bandwidth compared to the reference scenario only has impact on the sectors using more than 50 RBs, as one could expect, the throughput being influenced by the number of RBs as shown in (3.2). Regarding BSs throughput, one can observe in Figure 4.22-a) that there is a trend for the throughput to be higher for the 20 MHz bandwidth situation compared to the 10 MHz bandwidth situation, the centre of Lisbon presenting also higher throughputs compared to the edge. Also, one can see that there are greater variations of throughputs for the 20 MHz bandwidth case. Focusing on the number of users that are served by each BS illustrated in Figure 4.22-b), one can see that there is a trend of increase in the number of served users along the bandwidth, although on average only one additional user is served per BS with the double number of available RBs, the centre of Lisbon presenting again a higher density of users compared to the edge.

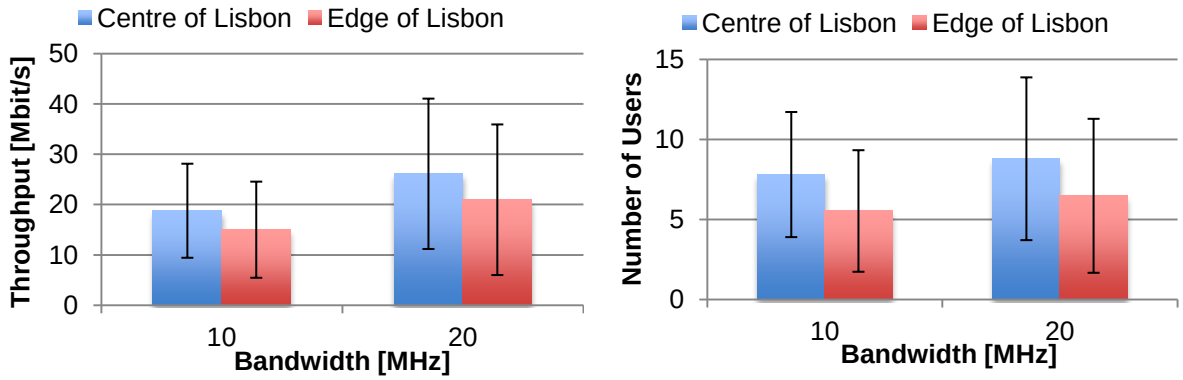

a) BS throughput b) Number of served users per BS

Figure 4.22. BSs throughput and served users for 10 and 20 MHz bandwidth.

Regarding the number of used RBs, in Figure 4.23 there seems to be a trend of almost doubling the number of used RBs with an increase in the usage of around 70%, which is expected as long as there is enough RBs starvation for the network to use all the available resources. Again, the centre of Lisbon tends to present a higher load in the resources usage compared to the edge.

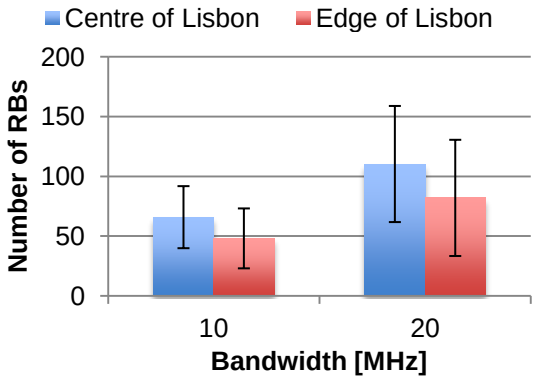

Figure 4.23.Number of used RBs per BS for 10 and 20 MHz bandwidth.

Regarding users key performance indicators, one can see in Figure 4.24 that there is a trend for users to have higher throughputs with an increase around 0.5 Mbit/s on average when going from 10 to 20 MHz bandwidth cases. Cell-centre users experience higher throughputs than cell-edge ones, as expected, and the variation of the users throughputs is very big, as one can see from the respective standard deviations, reflecting the different services nature and respective wanted throughput. Also one can see that there is a trend for users throughputs to be bigger on the edge of Lisbon than in the centre.

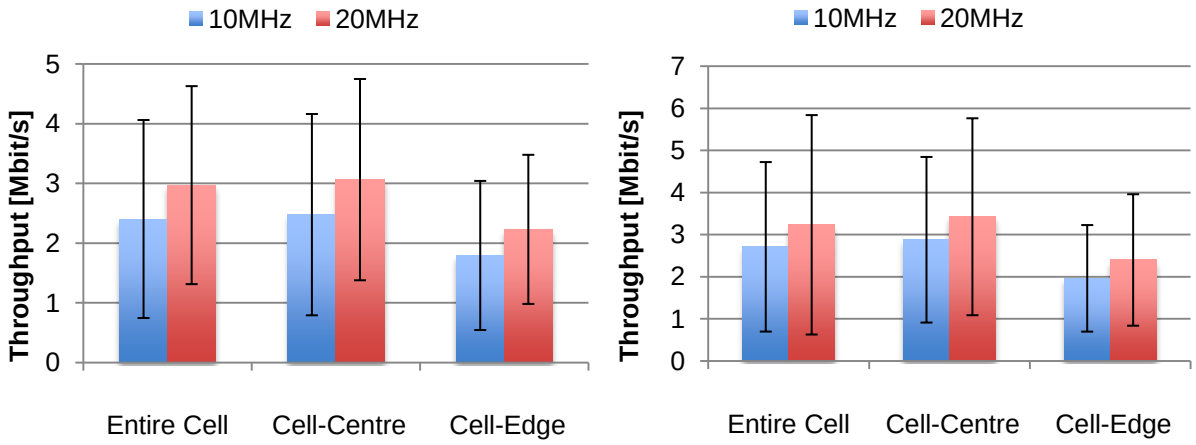

a) Centre of Lisbon

b) Edge of Lisbon

Figure 4.24. Users throughput along the cell for 10 and 20 MHz in the centre and edge of Lisbon.

Considering the number of served users by respective service in Figure 4.25, one can see that the distribution of users along the services is approximate for the centre and edge of Lisbon, being noticeable the higher number of served users in the edge of the city compared to the centre. Comparing the served users for 10 and 20 MHz bandwidth situations, there is a trend to be a higher number of users in the 20 MHz case, although the increase is indeed very small compared to the

theoretical double number of users for the same throughputs, that twice the RBs would allow.

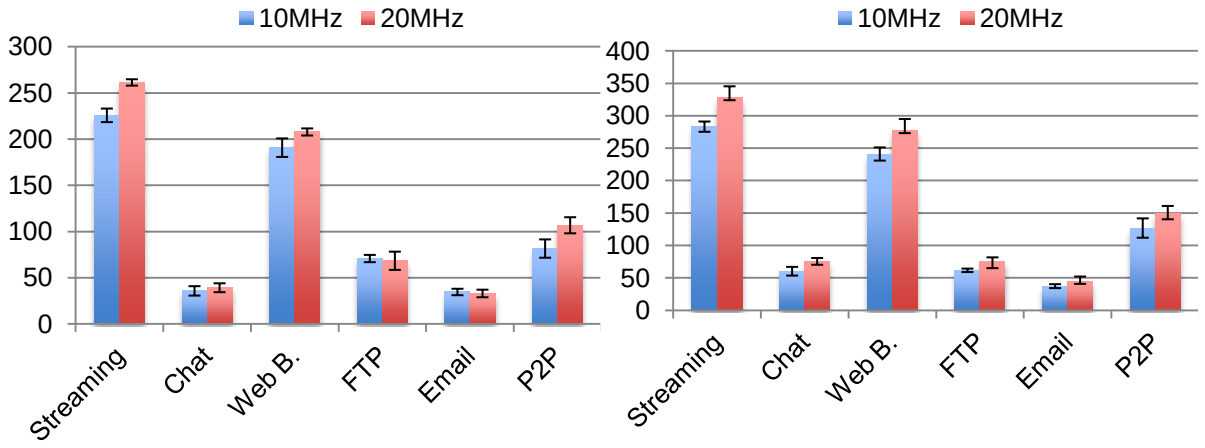

a) Centre of Lisbon

b) Edge of Lisbon

Figure 4.25. Number of served users by service for 10 and 20MHz bandwidth in the centre and edge of Lisbon.

4.3.3 Frequency Band

Regarding simulations along the frequency band, these were performed for 10MHz bandwidth only, since it is the maximum available bandwidth in the 800 MHz band.

Considering the results presented in Figure 4.26-a), one can see that BSs throughputs present a different behaviour along the frequency band in the centre and edge of Lisbon. Regarding the centre, one can see that there is a trend to achieve higher throughputs with an increase near 50% in the 2600 MHz band compared to the 800 MHz one, although variations are bigger than the difference between the average values. This fact can be justified by the decrease of the pathloss between users and serving BSs, and thus, between users and interfering BSs, creating a much bigger overlapping coverage area between neighbour cells, which seems to be having a more negative effect in the overall BSs throughput due to interference. Regarding the edge of Lisbon, throughput seems to have no effect whatsoever by the frequency band, although a higher variation can be seen in the 2600 MHz band.

Regarding the number of served users per BS presented in Figure 4.26-b), one can see that results appear to take somehow a similar behaviour as the previous ones, the number of users in the edge of Lisbon being around 6 for 800 and 2600 MHz presenting higher variations for the latter. Higher differences are in the number of served users for the two frequency bands in the centre of Lisbon, the 2600 MHz band presenting an average of 8 users per BS and the 800 MHz band around 6 users, the former presenting again higher variations.

Considering the number of used RBs per BS without null throughput illustrated on Figure 4.27-a), one can see there is a huge difference along the frequency band, with centre and edge of Lisbon in the 800 MHz band presenting a number of RBs three and two times lower than the 2600 MHz band,

respectively.

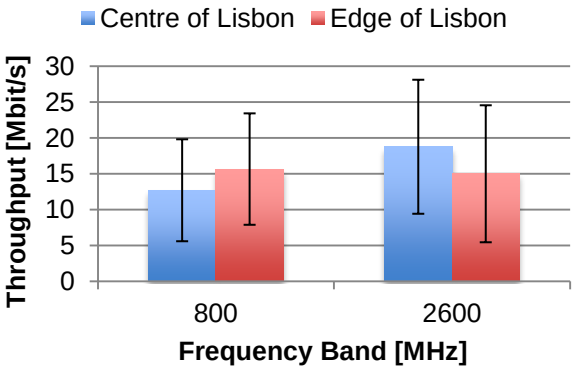

a) BS throughput

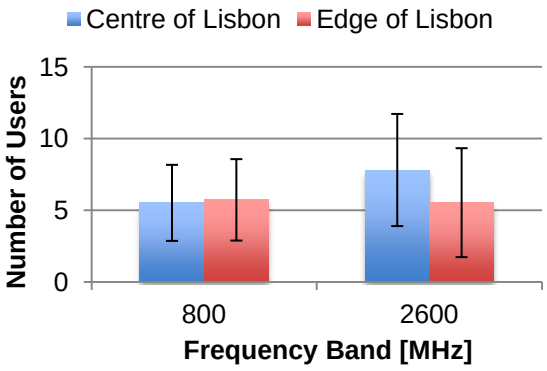

b) Number of served users per BS

Figure 4.26. BSs throughput and number of served users per BS for 800 and 2600MHz bands.

This difference can be explained because this number of RBs does not include the allocated RBs that had their SINR lowered below -2 dB, the minimum value to obtain throughput, i.e., the number of destructively affected RBs by interference in the 800 MHz is much higher than in the 2600 MHz for the same BSs distribution and transmission power, as one could expect.

Regarding cell radius illustrated in Figure 4.27-b), which again is given by the served user further away from the serving BS, one can see that they are a little bit higher for the 800 MHz band, but essentially take larger variations when compared to the 2600 MHz band case. Larger cell radius were already expected, but the increase is limited by the inner distribution of the BSs along the network and by the distance between them.

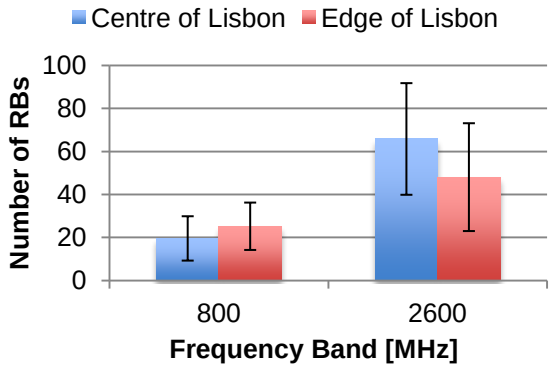

a) Number of RBs per BS

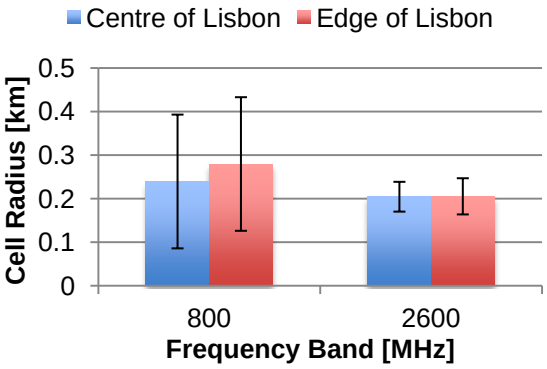

b) Cell radius

Figure 4.27. Number of used RBs per BS and cell radius for the 800 and 2600 MHz frequency bands.

Taking into account the users performance parameters for the frequency band variation, one can see in Figure 4.28-a) that in the centre of Lisbon there are little differences between the average throughputs and all but one are above 2 Mbit/s, but the variations of the throughputs are enormous compared to the average values, representing again the heterogeneity of the users in terms of services and required throughputs. The same behaviour can be observed in the edge of Lisbon in Figure 4.28-b), the throughputs taking higher values on average and the differences in terms of

throughput being a little bit higher between cell-centre and cell-edge. Comparing both graphics, one can see there is almost no difference in the users throughput along the frequency bands, besides the radio interface differences presented below.

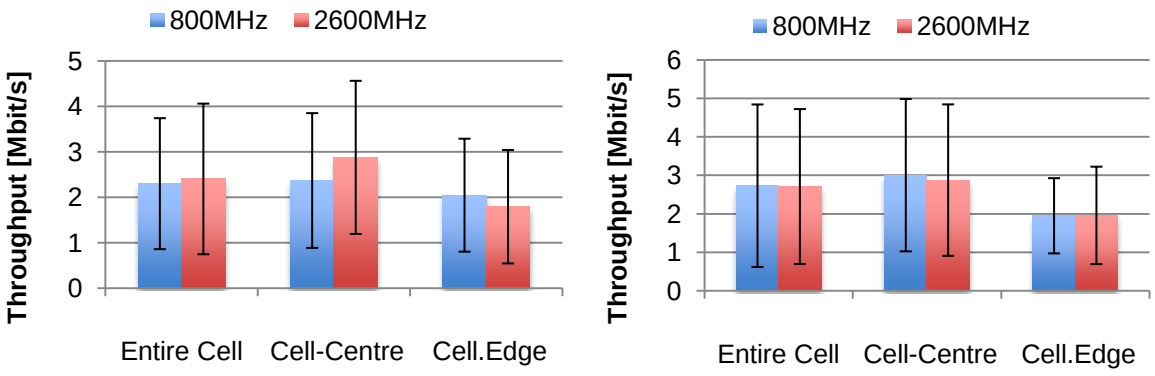

a) Centre of Lisbon b) Edge of Lisbon

Figure 4.28. Users throughput along the cell for 800 and 2600 MHz bands in the centre and edge of Lisbon.

Considering the results of the number of used RBs per user in Figure 4.29-a), one can observe an identical pattern as in Figure 4.27-a), although the differences between the frequency bands are smoother: the number of used RBs is lower for 800 than for 2600 MHz due to interference, which is more critical in the centre of Lisbon, where the overlapping coverage cell areas are bigger. One can see from Figure 4.29-b) the number of RBs per user that were not due to the reduced values of SINR caused by interference, and one can see that although average values are lower than half of a RB, variations are enormous, and both parameters are bigger for the 800 MHz band rather than for 2600 MHz band.

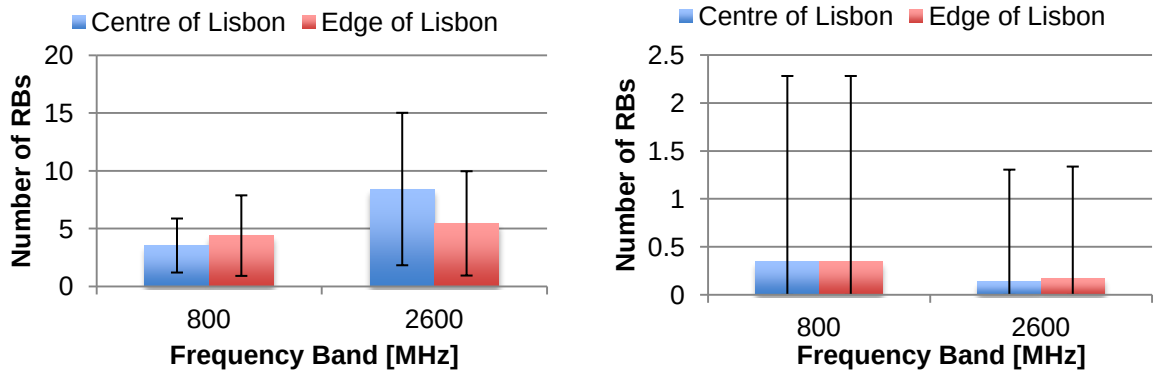

a) Number of used RBs per user b) Number of interference RBs per user

Figure 4.29. Number of used RBs and interference RBs without throughput due to interference per active user for 800 and 2600 MHz bands.

In Figure 4.30, one can see the radio channel condition by means of SNR and SINR in the centre and edge and observe that both zones present similar behaviour. However, between the two frequency bands there is a tremendous gap, especially for the SNR: the difference between the SNR in the two

frequency bands is around 25 dB, approximately the difference between the pathloss calculated for the two frequency bands by the COST 213 Walfisch Ikegami Model, detailed in Annex C. SINR is obviously lower than SNR, the decrease in the 800 MHz band, being much higher than in the 2600 MHz one, the differences being around 14 dB and 2 dB on average, respectively.

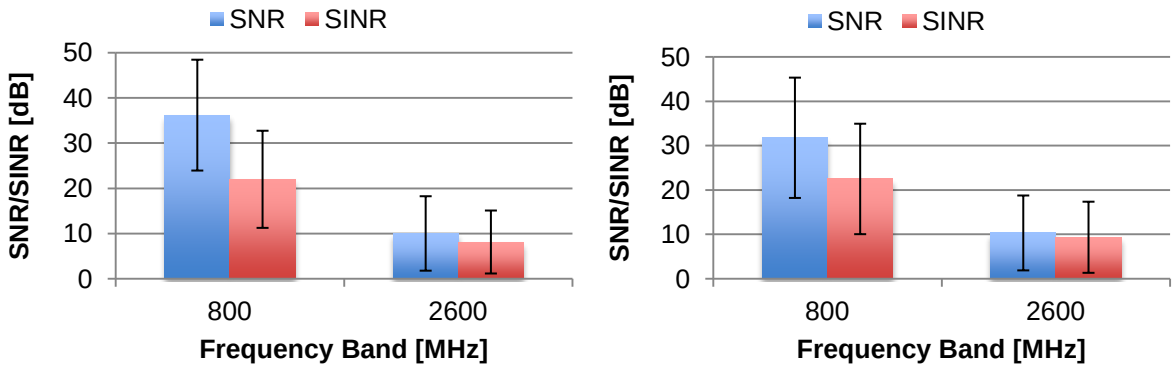

a) Centre of Lisbon b) Edge of Lisbon

Figure 4.30. Users SNR and SINR for 800 and 2600 MHz bands for the centre and edge of Lisbon.

In Figure 4.31-a), one can observe that in the centre, streaming, chat and P2P have their served users significantly reduced in the 800 MHz band, two of them below half of the number of served ones in the 2600 MHz band, which can be explained by the reduced number of RBs allocated, limiting the number of users. In the edge of Lisbon illustrated by Figure 4.31-b), the most significantly differences occur in the opposite way, as the 800 MHz favours a higher number of served users regarding the web browsing and FTP services, while chat and P2P services perform below compared to the 2600 MHz frequency band.

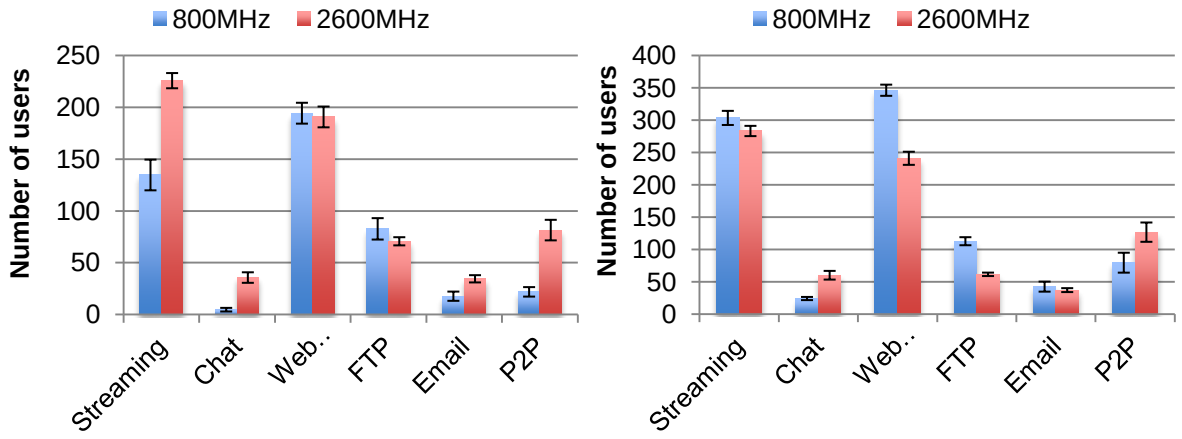

a) Centre of Lisbon b) Edge of Lisbon

Figure 4.31. Number of served users grouped by service for 800 and 2600MHz bands in the centre and edge of Lisbon.

4.3.4 Number of users

In the simulations regarding a variable number of users placed in the network, the aim is to evaluate performance taking into account its scalability, i.e., how the performance will be affected with the increase of the cells load, which will degrade as one can expect due to the radio resources shared channel and the higher number of users competing for them.

In Figure 4.32-a), one can observe the increase of the BSs throughput along the number of covered users in the network and that the increase is greater for the centre of Lisbon than for the edge. This can be explained by the higher density of users in this part of the city, which can also explain the reason for the earlier beginning of the saturation, i.e., throughput increase starts to slow down with the number of users until it increases no more.

The same trend can be found in Figure 4.32-b), the number of served users per BS being approximately around 500, and then the increase being faster in the centre than in the edge, to the point that around 3500 covered users, the number of served users is almost the double in the centre compared to the edge, 11 against 6 respectively.

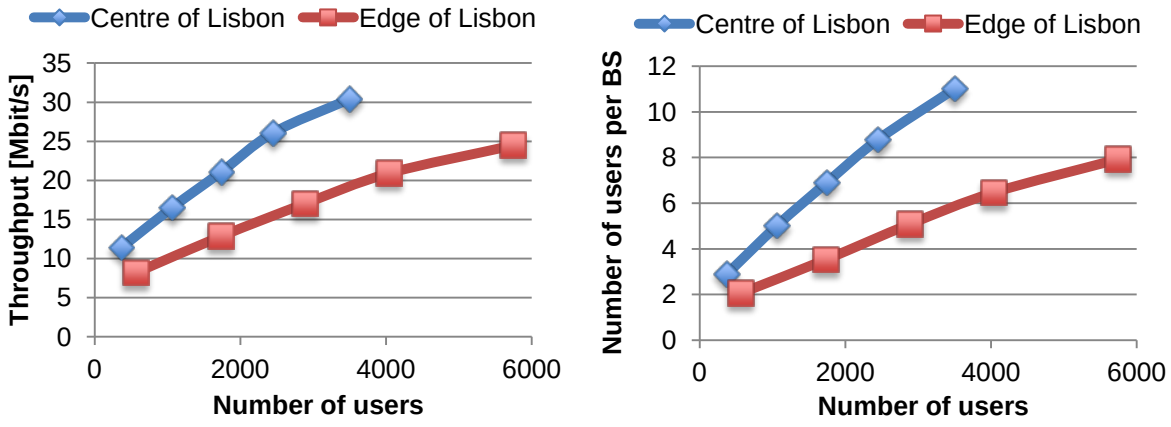

a) BS throughput

b) Number of served users per BS

Figure 4.32. BSs average throughput and number of served users per BS along the number of covered users.

In Figure 4.33-a), one can see the higher number of used RBs per BS in the centre and the difference getting higher with the number of users, as one could expect from the previous results. In Figure 4.33-b) one can observe the overall served users in the network along the covered ones, and observe that until 4000 covered users, the number of served users increases approximately in proportion, and after that, considering that only data from users belonging to the edge of Lisbon is available, the number of served users does not increase anymore, so that the saturation of the network is achieved for the given users distribution.

Regarding users performance indicators, one can see in Figure 4.34 that there is an overall trend for users throughputs to decrease along the number of users, which is expected due to the gradually higher scarce of RBs and interference power reaching users MTs. The throughput variance along the

number of users is around 1 Mbit/s for the cell-centre users, while one can see that cell-edge users throughputs do not vary significantly along the number of users, not having a so well defined decreasing trend.

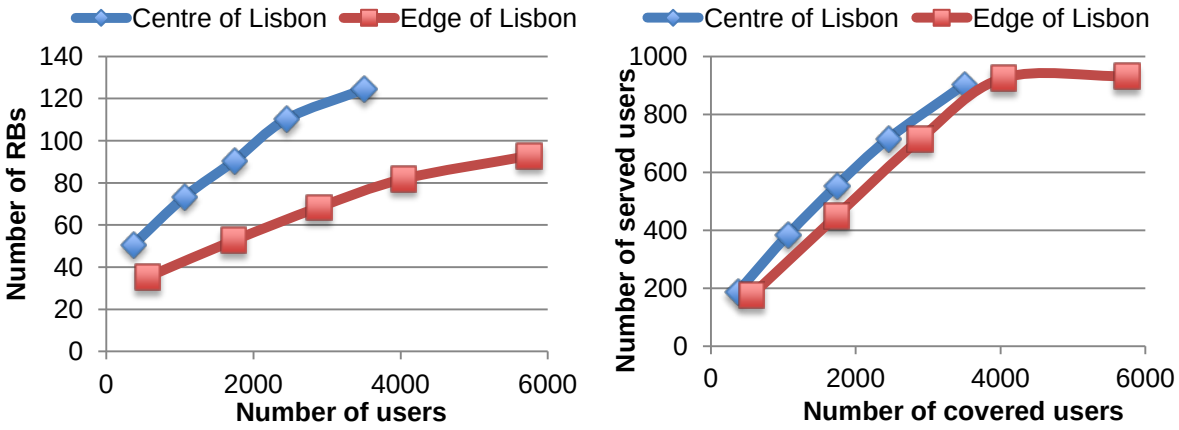

a) Number of used RBs per BS

b) Number of served users in the network

Figure 4.33. Number of used RBs per BS and number of served users in the network along the number of covered users.

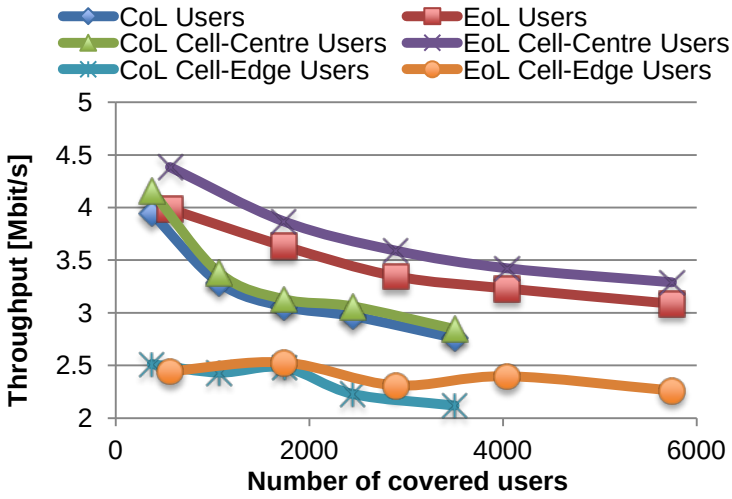

Figure 4.34. Users average throughput along the number of covered users.

Figure 4.35 illustrates the variation of the number of used RBs per user along the number of users in the network for the centre and edge, and one can see that its number decreases with the number of users as expected, due to the higher demand of resources to satisfy users services associated throughputs and the associated reduction algorithms when capacity is exceeded.

Regarding previous results illustrated in Figure 4.34 and Figure 4.35, one could somehow expect the results shown in Figure 4.36, i.e., because on average with such a reasonable number of used RBs per user, and relatively low associated throughputs compared to the high peak data rates that characterize LTE, radio channel conditions had to be the limiting performance factor, as one can see from Table 2.2.

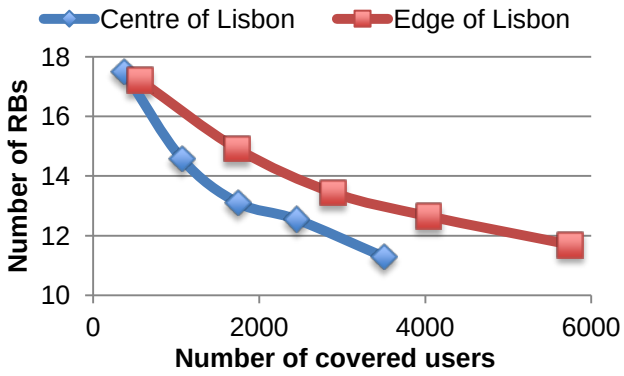

Figure 4.35. Number of used RBs per user along the number of covered users.

Even though the variance of the SNR and SINR among the number of users is unexpected, as from 500 to 1000 users these ratios decrease rapidly, but then slowly increase until the maximum of users in the network. Graphically one can see that users SNR take similar values in the centre and edge, while SINR take lower values in the centre compared to the edge, which can be explained by the higher density of BSs, thus higher interference power at the MT.

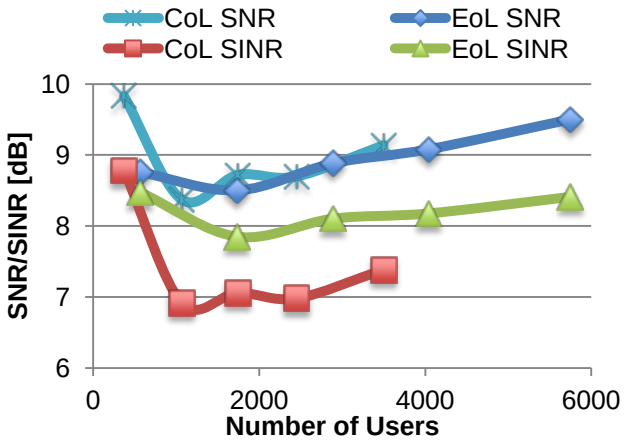

Figure 4.36. Active users average SNR and SINR along the number of covered users.

4.3.5 Frequency Reuse Schemes

Four FRSs were used in the simulations with the attempt to reduce interference, and results were obtained without raised power to the cell-edge users regarding SFR and PFR.

Results regarding BSs throughputs are shown in Figure 4.37-a), and one can see there is little variation between the schemes, with the exception of Reuse-3 where only half of the RBs are used in each sector, thus throughputs are expected to be lower than others, and one can see that they are around half of the value of the others schemes.

One can observe in Figure 4.37-b) that it seems to exist little correlation between the number of served users per BS and the used FRS; on all the schemes but Reuse-3, their average values and high variations are present on all of them, Reuse-3 presenting 6 and 4 instead of 8 and 6 served users per BS for the centre and edge respectively, due to the reduced number of available RBs per sector.

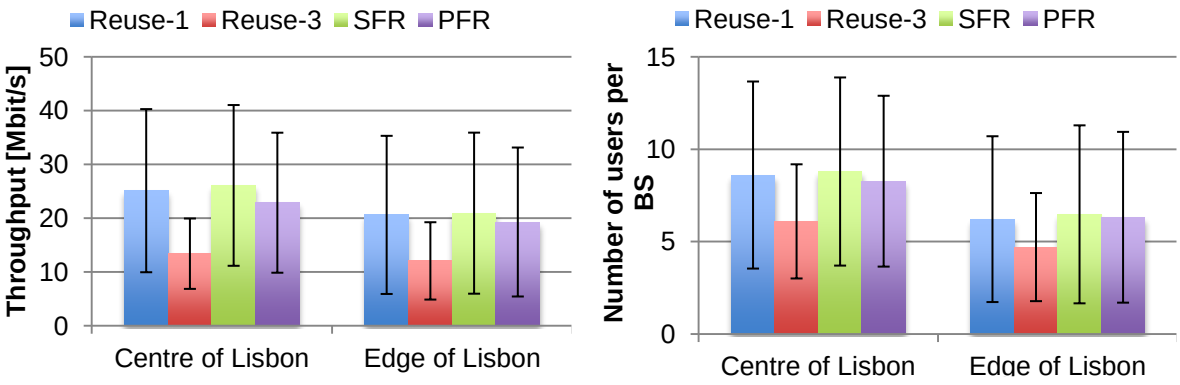

a) BS throughput

b) Number of served users per BS

Figure 4.37. BSs throughput and number of served users per BS along the FRS.

In Figure 4.38, one can see the usage of RBs per BS along the FRS, and observe that Reuse-1 and SRF schemes are the ones that distribute the higher number of RBs between users, the PFR and Reuse-3 having less RBs per BS due to the restrictions of 2/9 and 2/3 of the bandwidth per sector.

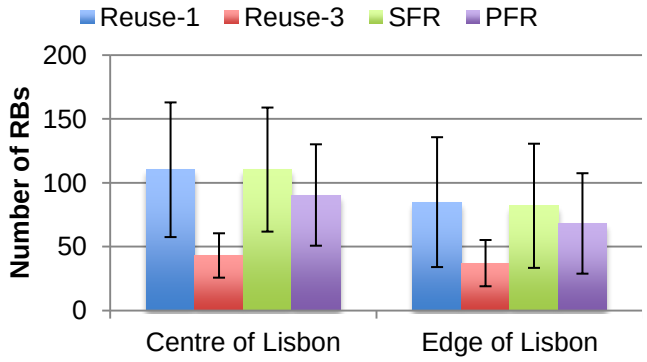

Figure 4.38. Number of used RBs per BS along the FRS.

Regarding users performance, one can see in Figure 4.39, users throughput in the centre and edge, that there seems to be little differences in the throughput along the FSR, the respective values being around 3 Mbit/s on average and having high variances, with the exception of Reuse-3 scheme which is the one to have higher bandwidth restrictions among sectors. As one can expect, cell-edge users have lower throughputs than cell-centre ones, even through the difference between them is small, with the throughputs reaching on average 2 Mbit/s.

In Figure 4.40, the RBs usage per user is shown for the centre and edge, being identical for the two regions, with an average number of used RBs around 10. One can again see the FRS influences the distribution of RBs, more specifically by theirs RBs restrictions: Reuse-1 and SFR using the entire bandwidth per sector, PFR using 7/9 of the bandwidth and Reuse-3 1/3 of the bandwidth.

In Figure 4.41, users SNR and SINR are shown for the centre and edge, and one can see the radio channel condition seems to be slightly better in the edge compared to the centre, although variances between users are again tremendous due to the heterogeneity of the network and the high number of BSs and users along the coverage area.

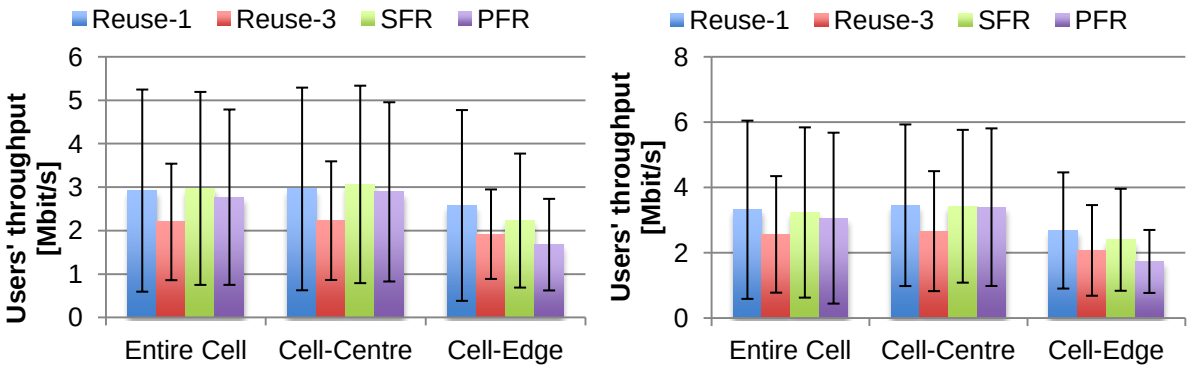

a) Centre of Lisbon b) Edge of Lisbon

Figure 4.39. Users' throughput along the cell and along the FRS in the centre of Lisbon.

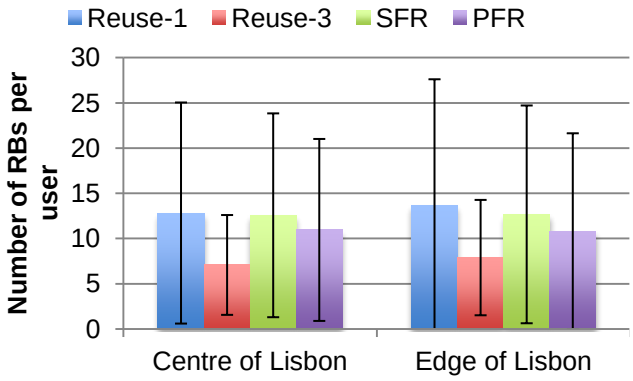

Figure 4.40. Number of used RBs per user along the FSR.

For the same reason, the differences between the used schemes are subtle and do not have a direct impact on the radio channel, with the exception of Reuse-3 that has on average the SNR and SINR 2 dB higher, probably due to the lower noise power at the receiver, which is a consequence of the lower RBs usage.

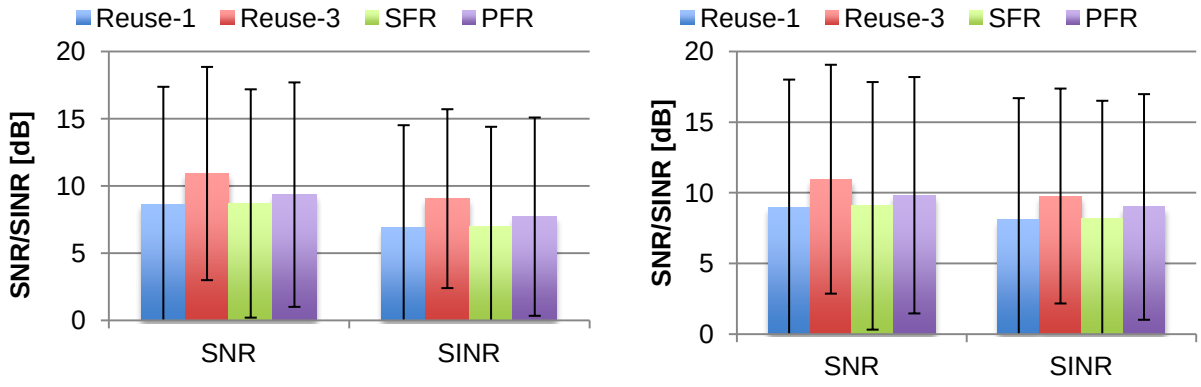

a) Centre of Lisbon b) Edge of Lisbon

Figure 4.41. Users SNR and SINR along the FSR in the centre and edge of Lisbon.

4.3.6 Scheduling Algorithms

Performance indicators variance along the scheduling algorithms are presented in this subsection, and have great importance, because the overall performance evaluation is highly dependent on the algorithms that manage the requested load by users when capacity is exceeded, which happens most of the time for all the sectors for the high load scenarios analysis.

In Figure 4.42-a), BSs throughput is shown for the three scheduling algorithms, and one can see that there are some differences in the throughput achieved, although the differences between them are lower than their standard deviations. As one could expect, on average Max SNR has the higher throughput on average, because higher SNR users have higher throughput for the same number of RBs and interference power at the MT and RR has the lower throughput because users are limited to a given reduced number of RBs, independent from their throughput needs.

In Figure 4.42-b), one can see the number of users per BS for the three scheduling algorithms for the centre and edge, and results show there are very few differences between Max SNR, RR and PF regarding the number of users served per BS, presenting an average of 9 and 6 users for the centre and edge, respectively, and high variations due to the heterogeneity of the network as well as the numbers of users per BSs requesting services.

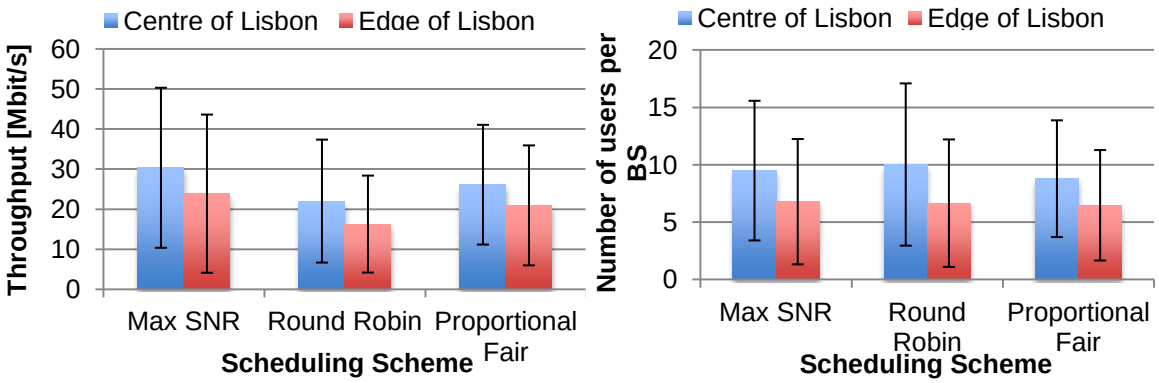

a) BSs throughput

b) Number of served users per BS

Figure 4.42. BSs throughput and number of served users per BS for the three scheduling algorithms in the centre and edge of Lisbon.

Regarding the distribution of radio resources among users, results from Figure 4.43 show the number of allocated RBs per BS for the three scheduling schemes, and one can see that Max SNR and PF are the schemes that have higher number of RBs, around 115 and 80 for the centre and edge, respectively, while RR presents approximately half of those same values. These results are subject to the fact that RR distributes resources equally among users, allocating for some users more resources than needed to satisfy the required throughput, resulting in a waste of RBs and allocating less for others that required higher throughput, or face a less favourable radio channel condition to achieve the wanted throughput for the respective service. One could also expect a worse behaviour by PF compared to Max SNR, because of the non allocation of the entire number of RBs users require, being provided resources with such to achieve the average throughput, but probably due to capacity

exceeder at most BSs, PF proved to be as performing as Max SNR as long as RBs distribution is concerned.

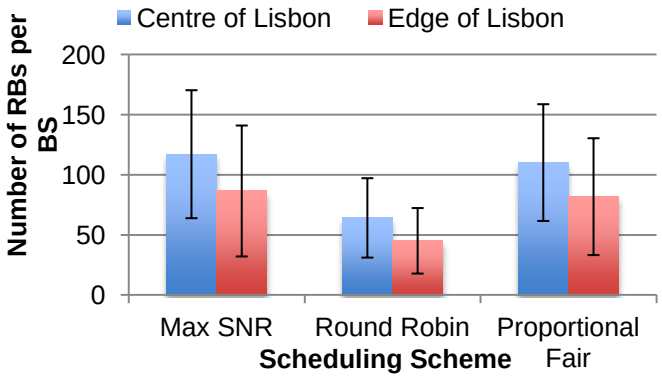

Figure 4.43. Number of RBs per BS along the scheduling algorithms in the centre and edge of Lisbon.

Regarding users performance at the throughput level, in Figure 4.44 results are shown for the centre and edge. One can see that users throughput reaches slightly higher values in the edge compared to the centre and that users throughput take similar and higher values for the Max SNR and PF schemes compared to the RR one. Even though, throughput variance is very big compared to both average values, and especially to the difference between the average values from the three scheduling schemes. Also cell-edge users have both lower average and variance throughputs.

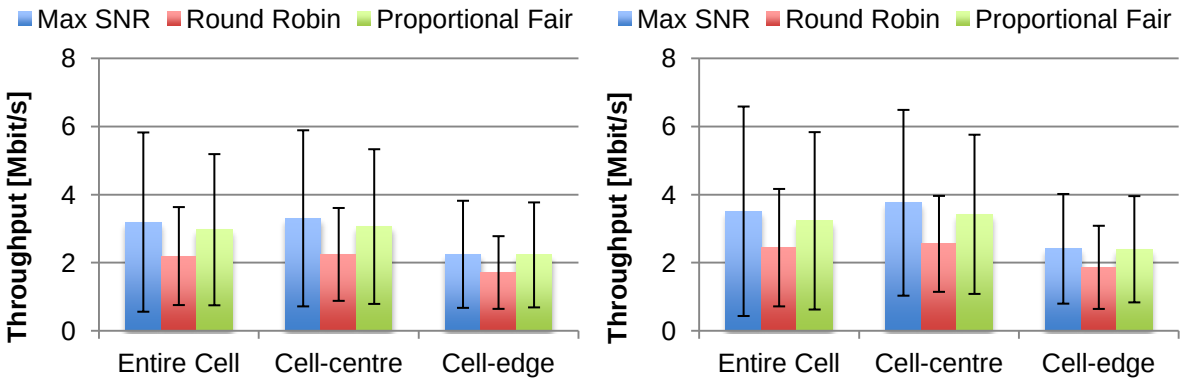

a) Centre of Lisbon

b) Edge of Lisbon

Figure 4.44. Users throughput in the cell areas for the three scheduling algorithms in the centre and edge of Lisbon.

In Figure 4.45, one can observe the distribution of the number of RBs among users, which is somehow similar to the one presented in Figure 4.43 for the BSs with the exception of the similar quantity of RBs on the centre and edge. Both centre and edge users have on average the same number of RBs, but edge BSs have a lower number of allocated RBs; there are less users per BS in this part of the city, which is confirmed in Figure 4.42-b). Results from Figure 4.45 show that Max SNR and PF have approximately the same distribution of allocated radio resources, taking similar values of average and standard deviation, while RR takes practically half of the same values. This fact may cause some surprise, because with half of the RBs per user on average, users reach throughputs that are not even 1/3 lower than other with Max SNR or PF, the number of served users per BS being

identical between all the schemes, as Figure 4.42 shows.

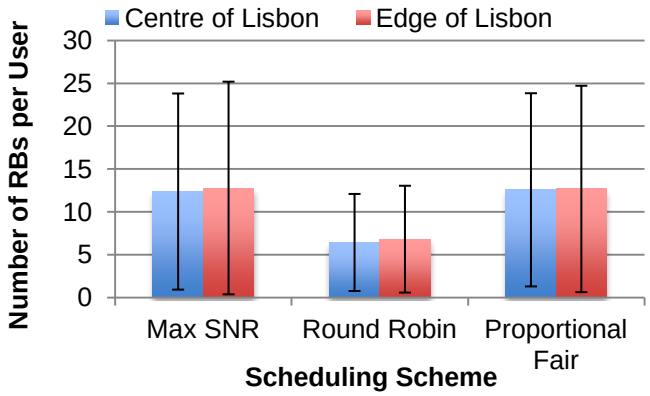

Figure 4.45. Number of RBs per user along the scheduling algorithms in the centre and edge of Lisbon.

One can see from Figure 4.46 results regarding users radio channel condition for the three scheduling schemes and considering the previous anaçysis, there is no surprise that RR is the scheme that presents higher SNR and SINR values than Max SNR and PF, whose performance is very similar, even though the difference between the average scheme values is much lower than their standard deviation values, as one could expect from a loaded network filled with 6500 covered users with distances from serving BSs and number of collision RBs as dispersed as possible. Results are identical for the centre and edge, although the edge seems to have a lower degradation of the radio channel condition taking interference into account. In fact, the RR scheme that distributes a smaller number of RBs among users, half compared to others schemes, can achieve a performance not even 1/3 below compared to the other schemes. Also, one can see from the results regarding the edge, which happen to have a lower load due to lower density of users per BS, that radio channel degradation seems to be lower compared to the centre.

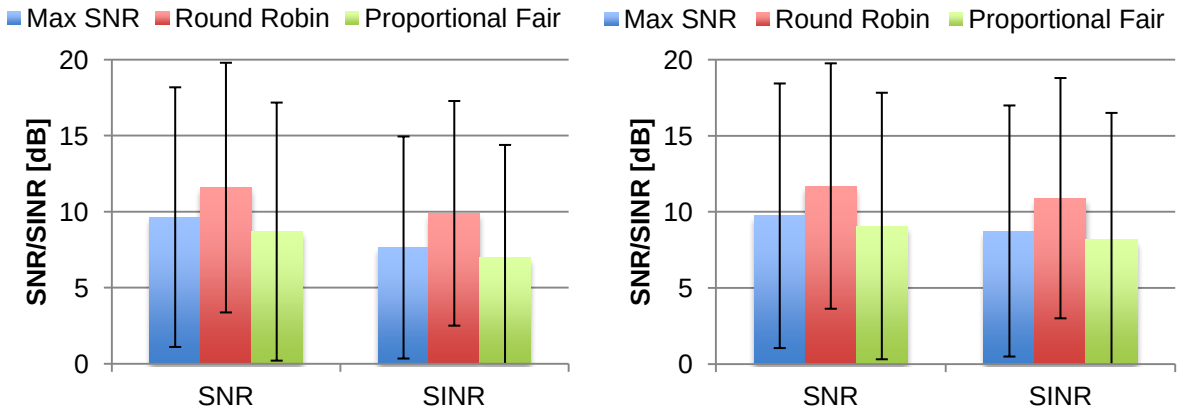

a) Centre of Lisbon

b) Edge of Lisbon

Figure 4.46. Users SNR and SINR along the scheduling algorithms in the centre and edge of Lisbon.

4.3.7 Antennas transmission power

Transmission power variation results are presented below, being an approach made in order to characterize its influence in the overlapping cells coverage areas and radio channel degradation caused by interference, as well as in the obtained throughputs.

Variation of the BSs throughput along transmission power is presented in Figure 4.47-a) and one can see that there is a trend that the higher transmission power is, the higher the obtained throughput for both centre and edge, besides the differences between the throughputs for the respective powers are much lower than the standard deviations.

Continuing with a capacity-focused analysis, in Figure 4.47-b) one can see the variation of the number of served users per BS along the transmission power, and observe that there is an increasing trend of the number of served users from 37 to 43 dBm, but the number of served users per BS for 46 dBm is on average the same for the 43 dBm case, which means that a saturation point might have been achieved, regarding the number of served users per BS.

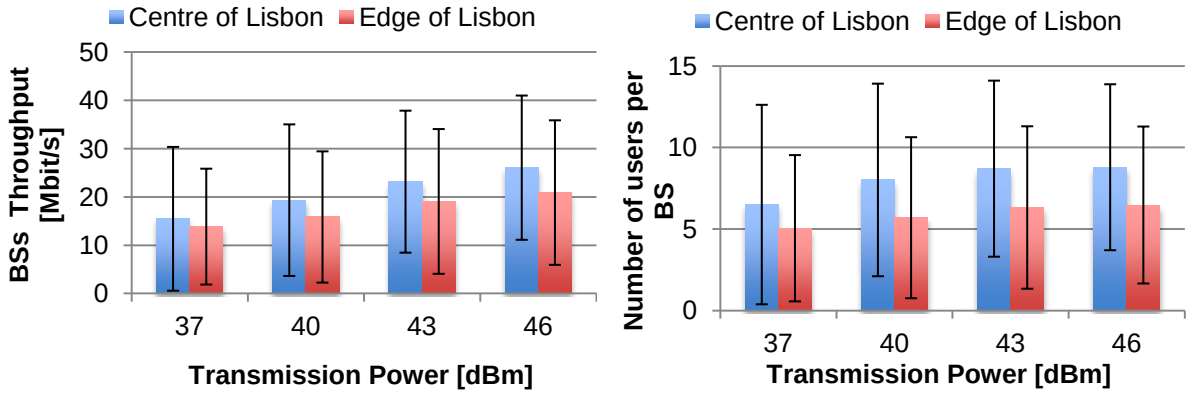

a) BSs throughput b) Number of served users per BS

Figure 4.47. BSs throughput and number of served users per BS along transmission power for the centre and edge of Lisbon.

In Figure 4.48, one can see the variation of the cell radius, which again is defined as the further user away from the serving BS, and is obvious limited by the distribution of the BSs in the network and by the distance between them in the centre and edge. So, one can expect the radius variation along the transmission power to be small as one can observe in Figure 4.48, being higher from the first power increase step from 37 do 40 dBm, and lower from the last power increase step of 43 to 46 dBm.

Regarding users performance indicators, one can observe the results from users throughput in Figure 4.49 to be increasing with the transmission power, but this trend is very subtle, and on average the throughput gain from 37 to 46 dBm is only around 0.5 Mbit/s for the centre and edge. Again, standard deviations values are enormous compared to the average values, and even bigger when compared to the difference between the average throughputs for the respective transmission powers.

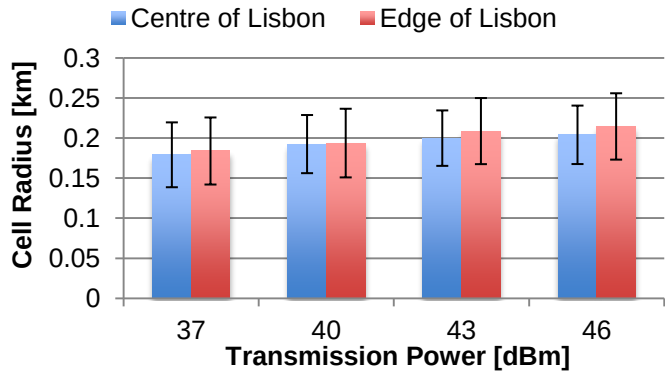

Figure 4.48. Cell radius along the transmission power in the centre and edge of Lisbon.

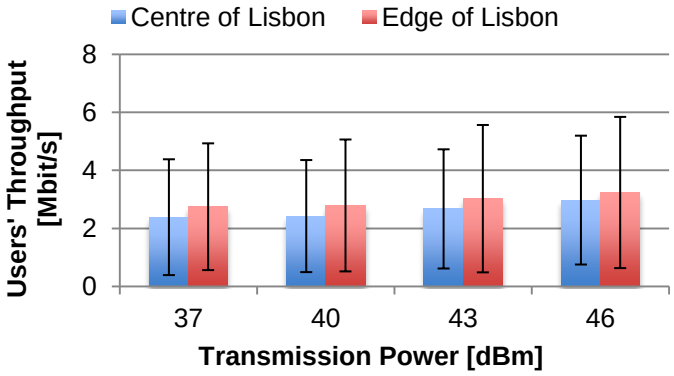

Figure 4.49. Users' throughput along the transmission power in the centre and edge of Lisbon.

Taking into account the influence of the transmission power in the radio channel condition, one can observe in Figure 4.50 the variation of the SNR and SINR along the transmission power in the centre and edge. First of all, it is noticeable the huge standard deviation of the SNR and SINR, taking higher values than the average ones. Also, there is no significant difference in the radio channel condition between the users from the centre and edge, and no significant decrease of the radio channel condition including interference for the throughput mapping. Besides these tremendous variations, one can observe an increase trend of the SNR and SINR, especially in the last step from 43 to 46 dBm, where SNR and SINR take values around 8 dB.

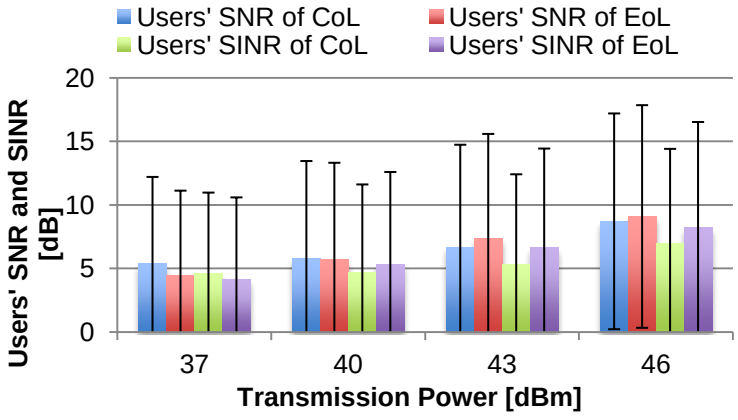

Figure 4.50. Users SNR and SINR along transmission power in the centre and edge of Lisbon.

In Figure 4.51, the variation of the covered and served users in the network along the transmission power is shown, and since it affects directly the link budget, not only by the radio channel condition but also by including or excluding users as coverage is concerned, the aim is to analyse and compare the number of covered users versus served ones. One can see that the number of covered users increases in both centre and edge, the bigger increase being at the edge of the city with an increase of 400 users per 3 dB power increase on average, against around 100 users per 3 dB power increase on average in the centre. Even though, the increase of the active users is much slower compared to the covered ones, being of 85 and 75 users per 3 dB power increase for the edge and centre, respectively.

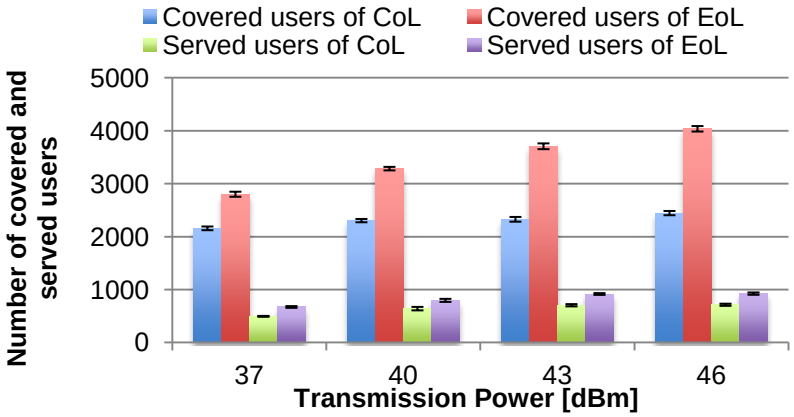

Figure 4.51. Number of covered and served users along transmission power in the centre and edge of Lisbon.

4.3.8 Antennas downtilt angle

Antennas downtilt angle variation results are presented in this subsection, and such as the transmission power variation, are important in the cell overlapping coverage area and interference mitigation analysis.

BSs throughput along the downtilt angle is shown Figure 4.52-a), and one can see that instead of having a monotonous behaviour, throughput seems to be maximised by a certain optimal angle, which is different for the centre and edge. Although differences between BSs throughputs, which only reach 5 Mbit/s, are much smaller than their standard deviation that are bigger than 10 Mbit/s, one can say that on average, 8° and 7° are the downtilt angles that maximize BSs throughput in the centre and edge, respectively.

In Figure 4.52-b), one can see number of served users per BS along the downtilt angle and observe some differences compared to the previous one, as the angles that maximize served users on average have changed, the values being 7° and 6° for the centre and edge of Lisbon, at least for the available data. One can also see that for the edge, which is an area of larger cell radius, downtilt has an exclusively decreasing capacity effect from 6° to 11°, reaching for the latter almost half of the served user on average of the former.

Regarding downtilt angle as a direct influence in cell coverage radius, one can see in Figure 4.53 that

cell radius is decreasing with the downtilt angle as one could expect, because is moves the maximum of vertical radiation diagram down, which takes an initial 0º tilt that is represented in red in Figure H.1. Considering cell radius values for 6º and 11º, one can see that the differences between the cell radius for these downtilt angles reach almost 100 m in the edge, considering coverage areas whose radii varied from 240 and 280 m to 160 and 190 m for the centre and edge respectively, corresponding to decreases of around 33%.

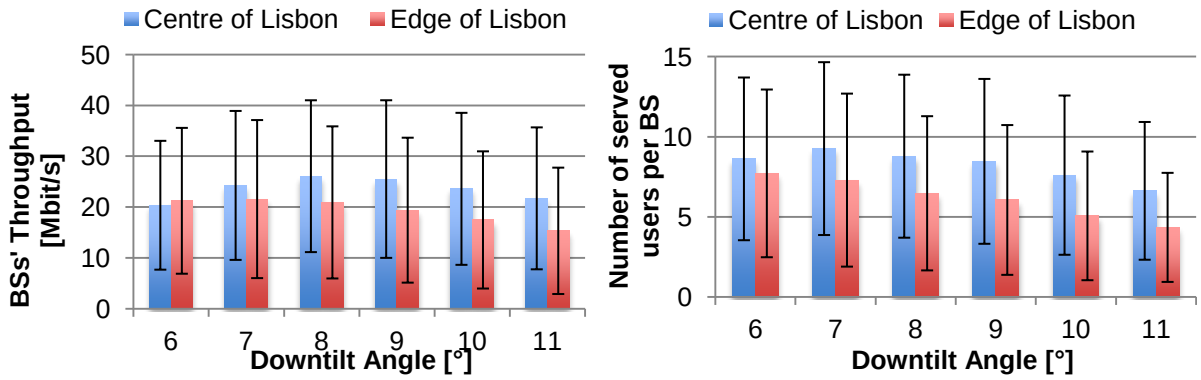

a) BSs throughput b) Number of served users per BS

Figure 4.52. BSs throughput and number of users per BS along the downtilt angle for the centre and edge of Lisbon.

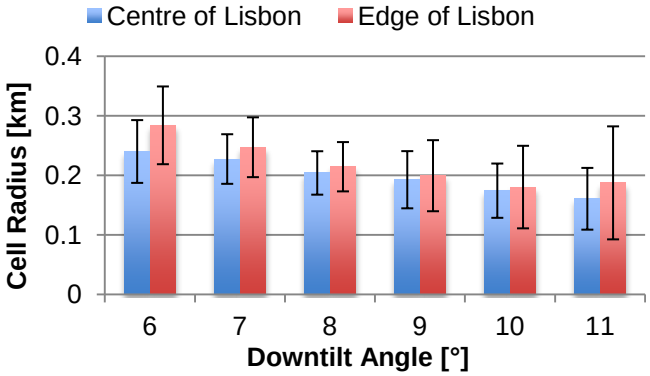

Figure 4.53. Cell radius along downtilt angle in the centre and edge of Lisbon.

Regarding users performance, in Figure 4.54-a) users throughput results are shown and one can see that, besides the huge variance of the throughput for each downtilt angle and the small difference between throughputs along downtilt angle, there seems to be a trend of throughput to increase with the downtilt angle. This fact can be explained by a lower number of covered users per BS, which leads to a lower number of users competing for RBs, and thus users can get more RBs to themselves. Also downtilt angles decreases overlapping cells coverage areas, which decrease interference between neighbour cell, and also improves the cell users radio channel condition, because the maximum vertical pattern is now more pointed to covered users rather than to users from other cells.

The same trend of decrease in the cell radius along the downtilt angle shown in Figure 4.53 can be found for the users distance to the serving BS presented below Figure 4.54-b), the relative differences between maximum and minimum distances being in the order of the ones regarding radius, around

33% and 35% in the centre and edge, taking into account the average values for 6º and 11º.

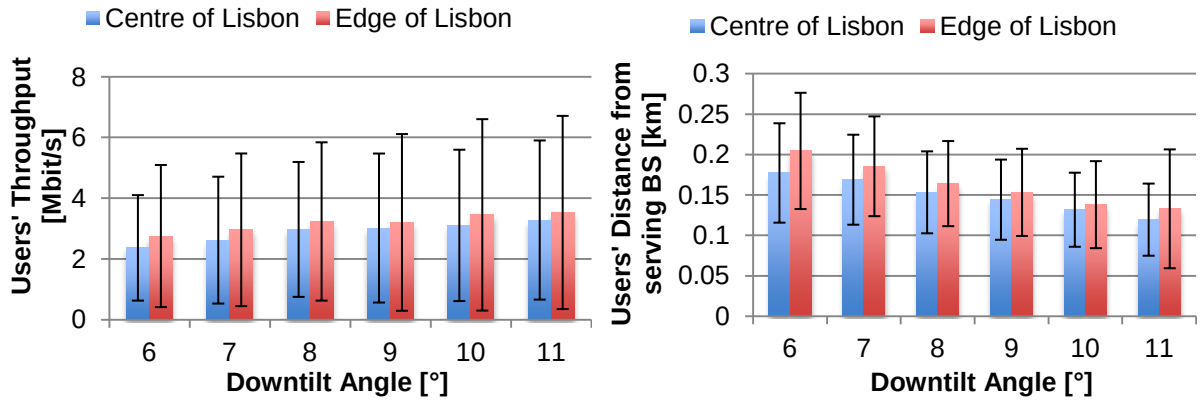

Figure 4.54. Users throughput along downtilt angle in the centre and edge.

Considering the users radio channel condition, one can see in Figure 4.55 the users SNR and SINR along the downtilt angle in the centre and edge and observe, first of all, that variations for each downtilt angle are huge since SNR and SINR standard deviation values are bigger than average ones, reflecting the heterogeneous distribution of users along the cells as well as the BSs ones. Also, one can say that there is little difference between the areas being considered, whether they are the centre or edge. Radio channel degradation seems to be higher due to interference for lower values of downtilt angle rather than for higher ones, which one could expect from the reduction in the overlapping coverage areas.

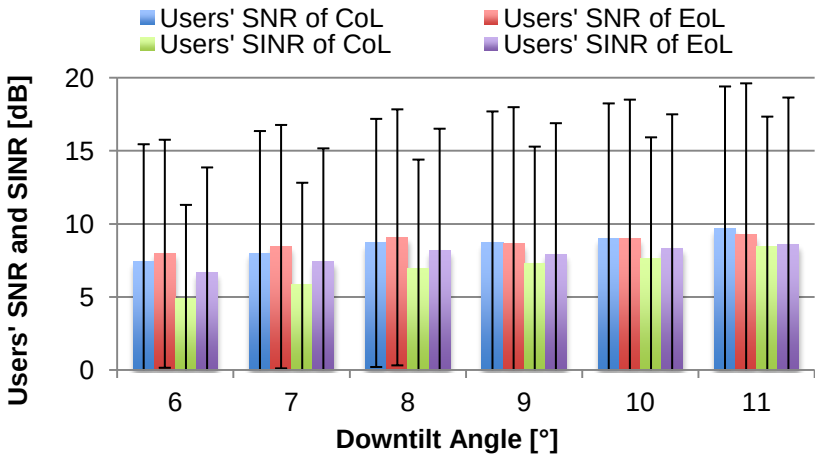

Figure 4.55. Users SNR and SINR along downtilt angle in the centre and edge of Lisbon.

Taking into account the absolute number of served users instead of per BS, one can see in Figure 4.56 the influence of the downtilt angle parameter in active users. For the centre, 7º is the optimal downtilt angle that maximizes the number of active users and the variations around that angles seem to be smooth compared to the edge, which presents a much stronger trend of decrease regarding the number of served users, which takes its maximum for 6º, presenting a number of users that almost doubles the one from the centre, and then decreasing rapidly with the downtilt angle to the point that for 11º, the number of served users in the two areas are almost the same.

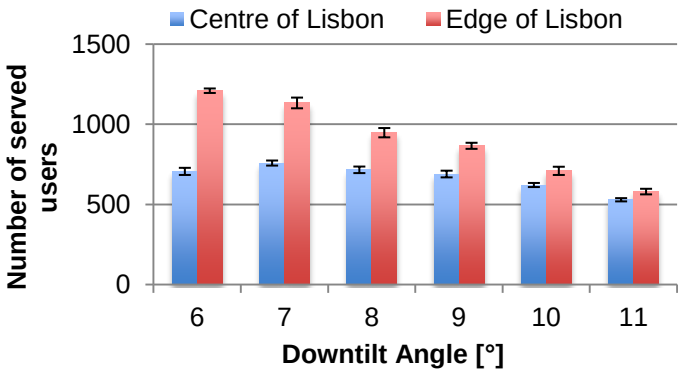

Figure 4.56. Number of served users along downtilt angle in the centre and edge of Lisbon.

Chapter 5

Conclusions

This chapter finalises the developed work, summarising conclusions and pointing out aspects to be developed in future work.

The main objective of this thesis was to study and quantify LTE coverage and capacity performance in urban scenarios, giving special emphasis to intra- and inter-cell interference aspects in the radio interface. LTE overall performance was evaluated through measurements and simulations for low load scenarios, and through intensive simulations for high load ones.

Chapter 2 is focused on LTE fundamental concepts, such as its basic aspects regarding radio interface, performance aspects and services, and state of the art. The first section addresses the network architecture, describing the network elements and the IP-packet oriented system. The second section addresses the spectrum organisation and licensing, as well as the radio channel characteristics, such as the modulations used, resources organisation and distribution and new aspects regarding LTE-A. In the third section, performance aspects are discussed, regarding throughput and addressing LTE peak data rates, interference and respective mitigation techniques and scheduling algorithms. In the next section, associated services and applications are described and characterised as far as data rates, associated delay and error rates tolerance are concerned. Finally, in the state of the art section, other authors' work related to this thesis is described, giving special importance to relevant performance aspects, such as dimensioning and maintenance regarding LTE network in urban scenarios.

Chapter 3 presents the developed model in order to access LTE performance on a multi-user scenario. In Section 3.1, the model description is presented, addressing the calculations regarding radio channel condition, pathloss models and additional urban scenario penetration margins. FRSs are described as well as their frequency allocation restrictions, along with the real interference situation approach for the intra- and inter-cell interferences analysis. Next, performance aspects are addressed and quantified in order to obtain results from the simulation that characterize the LTE overall performance. Users and BSs throughput, number and density of served users, users distance and cell radius are some of the aspects that are defined at this section. Also FRSs and scheduling algorithms are explained regarding the developed simulator. In Section 3.2, the implementation process is fully described, as well as the modules in the simulator, the respective information outflow, and the configurable parameters and options that are possible to use, starting from the insertion of users in the city, from the generation of the BSs network to the radio interface, FSR and scheduling algorithms parameters configuration. At the end of the chapter, the model is assessed in order to confirm its assertiveness.

In Chapter 4, the scenarios description are addressed and results are obtained for the city of Lisbon, regarding a high heterogeneous distribution of both users and BSs, with part of the city full loaded and many users being delayed and some other parts of the city being almost empty. In high-density BSs zones, overlapping coverage areas are bigger and more interference-susceptible, while on others there are some parts of the districts, which have no coverage whatsoever. Also one has to know that in reality there are many characteristics to be taken into account, which were not considered, as the tilt of the terrain, the different urban structure from the districts, the sporadic high buildings that act as a shield of signal, and shapes coverage areas, avoiding overlapping areas, and the fact that some BSs might not always be tri-sectorised as it was assumed.

In addition to the developed models, measurements were done in the Vodafone LTE network along the main avenues of Lisbon and through some neighbourhoods in the centre and in the edge of the city. Measurements were done during high load FTP sessions in order to achieve the maximum throughputs, the route having been performed by car, where several data was collected. Afterwards, the results analyses of all measurements and simulations are shown. Simulations, with parameters configured to approach the measurements environment with few FTP users with 100 Mbit/s required throughput and additional vehicular penetration margin, LoS COST 231 Walfisch-Ikegami propagation model and Max SNR scheduling algorithm, were made and results compared to the ones obtained though measurements.

Intensive simulations regarding the reference scenario, as well as successive variations of one parameter at a time, were made in order to analyse performance in the reference scenario, and the influence of these parameters in the overall performance. The tested variation of parameters include bandwidth, frequency band, number of users in the network, FRSs, scheduling algorithms, antennas transmission power, and antennas downtilt angle. One can see from the results that some parameters have a clear influence in the results and some are not so conclusive. The fact that the network is big, being composed almost by 300 BSs and 7000 users placed in the city with their randomness and heterogeneity, make some results, such as users throughput, harder to characterize due to the specific disparate radio interface of each user when requesting services, although this might be a good approximation to real urban cellular networks, in the sense of the unpredictable and highly statistically variable requests of throughput by users. The reference scenario simulations were made using penetration margins of pedestrian, vehicular, urban and dense urban, focusing on the fact that in the urban scenario the majority of users perform their telecommunication services indoor, which introduces higher pathloss, especially taking into account the higher frequency band of 2600 MHz that seems to be one of the most consensual frequency bands for LTE deployment.

The obtained results show that the performance differences obtained from low and high load, regarding the number of users in the network and the required RBs, are tremendous, with users in the former obtaining peak data rates of 80 Mbit/s and in the latter being limited to relative low throughputs regarding the potential peak data rates, mainly because of the number of available RBs per user. Indeed, average users throughput in low load scenarios is around 15 times higher than in high load ones, the difference being only the number of users in the network and being or not in LoS with the BS. From measurements and low load simulation results, one can see the variation of the throughput, which is highly dependent of the radio channel condition, increasing along the RSRP and RS SNR. From high load simulations, one can see that the radio channel condition of the majority of users is performance limiting regarding obtainable throughputs and compared to peak data rates. The centre of Lisbon shows a higher percentage of served users compared to the edge, around 30% against 23% of served users over covered ones. In spite of the percentage of served users being relatively low, one can see from the users service penetration in the network, that the QoS criteria took place and increase slightly the number users with higher priority and decrease slightly those with lower priority services, but the differences from the penetration services being very smooth. Results show also that cell-edge users have lower throughputs compared to both cell-centre throughputs and overall users.

In terms of parameters variation, regarding bandwidth, results show that the reduction in the number of RBs by 40% have fewer influence than one could expect, with the most significant difference to be lowered throughput with an average 0.5 Mbit/s reduction, but the number of served users stays approximately the same. For the frequency band results analysis, one can see that there are higher differences than other results, because of the use of a much lower frequency carriers and the same transmission power, the 2600 MHz band has proved to be more performing than the 800 MHz one, with BSs throughput increasing 48% and number of served users per BS of 42% in the centre of Lisbon only, the edge registering similar values. In the case of radio channel condition, the 800 MHz band performs better, obviously due to the higher received power at the MT, with the disadvantage of generating much more interference, which is proved by the higher gap from SNR and SINR values, especially in the centre of Lisbon, where the distance between neighbour BSs is smaller. Thus, the number of RBs unusable due to interference is bigger as well as the number of throughput RBs is smaller for the 800 MHz due to interference. Also cell radii are bigger for the 800 MHz, as one could expect. With the variation of the number of users, one could test in a simple way the scalability of the system, and find for some cases the saturation in the system, where BS aggregated throughput and number of served users raises with the users in the network and the individual users performance indicators degrade although with low relevance, regarding throughput, number of attributed RBs and SINR, as one could expect. Regarding FRSs, there are little differences between them, with the exception of Reuse-3 that has restrictions in the use of RBs of 2/3 of the entire bandwidth per sector. This scheme leads to lower throughputs and fewer served users, but turnes out to be the scheme that maximizes radio channel condition. Regarding scheduling algorithms, one can see little differences between Max SNR and PF, the former presenting little superiority in the performance indicators, with the exception in the SNR and SINR for the RR, which performs worse with less resources and better on interference purposes. Variations of the transmission power show results with a trend to improve along the used power, especially for the users throughput, SNR and SINR with smooth variations and the minimum and maximum power gap being 9 dB. Antennas downtilt angle proves to have a slightly difference behaviour compared to previous results, because instead of monotonous behaviour in the results, there seems to be an optimal value that maximizes performance indicators, this value varying according to the performance indicator being evaluated. A trend of the number of served users and cell radius to decrease with the downtilt angle is shown, as one could expect from the increasingly smaller coverage area, and the users throughput, SNR and SINR raise with better collocation of the half-power beamwidth and reduce interference.

The developed simulator proved to be a reasonable tool to make an approach to urban LTE network in the case of low load as one can see from the comparison of the results obtained from the measurements and simulations but it has obviously inherent limitations. It is based on the allocation of resources on a snapshot basis, instead of having temporal depth, which would bring a more realistic approach to the scheduling of users when capacity is exceeded, especially for the PF scheme, which is intended to take into account the recent history from users to promote fairness between them. Also the simulator was used either for LoS situation for measurements comparison or for NLoS, and one could expect obviously the mix of the two in reality. In fact, Lisbon is known to be a very

heterogeneous city, in terms urban structure regarding construction material, terrain tilt, density of users and buildings, streets width and building distance, characteristic that are known to interfere with the signal propagation and that were not taken into account. Another aspect that might have conditioned the obtained results is the reduction algorithm based on the reduction of the number attributed RBs when maximum capacity is exceeded, playing a very important role in the overall performance. Also, the MT for the 2600 MHz band and the MIMO 2×2 antennas configuration conditioned measurements to the maximum 100 Mbit/s throughput imposed.

LTE performance obtained through simulations regarding the low load scenarios proved to be much better for users, as far as throughput is concerned, as one could expect. It will certainly be interesting to repeat the measurement campaign done in this thesis 5 years from now, when certainly more subscribers will exist in the network to compete for RBs, and create a more interference challenging and scheduling dependent environment. Along with the higher load required to the network, the improvements described below will also be important to keep up the simulator with the potential that LTE has.

Regarding future work, there are many improvements to be made that were not addresses in this thesis, namely the dynamic RBs allocation scheme in the subcarriers attribution between neighbour sectors and cells in order to avoid interference, though the X1 connections that link the eNBs. In fact interference can have worse consequences than lowering users throughput: it is important to avoid interference to the RBs dedicated to channels of signalling and controlling that are responsible for the numerous function that assure the correct performance of the LTE system. Relaying techniques can also be implemented in order to increase both coverage and capacity, without creating interference by installing more BSs. Another aspect to take into account is the inherent importance of UL in LTE network, which was not analysed in this thesis, and is crucial for the provided services. It is important to quantity its performance, as it uses SC-FDMA and this one is not as robust as OFDMA, and because MTs use less transmission power, and typically no MIMO antennas configuration due to power purposes. In fact, although services do not tend to be symmetric, in the sense that the highest user data rates are usually in the DL, more and more users are becoming content producers, as the nowadays tendency is the paradigm of users to create their own contents regarding numerous services of content sharing of textual information, music, video, social networks, etc. Moreover, it is interesting to address LTE-A performance at MT and spectrum levels when the augmented bandwidth will prove to value the additional cost it inherently will bring.

Annex A

Frequency bands assignment auction results by ANACOM

This annex presents the available frequency bands and respective bandwidths during the auction performed by ANACOM, as well as the ones assigned to each Telecommunications Operator.

In Portugal, the frequency bands assignment auction performed by ANACOM (the Portuguese National Authority for Communications), occurred in November 2011, the results being presented in Table A.1. The blocks lacking price and operator assignment were the ones not bided by any Telecommunications Operator. The auction lasted for three days and the total value of the frequency blocks bided was €372.000.000. Note that frequency block of 450 MHz is not specified by 3GPP as an LTE operating band.

Table A.1. Results of the frequency bands assignment auction (extracted from [ANAC12]).

Block designation	Frequency band [MHz]	Block bandwidth [MHz]	Block price [€]	Operator assigned
A1	450	2 × 1.25	-	-
B1	800	2 × 5	45.000.000	TMN
B2	800	2 × 5	45.000.000	TMN
B3	800	2 × 5	45.000.000	VODAFONE
B4	800	2 × 5	45.000.000	VODAFONE
B5	800	2 × 5	45.000.000	OPTIMUS
B6	800	2 × 5	45.000.000	OPTIMUS
C1	900	2 × 5	-	-
C2	900	2 × 5	30.000.000	VODAFONE
D1	1800	2 × 5	4.000.000	TMN
D2	1800	2 × 5	4.000.000	TMN
D3	1800	2 × 5	4.000.000	VODAFONE
D4	1800	2 × 5	4.000.000	VODAFONE
D5	1800	2 × 5	4.000.000	OPTIMUS
D6	1800	2 × 5	4.000.000	OPTIMUS
D7	1800	2 × 5	-	-
D8	1800	2 × 5	-	-
D9	1800	2 × 5	-	-
E1	1800	2 × 5	3.000.000	TMN
E2	1800	2 × 5	3.000.000	VODAFONE
E3	1800	2 × 5	3.000.000	OPTIMUS
F1	2100	5	-	-

Table A.1 (contd.). Results of the frequency bands assignment auction (extracted from [ANAC12]).

F2	2100	5	-	-
G1	2600	2 × 5	3.000.000	TMN
G2	2600	2 × 5	3.000.000	TMN
G3	2600	2 × 5	3.000.000	TMN
G4	2600	2 × 5	3.000.000	TMN
G5	2600	2 × 5	3.000.000	VODAFONE
G6	2600	2 × 5	3.000.000	VODAFONE
G7	2600	2 × 5	3.000.000	VODAFONE
G8	2600	2 × 5	3.000.000	VODAFONE
G9	2600	2 × 5	3.000.000	OPTIMUS
G10	2600	2 × 5	3.000.000	OPTIMUS
G11	2600	2 × 5	3.000.000	OPTIMUS
G12	2600	2 × 5	3.000.000	OPTIMUS
G13	2600	2 × 5	-	-
G14	2600	2 × 5	-	-
H1	2600	25	3.000.000	VODAFONE
I1	2600	25	-	-

Annex B

Link Budget

This annex presents the link budget calculation regarding propagation between the transmitter and receiver, through the calculation of the losses along the link.

Link budget is a necessary tool to calculate the coverage of a cell and the appropriate modulation and code for all MTs, even though radio condition cannot be predicted it can be properly estimated.

The signal power at the receiving antenna can be calculated by the following expression:

$$P_{r[\text{dBm}]} = P_{t[\text{dBm}]} + G_{t[\text{dBi}]} + G_{r[\text{dBi}]} - L_{p[\text{dB}]} \quad \text{(B.1)}$$

where:

- P_r is the power available at the receiving antenna.
- P_t is the power fed to the antenna;
- G_t is the gain of the transmitting antenna;
- G_r is the gain of the receiving antenna;
- L_p is the pathloss.

The power fed to the antenna in the DL is given by:

$$P_{t[\text{dBm}]}{}^{DL} = P_{Tx[\text{dBm}]} - L_{c[\text{dB}]} \quad \text{(B.2)}$$

where:

- P_{Tx} is the transmitter output power;
- L_c is the losses in the cable between the transmitter and the antenna.

The power fed to the antenna in the UL is given by:

$$P_{t[\text{dBm}]}{}^{UL} = P_{Tx[\text{dBm}]} - L_{u[\text{dB}]} \quad \text{(B.3)}$$

where:

- L_u is the losses due to the user's body.

The power at the receiver in the DL is given by:

$$P_{Rx[\text{dBm}]}{}^{DL} = P_{r[\text{dBm}]} - L_{u[\text{dB}]} \quad \text{(B.4)}$$

where:

- P_{Rx} is the receiver input power.

The power at the receiver in the UL is given by:

$$P_{Rx[\text{dBm}]}{}^{UL} = P_{r[\text{dBm}]} - L_{c[\text{dB}]} \quad \text{(B.5)}$$

The pathloss can be calculated as:

$$L_{p\,[\text{dB}]} = L_{p,\ COST\ 231\ WI\,[\text{dB}]} + L_{p,\ environment\,[\text{dB}]} + M_{SF\,[\text{dB}]} \quad \text{(B.6)}$$

where:

- $L_{p,COST\ 231\ WI}$ is the pathloss from the COST 231 Walfisch-Ikegami Model;
- $L_{p,environment}$ is the pathloss from the user environment;
- M_{SF} is the slow fading margin.

SNR can be computed using the signal and noise power available at the receiver antenna:

$$\rho_{N\,[\mathrm{dB}]} = P_{r\,[\mathrm{dBm}]} - N_{[\mathrm{dBm}]} \tag{B.7}$$

where:

- ρ_N is the SNR;
- P_r is the average signal power at the receiver;
- N is the average noise power at the receiver;

The noise power at the receiver can be calculated by the expression (3.4).

$$N_{[\mathrm{dBm}]} = -174 + 10\log_{10}\Delta f_{[\mathrm{Hz}]} + F_{N\,[\mathrm{dB}]} \tag{B.8}$$

where:

- Δf is the bandwidth of the radio channel being used;
- F_N is the noise figure at the receiver.

SINR can be calculated by the following expression:

$$\rho_{IN\,[\mathrm{dB}]} = 10\log_{10}\left(\frac{P_{r\,[\mathrm{mW}]}}{N_{\,[\mathrm{mW}]}+I_{\,[\mathrm{mW}]}}\right) \tag{B.9}$$

where:

- ρ_{IN} is the SINR;
- I is the interference power at the receiver.

Annex C

COST 231 Walfisch-Ikegami

This annex presents the propagation model used to calculate the pathloss in the urban environment.

To calculate the path loss for urban scenarios, one can use the COST 231 Walfisch-Ikegami Model, whose parameters are illustrated by Figure C.1.

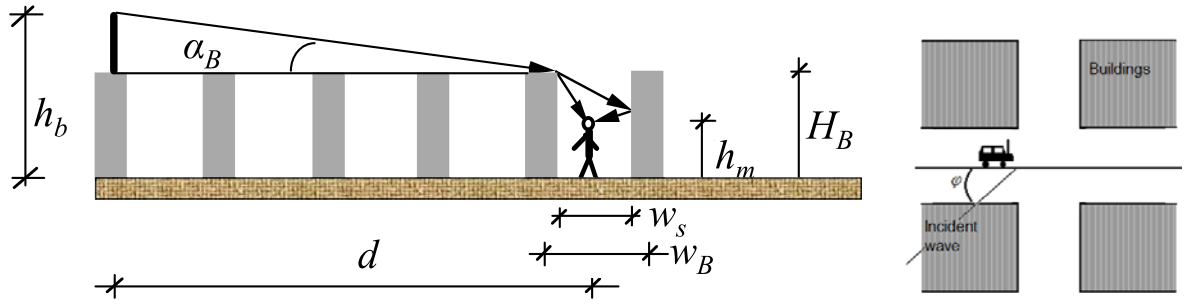

Figure C.1. COST 231 Walfisch-Ikegami Model diagram and parameters (extracted from [Corr09] and [Carr11]).

For LoS propagation, path loss is given by:

$$L_{p[\text{dB}]} = 42.6 + 26 \log d_{[\text{km}]} + 20 \log f_{[\text{MHz}]} \text{ , for } d > 0.02 \text{ km} \quad \text{(C.1)}$$

where:

- d is the horizontal distance between the BS and the MT;
- f is the frequency carrier of the signal.

For NLoS propagation in a street, path loss is given by:

$$L_{p[\text{dB}]} = \begin{cases} L_{0[\text{dB}]} + L_{rt[\text{dB}]} + L_{rm[\text{dB}]} \text{ , for } L_{rt} + L_{rm} > 0 \\ L_{0[\text{dB}]} \text{ , for } L_{rt} + L_{rm} \leq 0 \end{cases} \quad \text{(C.2)}$$

where:

- L_0 is the free space propagation path loss;
- L_{rt} is the loss between the last rooftop and the MT;
- L_{rm} is the loss between the BS and the last rooftop.

The free space propagation path loss is given by:

$$L_{0[\text{dB}]} = 32.44 + 20 \log d_{[\text{km}]} + 20 \log f_{[\text{MHz}]} \quad \text{(C.3)}$$

The loss between the last rooftop and the MT is given by:

$$L_{rt[\text{dB}]} = L_{bsh[\text{dB}]} + k_a + k_d \log d_{[\text{km}]} + k_f \log f_{[\text{MHz}]} - 9 \log w_{B[\text{m}]} \quad \text{(C.4)}$$

where:

- L_{bsh} is the loss due to the height difference between the rooftop and the antennas;
- k_a is the increase of path loss for the BS antennas below the roof tops of the adjacent buildings;
- k_d controls the dependence of the multi-screen diffraction loss versus distance;
- k_f controls the dependence of the multi-screen diffraction loss versus frequency;
- w_B is the buildings separation distance.

The loss due to the height difference between the rooftop and the antennas is given by:

$$L_{bsh[\text{dB}]} = \begin{cases} -18\log\left(h_{b[\text{m}]} - H_{B[\text{m}]} + 1\right), & \text{for } h_b > H_B \\ 0, & \text{for } h_b \leq H_B \end{cases} \quad \text{(C.5)}$$

where:

- h_b is the BS height;
- H_B is the buildings height;

The other parameters are given by:

$$k_a = \begin{cases} 54, & \text{for } h_b > H_B \\ 54 - 0.8\left(h_{b[\text{m}]} - H_{B[\text{m}]}\right), & \text{for } h_b \leq H_B \text{ and } d \geq 0.5 \text{ km} \\ 54 - 1.6\left(h_{b[\text{m}]} - H_{B[\text{m}]}\right)d_{[\text{km}]}, & \text{for } h_b \leq H_B \text{ and } d \geq 0.5 \text{ km} \end{cases} \quad \text{(C.6)}$$

$$k_d = \begin{cases} 18, & \text{for } h_b > H_B \\ 18 - 15\frac{h_b - H_B}{H_B}, & \text{for } h_b \leq H_B \end{cases} \quad \text{(C.7)}$$

$$k_f = \begin{cases} -4 + 0.7\left(\frac{f_{[\text{MHz}]}}{925} - 1\right), & \text{for urban and suburban scenarios} \\ -4 + 1.5\left(\frac{f_{[\text{MHz}]}}{925} - 1\right), & \text{for dense urban scenarios} \end{cases} \quad \text{(C.8)}$$

The loss between the BS and the last rooftop is given by:

$$L_{rm[\text{dB}]} = -16.9 - 10\log w_{s[\text{m}]} + 10\log f_{[\text{MHz}]} + 20\log\left(H_{B[\text{m}]} - h_{m[\text{m}]}\right) + L_{ori[\text{dB}]} \quad \text{(C.9)}$$

where:

- w_s is the width of the street;
- h_m is the height of the MT;
- L_{ori} is the street orientation loss.

The street orientation loss is given by:

$$L_{ori[\text{dB}]} = \begin{cases} -10.0 + 0.354\phi_{[^\circ]}, & \text{for } 0^\circ < \phi < 35^\circ \\ 2.5 + 0.075\left(\phi_{[^\circ]} - 35\right), & \text{for } 35^\circ \leq \phi < 55^\circ \\ 4.0 - 0.114\left(\phi_{[^\circ]} - 55\right), & \text{for } 55^\circ \leq \phi \leq 90^\circ \end{cases} \quad \text{(C.10)}$$

where:

- ϕ is the angle of incidence of the signal in the buildings, in the horizontal plane.

The COST 231 Walfisch-Ikegami model is valid for the following conditions:

- $f \in [800, 2000]$ MHz;
- $d \in [0.02, 5]$ km;
- $h_b \in [4, 50]$ m;
- $h_m \in [1, 3]$ m.

Finally, the model standard deviation takes values from 4 dB to 7 dB.

Annex D

Additional Results

This annex contains additional results that were obtained the same way as those presented in Chapter 4 and are not presented there due to being less relevant or conclusive.

Concerning the users distance from the serving BS, results are presented for the variation of the tested parameters along Chapter 4.

Considering the influence of the bandwidth in the cell radius which is given by the distance of the user further away from the serving BS, one can see in Figure D.1 that there is little variance between the 10 MHz and 20 MHz bandwidth situations, for both average and standard deviation values, with the exception of a trend for a little raise in the cell radius in the edge of Lisbon from the 10 MHz to the 20 MHz bandwidth situation.

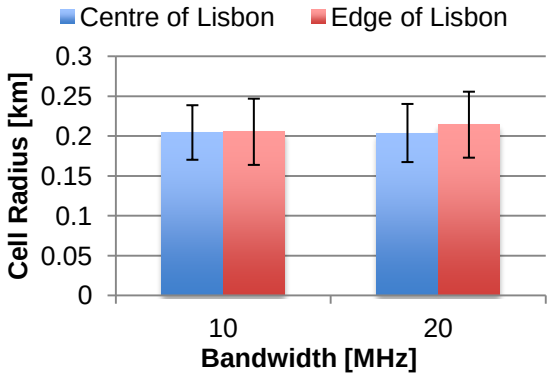

Figure D.1. Cell radius for 10MHz and 20MHz bandwidth.

In Figure D.2 one can observe that there is almost no relation of the frequency band in the distance of the served user to the BS, the 800 MHz frequency band case presenting higher variations than the 2600 MHz. In fact users are located equally along the network whether the frequency band is but it also shows that the lower pathloss from lower frequency has not increased significantly the number of served users further away from the serving BS.

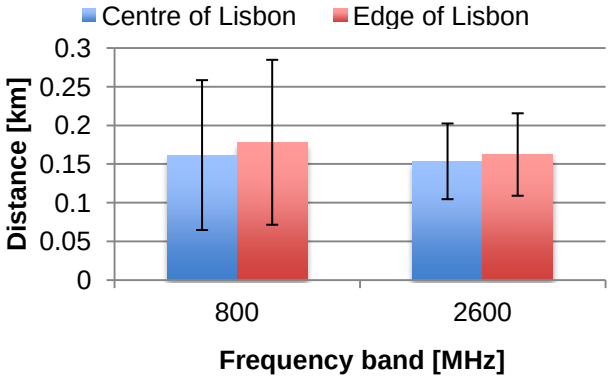

Figure D.2. Distance of users from serving BS for 800MHz and 2600MHz frequency bands.

Regarding the cell radius shown above illustrated in Figure 4.48, the same smooth increasing trend can be found for the users average distance from the serving BS, as shown Figure D.3, as one can expect from the additional power gain in the link budget.

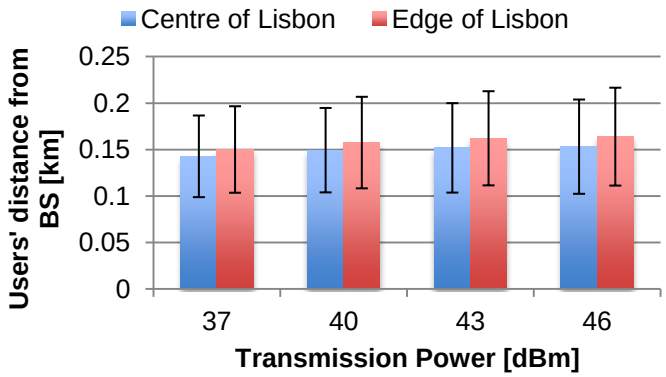

Figure D.3. Users' distance from serving BS along the transmission power in the centre and edge of Lisbon.

Annex E

User’s Manual

This annex explains how to configure the simulator parameters and run a simulation.

To start the applications, one must first run the file UMTS_Simul.MBX and then one must select three input files, as Figure E.1 shows for the radiation pattern:

- "Ant65deg.TAB", with the BS antennas gain structure;
- "DADOS_Lisboa.TAB" with the information regarding the city of Lisbon and its districts;
- "ZONAS_Lisboa.TAB", with area characterisation regarding the districts.

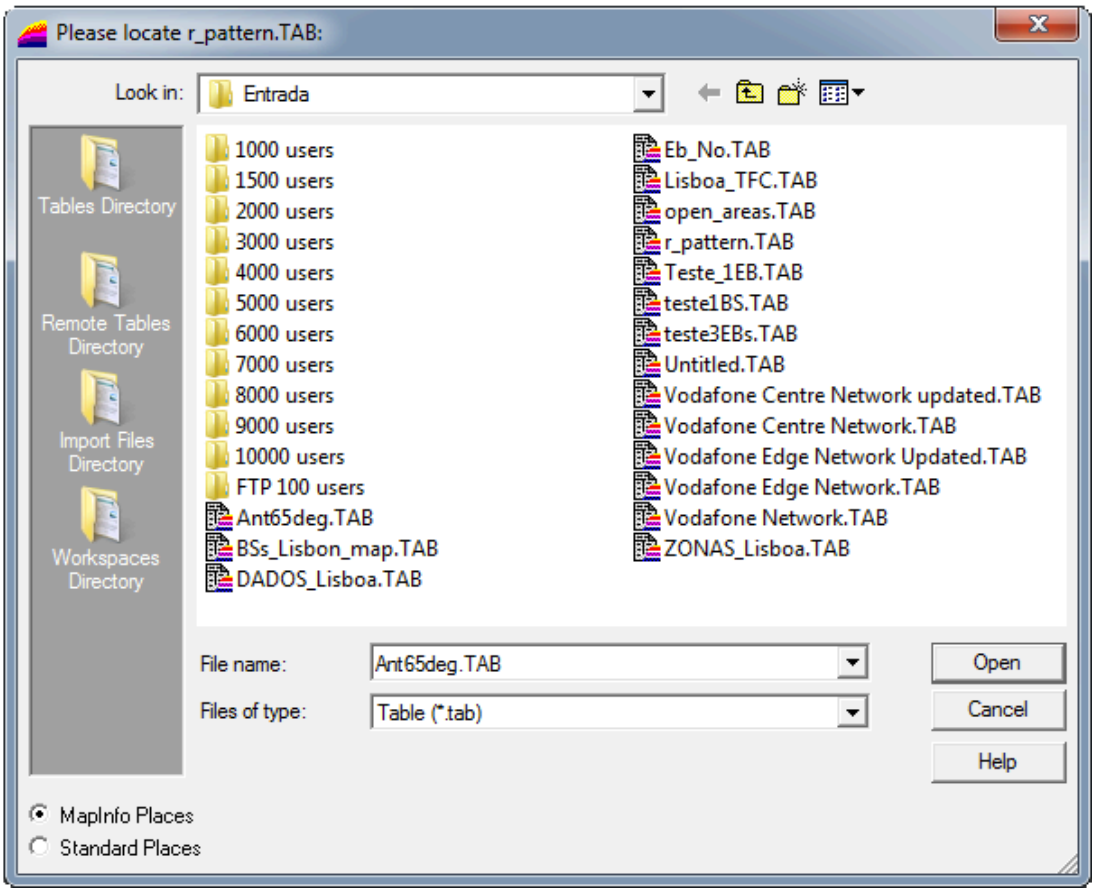

Figure E.1. Window for the selection of the radiation pattern file.

After the introduction of the geographical information, the map of Lisbon appears in the MapInfo program and a net tab called "System" is now available, where one should access to select the "LTE-DL" as shows Figure E.2.

Now one can configure several parameters that are spread on more than one window. The first window that one can open is the propagation model where one can chose the sizes of the urban area characterisation, the departing angle from the closest building and the MT height, as illustrated in Figure E.3.

The "LTE-DL Settings" window is the main panel where the majority of the parameters can be configured, from the transmission power to the indoor margins, FRS and scheduling algorithms and radio interface parameters such as bandwidth and frequency band, as illustrates Figure E.4. After selecting these parameters and choosing "ok" button, the "User Profile" tab gets available, where one can select the minimum and maximum throughput associated to each service, as shows Figure E.5.

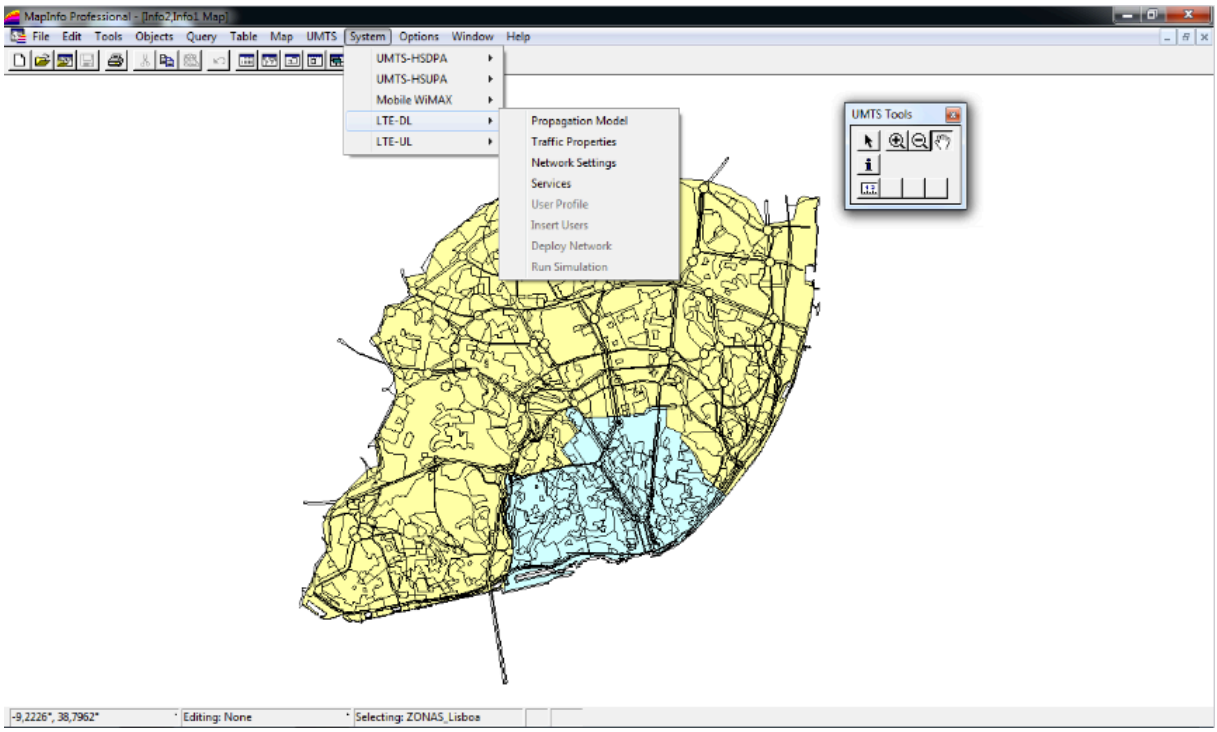

Figure E.2. System tab with the LTE-DL.

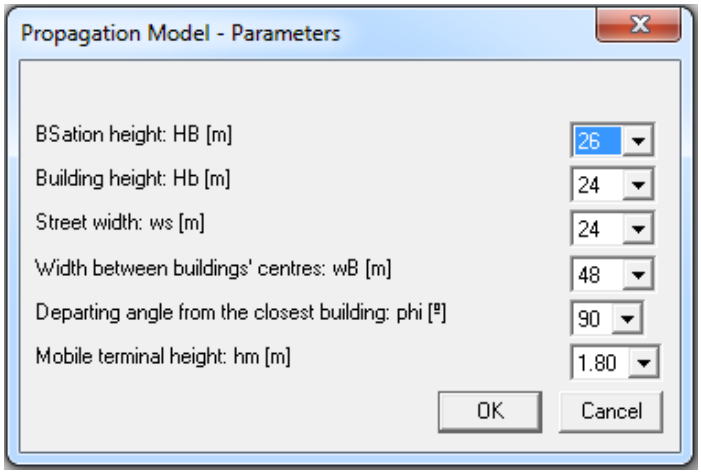

Figure E.3. Propagation model parameters.

After the associated services throughputs are set up, the tab “Insert users” is available and must select this tab and insert the files with the users that will be placed in the city of Lisbon, as in Figure E.6. The users files are created by the Users Generator (SIM) program developed whose functioning is detailed at [LaCo06]. After the users are loaded, users are represented in the map by flags, each one of a colour that represents the required service. Then one must load the BSs network, by selecting the “Deploy Network“ tab and choose the desired network table, which contains in each row the identification and coordinates of each BS, as illustrates Figure E.7. When the network is loaded, it is represented with the users along the map and one can finally select “Run Simulation” in order to run the simulation, as shown in Figure E.8. When the simulation ends, three windows appear, the first

presenting some statistical information regarding the simulation performed as shows Figure E.9.

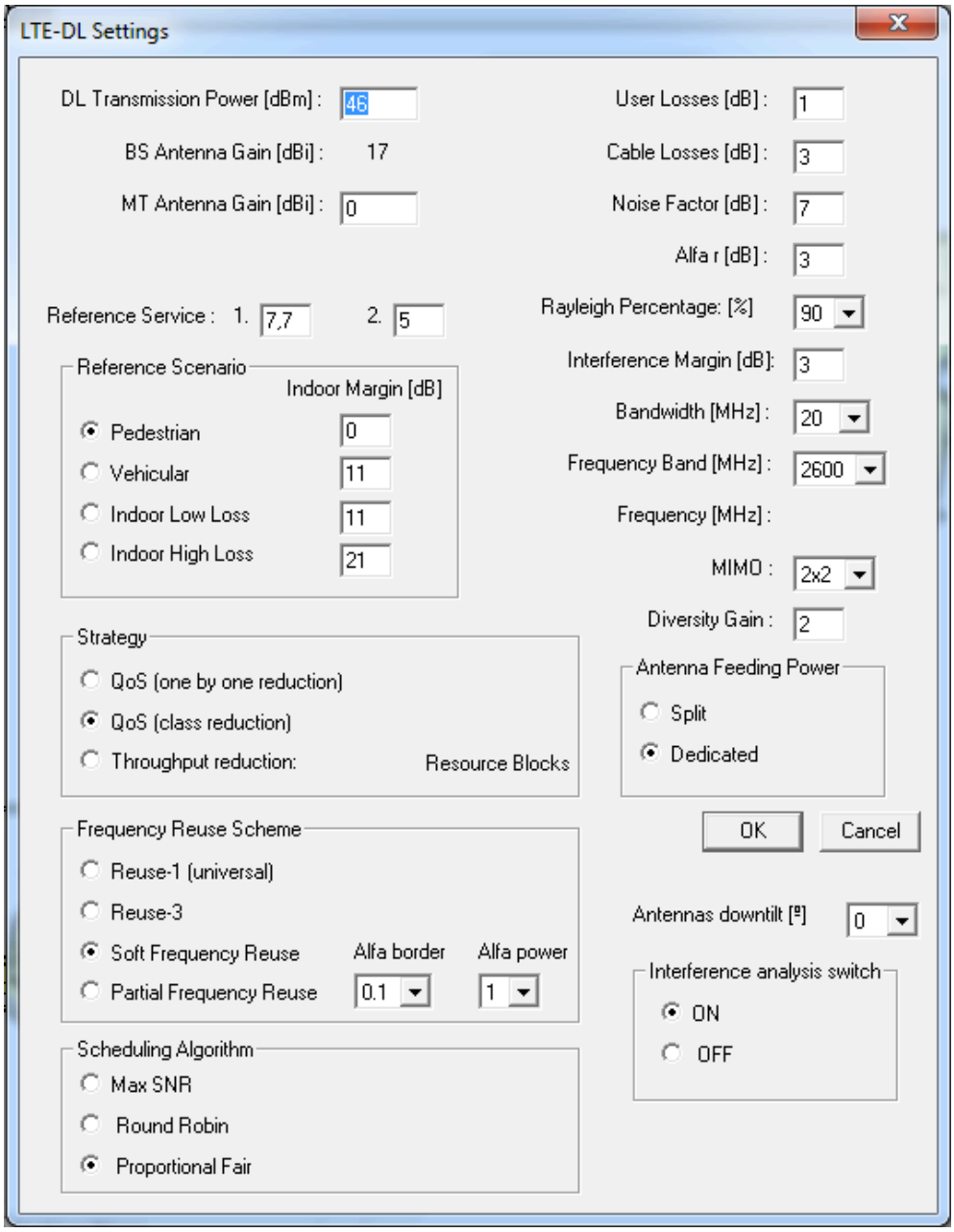

Figure E.4. Radio Interface parameters.

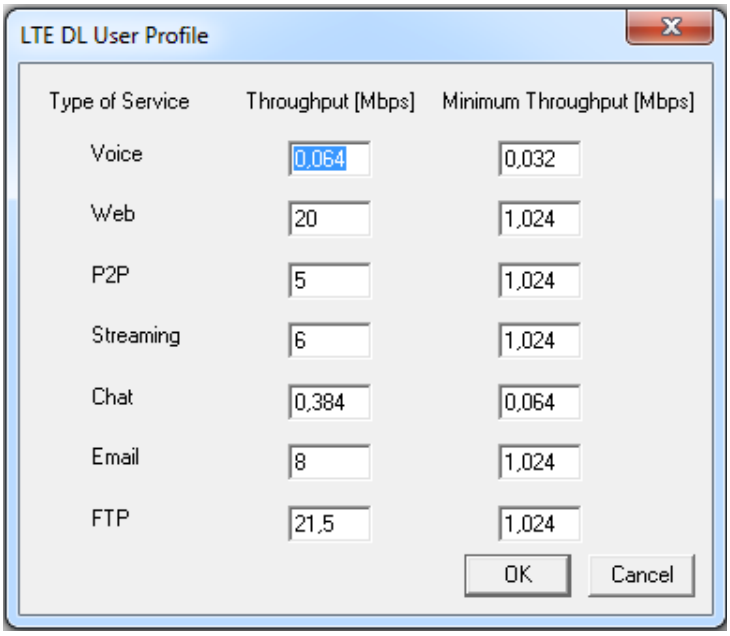

Figure E.5. User Profile parameters.

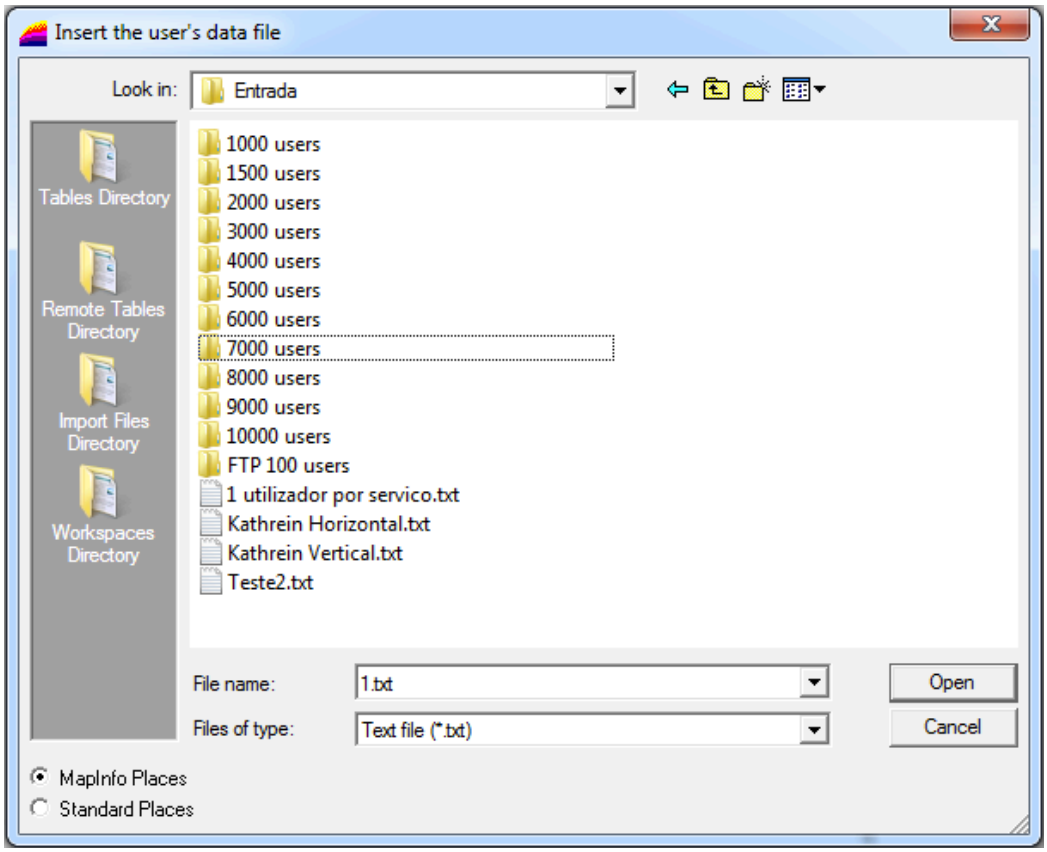

Figure E.6. Users data file.

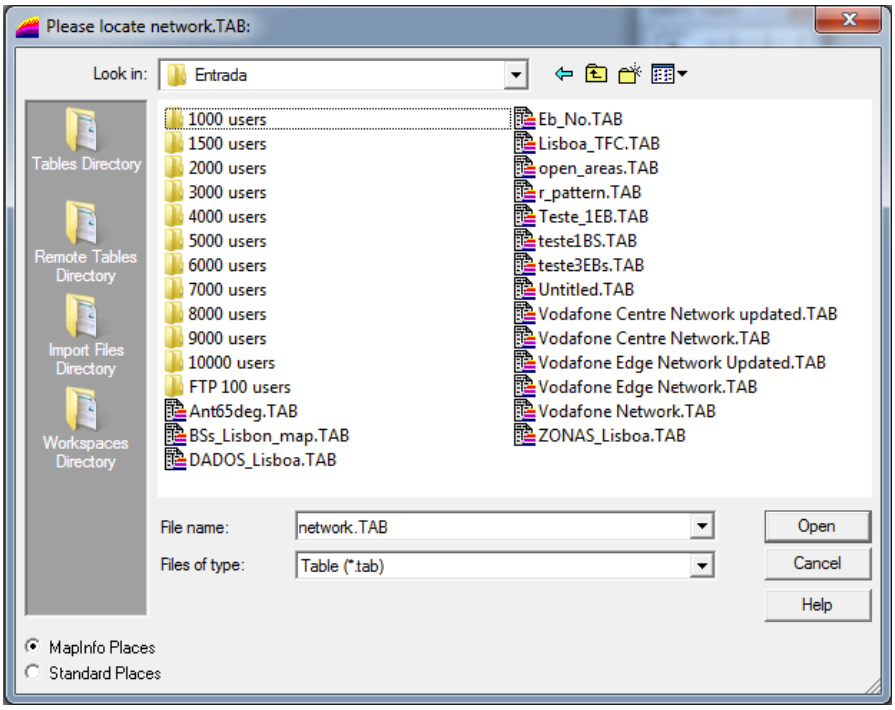

Figure E.7. Deploy Network window.

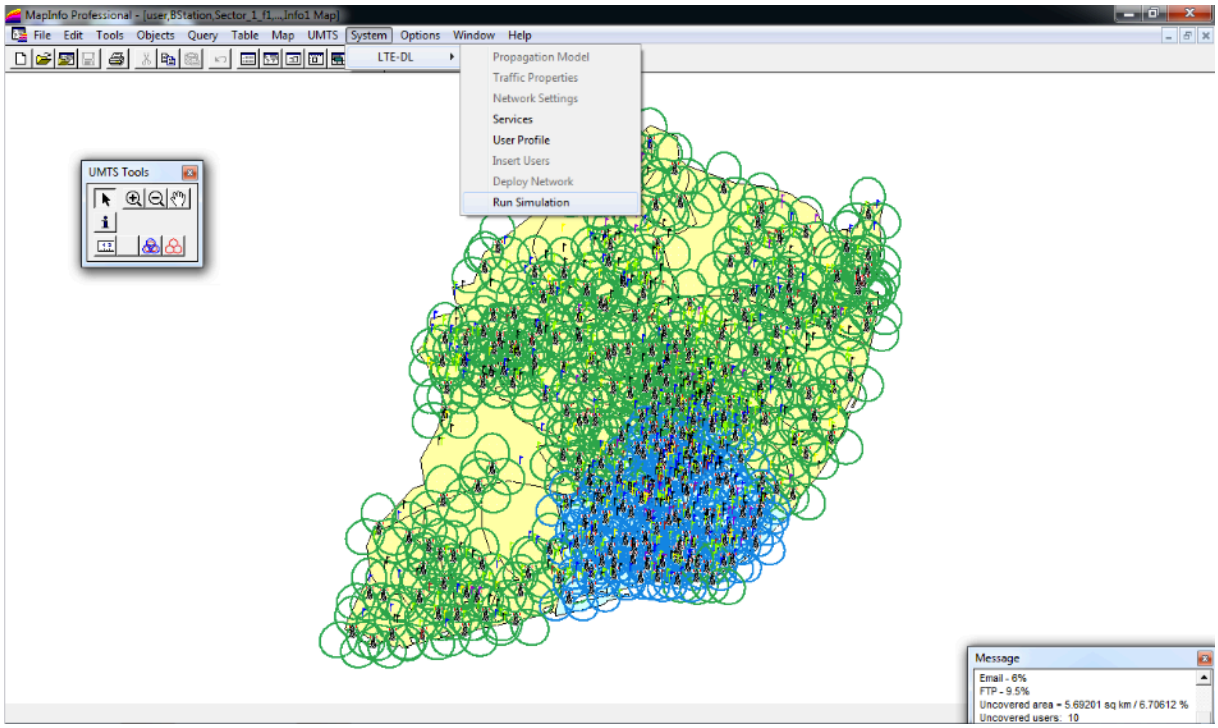

Figure E.8. Run Simulation command.

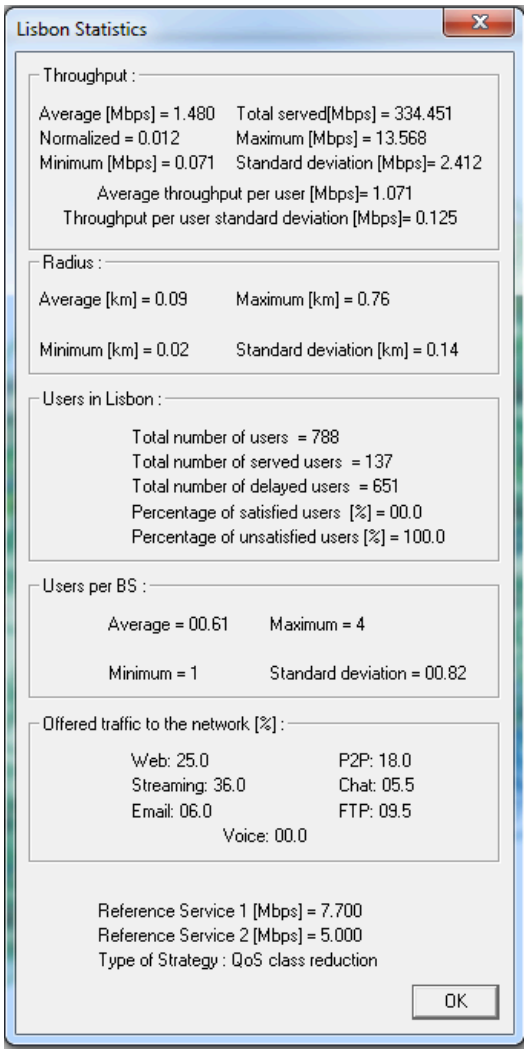

Figure E.9. Final simulation window.

Annex F

SINR and Data Rate Models

This annex describes the LTE SINR and throughput models and calculations of the obtainable throughputs regarding the physical layer.

Trial measurements documented by the 3GPP were taken as reference for deriving the expressions for throughput in the physical layer and SNR. The chosen channel models, Extended Pedestrian A (EPA), Extended Vehicular A (EVA) and Extended Typical Urban (ETU), are characterised in terms of the maximum Doppler frequency considered and maximum delay spread, as shows Table F.1. In addiction, Figure F.1 shows throughput as a function of the SNR for the EPA 5Hz channel, for some selected modulation schemes and MIMO configurations, regarding DL.

Table F.1. Channels mode characterisation in terms of Doppler frequency spread and delay spread (extracted from [Jaci09]).

Channel Mode	Doppler Frequency [Hz]	Delay Spread [ns]
EPA 5Hz	5 (low)	43 (low)
EVA 5Hz	5 (low)	357 (medium)
ETU 70Hz	70 (medium)	991 (high)

DL interpolations presented are based on the results in [Duar08], [Jaci09], [Carr11] and on simulation results from 3GPP. SIMO, MISO and MIMO configurations are considered for 10 MHz-bandwidth, using normal CP and considering the EPA5Hz channel mode, for low delay spreads. When results for the considered channel mode were not available, an extrapolation was made, base on the results for the EVA5Hz channel, as shown in Table F.2. This was the case of MIMO 4×2 with QPSK and 16QAM modulations and MIMO 2×2 using 16QAM. Furthermore, saturation of the curves for higher values of SINR was done to assure coherence between different MIMO and modulation configurations.

Because of the different radio channel models, the extrapolation factors used to derive results for the EPA5Hz can also be easily used to obtain results for the EVA5Hz channel mode. Thus, the interpolations obtained present mean errors lower or approximately equal to 5%.

Table F.2. Extrapolation EVA5Hz to EPA5Hz (extracted from [Duar08]).

M	$\frac{\text{EPA 5Hz}}{\text{EVA 5Hz}}$	$\bar{\varepsilon}_r[\%]$
QPSK	1.027	5.3
16QAM	1.061	4.6
64QAM	1.04	15.2

Also, results from higher order MISO and MIMO configurations in DL, namely 4×2 and 4×4 and 2×2 using QPSK, were obtained recurring to Relative MIMO Gain Model [KuCo08], together with the model for the receive diversity gain, via selection combining, explained in [OeCl08].

In order to easily obtain results for different bandwidths, throughput for a single RB is considered for the following expressions. An estimate of the channel throughput is obtained by multiplying the average throughput per RB by the number of RBs used for the required channel bandwidth, according to Table F.3.

Table F.3. Transmission band (extracted from [Carr11]).

Channel bandwidth [MHz]	Number of RBs	Transmission bandwidth [MHz]	Spectral efficiency [%]
1.4	6	1.08	77
3	15	2.7	90
5	25	4.5	90
10	50	9	90
15	75	13.5	90
20	100	18.0	90

For SIMO 1×2, coding rate of 1/3 and QPSK modulation, SNR in the DL is given by, based on [Duar08]:

- EPA5Hz

$$\rho_{N_{[\mathrm{dB}]}} = \begin{cases} 2.55 \times 10^7 {R_b}^5 - 6.303 \times 10^6 {R_b}^4 + 5.803 \times 10^5 {R_b}^3 - 2.502 \times 10^4 {R_b}^2 + \\ +609.1\ R_b - 12.93, \quad 0.02037304 \leq R_{b\,[\mathrm{Mbps}]} < 0.09338800 \\ 7.457 \times 10^9 {R_b}^3 - 2.126 \times 10^9 {R_b}^2 + 2.02 \times 10^8 R_b - \\ -6.397 \times 10^6, \quad 0.09338800 \leq R_{b\,[\mathrm{Mbps}]} \leq 0.096261 \end{cases} \tag{F.1}$$

- ETU70Hz

$$\rho_{N_{[\mathrm{dB}]}} = \begin{cases} -61.62 {R_b}^2 + 104.2\ R_b - 8.231, \quad 0.04145 \leq R_{b\,[\mathrm{Mbps}]} < 0.08313 \\ 4.465 \times 10^4 {R_b}^2 - 7476\ R_b + 313, \quad 0.08313 \leq R_{b\,[\mathrm{Mbps}]} \leq 0.0916893 \end{cases} \tag{F.2}$$

For SIMO 1×2, coding rate of 1/2 and using 16QAM, SNR in DL is obtained, according to the results in [Duar08], by:

- EPA5Hz

$$\rho_{N_{[\mathrm{dB}]}} = \begin{cases} -70.91 {R_b}^2 + 61.37 R_b - 5.045, \quad 0.09042 \leq R_{b\,[\mathrm{Mbps}]} < 0.2200675 \\ \left(820.7 {R_b}^5 + 1151 {R_b}^4 - 644.9 {R_b}^3 + 180.6 {R_b}^2 - 25.26 R_b + 1.412\right) \times 10^8, \\ 0.2200675 \leq R_{b\,[\mathrm{Mbps}]} \leq 0.29382 \end{cases} \tag{F.3}$$

- ETU70Hz

$$\rho_{N_{[\mathrm{dB}]}} = \begin{cases} 2968 {R_b}^4 - 1233 {R_b}^3 - 12.73 {R_b}^2 + \\ +93.33 R_b - 6.971, \quad 0.08175 \leq R_{b\,[\mathrm{Mbps}]} < 0.27310179 \\ (1664 {R_b}^4 - 1824 {R_b}^3 + 749.5 {R_b}^2 - \\ -136.9 R_b + 9.374) \times 10^9, \quad 0.27310179 \leq R_{b\,[\mathrm{Mbps}]} \leq 0.27500964 \end{cases} \tag{F.4}$$

In SIMO 1×2, coding rate of 3/4 and 64QAM modulation, one gets for DL, [Duar08]:

- EPA5Hz

$$\rho_{N_{[\mathrm{dB}]}} = \begin{cases} -3.891 \times 10^4 {R_b}^4 + 1.418 \times 10^4 {R_b}^3 - \\ -1756 {R_b}^2 + 110 R_b - 0.1967, \quad 0.003036 \le R_{b\,[\mathrm{Mbps}]} < 0.152616 \\ -7931 {R_b}^3 + 4946 {R_b}^2 - 946.6 R_b + 62.48, \quad 0.152616 \le R_{b\,[\mathrm{Mbps}]} < 0.25014 \\ 455.2 {R_b}^4 - 599.4 {R_b}^3 + 246.2 {R_b}^2 - \\ -11.18 R_b + 6.022, \quad 0.25014 \le R_{b\,[\mathrm{Mbps}]} < 0.637095 \\ 1.547 \times 10^4 {R_b}^2 - 1.972 \times 10^4 R_b + 6300, \quad 0.637095 \le R_{b\,[\mathrm{Mbps}]} < 0.648575 \end{cases} \quad \text{(F.5)}$$

- ETU70Hz

$$\rho_{N_{[\mathrm{dB}]}} = \begin{cases} \left(-9.862 {R_b}^4 + 3.195 {R_b}^3\right) \times 10^4 - \\ -3458 {R_b}^2 + 165.5 R_b + 0.8493, \quad 0 \le R_{b\,[\mathrm{Mbps}]} < 0.1428556 \\ 7838 {R_b}^3 - 3441 {R_b}^2 + 527 R_b - 21.91, \quad 0.1428556 \le R_{b\,[\mathrm{Mbps}]} < 0.220953 \\ 198.2 {R_b}^3 - 267.3 {R_b}^2 + 135.4 R_b - 7.904, \quad 0.220953 \le R_{b\,[\mathrm{Mbps}]} < 0.5656632 \\ 2290 {R_b}^2 - 2617 R_b + 766.5, \quad 0.5656632 \le R_{b\,[\mathrm{Mbps}]} < 0.6068352 \\ (3.684 {R_b}^2 - 4.472 R_b + 1.375) \times 10^4, \quad 0.6068352 \le R_{b\,[\mathrm{Mbps}]} \le 0.6076992 \end{cases} \quad \text{(F.6)}$$

For MIMO 2×2, coding rate of 1/2 and 16QAM, for DL, SNR is obtained based on the results in [3GPP08a], [3GPP08b], [3GPP08c] and [3GPP08d]:

- EPA5Hz

$$\rho_{N_{[\mathrm{dB}]}} = \begin{cases} 683.8 {R_b}^3 - 399.4 {R_b}^2 + 115.8 R_b - 7.195, \quad 0.081909 \le R_{b\,[\mathrm{Mbps}]} < 0.2619 \\ 5.149 \times 10^4 {R_b}^5 - 1.056 \times 10^5 {R_b}^4 + 8.561 \times 10^4 {R_b}^3 - \\ -3.43 \times 10^4 {R_b}^2 + 6812 R_b - 528, \quad 0.2619 \le R_{b\,[\mathrm{Mbps}]} < 0.52724 \\ 2740 {R_b}^2 - 2868 R_b + 766.7, \quad 0.52724 \le R_{b\,[\mathrm{Mbps}]} < 0.5507425 \\ 2.851 \times 10^4 {R_b}^2 - 3.105 \times 10^4 R_b + 8472, \quad 0.5507425 \le R_{b\,[\mathrm{Mbps}]} \le 0.5531 \end{cases} \quad \text{(F.7)}$$

- ETU70Hz

$$\rho_{N_{[\mathrm{dB}]}} = \begin{cases} 23.21 {R_b}^2 + 27.73 R_b - 0.7635, \quad 0.02782 \le R_{b\,[\mathrm{Mbps}]} < 0.23376343 \\ 1.765 \times 10^4 {R_b}^3 - 1.391 \times 10^4 {R_b}^2 + \\ +3675 R_b - 317.4, \quad 0.23376343 \le R_{b\,[\mathrm{Mbps}]} < 0.3024 \\ 1.019 \times 10^4 {R_b}^4 - 1.595 \times 10^4 {R_b}^3 + \\ +9329 {R_b}^2 - 2396 R_b + 237.4, \quad 0.3024 \le R_{b\,[\mathrm{Mbps}]} < 0.5155584 \\ 197.8 R_b - 85.95, \quad 0.5155584 \le R_{b\,[\mathrm{Mbps}]} < 0.5206152 \\ (3.909 {R_b}^2 - 4.0689 R_b + 1.059) \times 10^5, \quad 0.5206152 \le R_{b\,[\mathrm{Mbps}]} < 0.5232 \end{cases} \quad \text{(F.8)}$$

For MIMO 2×2, coding rate of 3/4 and 64QAM, based on the results in [3GPP08a], DL SNR is given by:

- EPA5Hz

$$\rho_{N_{[\mathrm{dB}]}} = \begin{cases} 1.071 \times 10^5 {R_b}^3 - 1.023 \times 10^4 {R_b}^2 + 337.1 R_b + 2.201, \\ 0.000636 \le R_{b\,[\mathrm{Mbps}]} < 0.0510 \\ -1475 {R_b}^4 + 1090 {R_b}^3 - 283.9 {R_b}^2 + \\ +52.07 R_b + 4.943, \quad 0.0510 \le R_{b\,[\mathrm{Mbps}]} < 0.3522 \\ 97.69 {R_b}^3 - 179 {R_b}^2 + 118.4 R_b - 10.72, \quad 0.3522 \le R_{b\,[\mathrm{Mbps}]} < 0.7042 \\ 158.6 {R_b}^3 - 418.5 {R_b}^2 + 380.9 R_b - 98.1, \quad 0.7042 \le R_{b\,[\mathrm{Mbps}]} < 1.0780 \\ (3.49 {R_b}^3 - 11.55 {R_b}^2 + 12.75 R_b - 4.689) \times 10^4, \quad 1.0780 \le R_{b\,[\mathrm{Mbps}]} < 1.1434 \end{cases} \quad \text{(F.9)}$$

- ETU70Hz

$$\rho_{N_{[\mathrm{dB}]}} = \begin{cases} 3.69 \times 10^4 {R_b}^3 - 5182 {R_b}^2 + 269 R_b + 0.8425, 0 \le R_{b\,[\mathrm{Mbps}]} \le 0.07103922 \\ -10.14 {R_b}^3 + 5.678 {R_b}^2 + 24.37 R_b + 5.248, \ 0.07103922 \le R_{b\,[\mathrm{Mbps}]} \le 0.858 \\ 243.1 {R_b}^3 - 675.3 {R_b}^2 + 643.7 R_b - 184.8, 0.858 \le R_{b\,[\mathrm{Mbps}]} \le 1.1452 \end{cases} \quad \text{(F.10)}$$

Considering throughput in the physical layer as a function of the SNR in LTE, interpolated expressions were obtained.

For SIMO 1×2, coding rate of 1/3 and using QPSK, DL throughput is given by, [Duar08] and [3GPP08a]:

- EPA5Hz

$$R_{b\,[\mathrm{bps}]} = \begin{cases} (0.0190 {\rho_N}^3 - 0.1455 {\rho_N}^2 + 0.3516 \rho_N + 9.3388) \times 10^{-2}, & -2 \le \rho_{N_{[\mathrm{dB}]}} < 2 \\ (0.0063 \rho_N + 9.6009) \times 10^4, & 2 \le \rho_{N_{[\mathrm{dB}]}} < 4 \\ 96261, & 4 < \rho_{N_{[\mathrm{dB}]}} \le 6 \end{cases} \quad \text{(F.11)}$$

- ETU70Hz

$$R_{b\,[\mathrm{bps}]} = \begin{cases} (0.01035 \rho_N + 0.08285) \times 10^6, & -4 \le \rho_{N_{[\mathrm{dB}]}} < 0 \\ (0.0001279 {\rho_N}^3 - 0.001638 {\rho_N}^2 + 0.006616 \rho_N + 0.08313) \times 10^6, & 0 \le \rho_{N_{[\mathrm{dB}]}} \le 6 \\ 91484.4, & \rho_{N_{[\mathrm{dB}]}} > 6 \end{cases} \quad \text{(F.12)}$$

For SIMO 1×2, coding rate of 1/2 and 16QAM, DL throughput is given by, [Duar08] and [3GPP07]:

- EPA5Hz

$$R_{b\,[\mathrm{bps}]} = \begin{cases} -263.5 {\rho_N}^3 + 303 {\rho_N}^2 + 26360 \rho_N + 90420, & -4 \le \rho_{N_{[\mathrm{dB}]}} < 2 \\ (-0.000945 {\rho_N}^4 + 0.0103 {\rho_N}^3 - 0.0141 {\rho_N}^2 + 0.1696 \rho_N + 1.0083) \times 10^5, \\ 2 \le \rho_{N_{[\mathrm{dB}]}} < 6 \\ (0.0048 {\rho_N}^3 - 0.1503 {\rho_N}^2 + 1.5644 \rho_N - 2.4858) \times 10^5, & 6 \le \rho_{N_{[\mathrm{dB}]}} < 12 \\ 293820, & 12 \le \rho_{N_{[\mathrm{dB}]}} \le 14 \end{cases} \quad \text{(F.13)}$$

- ETU70Hz

$$R_{b\,[\mathrm{bps}]} = \begin{cases} (0.002862\rho_N{}^2 + 0.03113\rho_N + 0.07953) \times 10^6, -4 \le \rho_{N_{[\mathrm{dB}]}} \le 0 \\ (1.204\rho_N{}^2 + 12.02\rho_N + 81.75) \times 10^3, \quad 0 < \rho_{N_{[\mathrm{dB}]}} \le 8 \\ 66{,}41\rho_N{}^2 + 1909\rho_N + 261300, \quad 8 < \rho_{N_{[\mathrm{dB}]}} \le 14 \\ 275009.64, \quad \rho_{N_{[\mathrm{dB}]}} > 14 \end{cases} \tag{F.14}$$

For SIMO 1×2, coding rate of 3/4 and 64QAM, DL throughput is obtained by, [Duar08]:

- EPA5Hz

$$R_{b\,[\mathrm{bps}]} = \begin{cases} (-0.1292\rho_N{}^3 + 1.3299\rho_N{}^2 - 0.4279\rho_N + 0.3036) \times 10^4, \quad 0 \le \rho_{N_{[\mathrm{dB}]}} < 6 \\ (-0.1018\rho_N{}^2 + 2.92\rho_N + 3.8494) \times 10^4, \quad 6 \le \rho_{N_{[\mathrm{dB}]}} < 10 \\ (0.0585\rho_N{}^2 - 1.0032\rho_N + 6.4581) \times 10^5, \quad 10 \le \rho_{N_{[\mathrm{dB}]}} < 16 \\ (0.4354\rho_N - 1.6098) \times 10^5, \quad 16 \le \rho_{N_{[\mathrm{dB}]}} < 18 \\ (-0.0241\rho_N{}^2 + 1.0214\rho_N - 4.33555) \times 10^5, \quad 18 \le \rho_{N_{[\mathrm{dB}]}} < 22 \\ 647085, \quad 22 \le \rho_{N_{[\mathrm{dB}]}} \le 26 \end{cases} \tag{F.15}$$

- ETU70Hz

$$R_{b\,[\mathrm{bps}]} = \begin{cases} 727.4\rho_N, \quad 0 \le \rho_{N_{[\mathrm{dB}]}} < 2 \\ 127.6\rho_N{}^4 - 3709\rho_N{}^3 + 34850\rho_N{}^2 - 91410\rho_N + 72490, \quad 2 \le \rho_{N_{[\mathrm{dB}]}} < 10 \\ 3933\rho_N{}^2 - 71940\rho_N + 5.364 \times 10^5, \quad 10 \le \rho_{N_{[\mathrm{dB}]}} < 18 \\ -100.8\rho_N{}^4 + 9480\rho_N{}^3 - 334300\rho_N{}^2 + 5.239 \times 10^6\rho_N - \\ -30.18 \times 10^6, 18 \le \rho_{N_{[\mathrm{dB}]}} \le 26 \\ 604499.2, \quad , \quad 18\rho_{N_{[\mathrm{dB}]}} > 26 \end{cases} \tag{F.16}$$

For MIMO 2×2, coding rate of 1/2 and 16QAM, DL throughput is given based on the results in [3GPP08a], [3GPP08b], [3GPP08c] and [3GPP08d]:

- EPA5Hz

$$R_{b\,[\mathrm{bps}]} = \begin{cases} (-0.0348\rho_N{}^3 - 0.0922\rho_N{}^2 + 2.045\rho_N + 8.1909) \times 10^4, \quad -4 \le \rho_{N_{[\mathrm{dB}]}} < 2 \\ (0.0023\rho_N{}^2 + 2.4658\rho_N + 6.4636) \times 10^4, \quad 2 \le \rho_{N_{[\mathrm{dB}]}} < 8 \\ (-0.0049\rho_N{}^2 + 0.1405\rho_N + 1.8086) \times 10^5, \quad 8 \le \rho_{N_{[\mathrm{dB}]}} < 10 \\ (3.8501\rho_N - 9.1235) \times 10^4, \quad 10 \le \rho_{N_{[\mathrm{dB}]}} < 16 \\ 412.3468\rho_N{}^3 - 2.4976 \times 10^4 + 5.0302 \times 10^5 - 2.8162 \times 10^6, \quad 16 \le \rho_{N_{[\mathrm{dB}]}} \le 22 \\ 552524, \quad \rho_{N_{[\mathrm{dB}]}} > 22 \end{cases} \tag{F.17}$$

- ETU70Hz

$$R_{b\,[\mathrm{bps}]} = \begin{cases} 21.63\rho_N{}^4 - 335.4\rho_N{}^3 + 1058\rho_N{}^2 + 31030\rho_N + 27820, \quad 0 \le \rho_{N_{[\mathrm{dB}]}} < 10 \\ 330.4\rho_N{}^3 + 18560\rho_N{}^2 + 347600\rho_N - 1.648 \times 10^6, \quad 10 \le \rho_{N_{[\mathrm{dB}]}} \le 20 \\ 533200, \quad \rho_{N_{[\mathrm{dB}]}} > 20 \end{cases} \tag{F.18}$$

Considering MIMO 2×2, coding rate of 3/4 and 64QAM, based on the results in [3GPP08a], throughput in the DL is given by:

- EPA5Hz

$$R_{b\,[\mathrm{bps}]} = \begin{cases} (0.1853{\rho_N}^2 - 0.8564\rho_N + 1.0352) \times 10^4, & 2 \le \rho_{N_{[\mathrm{dB}]}} < 6 \\ (0.0005738{\rho_N}^4 - 0.02762{\rho_N}^3 & \\ +0.4778{\rho_N}^2 - 3.088\rho_N + 6.81) \times 10^5, & 6 \le \rho_{N_{[\mathrm{dB}]}} < 13 \\ (0.0893{\rho_N}^2 - 2.0808\rho_N + 15.3841) \times 10^5, & 13 \le \rho_{N_{[\mathrm{dB}]}} < 19 \\ (0.010304{\rho_N}^2 + 0.16608\rho_N - 1.247) \times 10^5, & 19 \le \rho_{N_{[\mathrm{dB}]}} < 24 \\ -4424{\rho_N}^2 + 281800\rho_N - 3344000, & 24 \le \rho_{N_{[\mathrm{dB}]}} \le 30 \\ 1143420, & \rho_{N_{[\mathrm{dB}]}} > 30 \end{cases} \quad \text{(F.19)}$$

- ETU70Hz

$$R_{b\,[\mathrm{bps}]} = \begin{cases} 36.62{\rho_N}^4 - 387.8{\rho_N}^3 + 2810{\rho_N}^2 - 3080\rho_N - 1.011 \times 10^{-11}, & 0 \le \rho_{N_{[\mathrm{dB}]}} < 8 \\ 80.56{\rho_N}^3 - 3033{\rho_N}^2 + 76910\rho_N - 3.55 \times 10^5, & 8 \le \rho_{N_{[\mathrm{dB}]}} < 24 \\ -2800{\rho_N}^2 + 192700\rho_N - 2.154 \times 10^6, & 24 \le \rho_{N_{[\mathrm{dB}]}} \le 32 \\ 1145200, & \rho_{N_{[\mathrm{dB}]}} > 32 \end{cases} \quad \text{(F.20)}$$

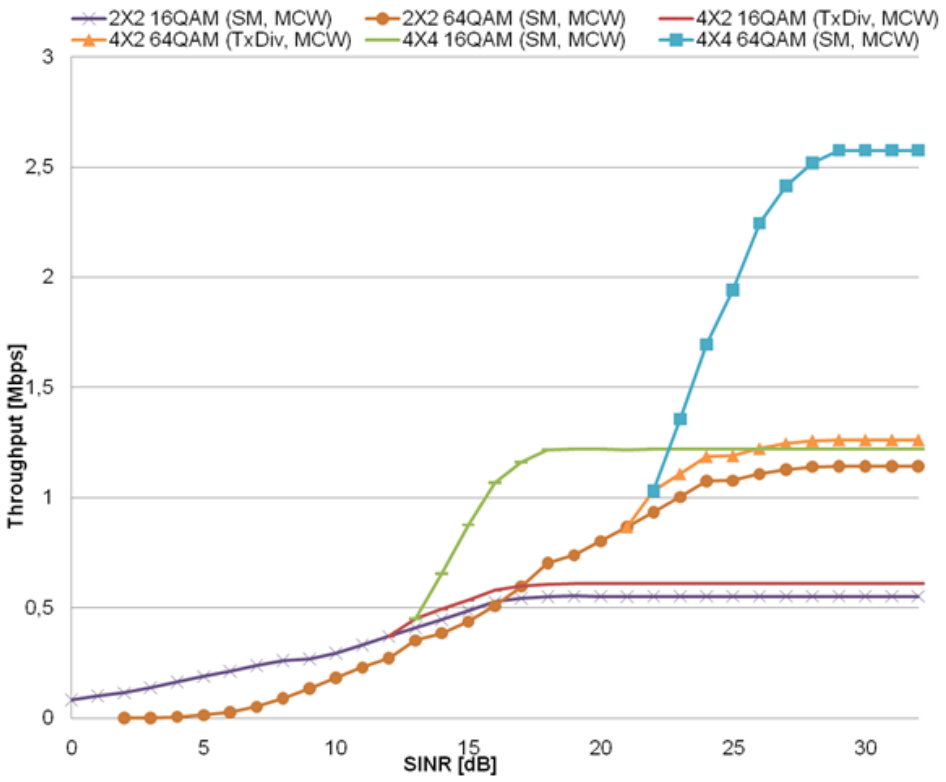

Figure F.1. LTE EPA5Hz downlink physical throughput per RB for two layer 16QAM and 64QAM modulation schemes as a function of SNR [extracted from [Carr11]).

Annex G

Relative MIMO Gain Model

This annex describes the MIMO model used in the calculations of the throughputs.

MIMO consists in the use of multiple antennas at both the transmitter and receiver, as its acronym definition suggests, and is used to improve the SINR and achieve a higher diversity gain against fading, when compared to the use of only multiple transmit antennas or multiple receiver antennas, SIMO and MISO respectively. Furthermore, MIMO allows MTs and BSs to explore special multiplexing through beam-forming, allowing higher efficient utilisation of high SINR and significantly higher data rates over the radio interface [DaPS11], as one can see from the maximum throughputs associated to the MIMO use for example in Table 2.2. SISO, SIMO and MIMO radio transmission is shown in Figure G.1, where radio streams as well as used antennas are illustrated.

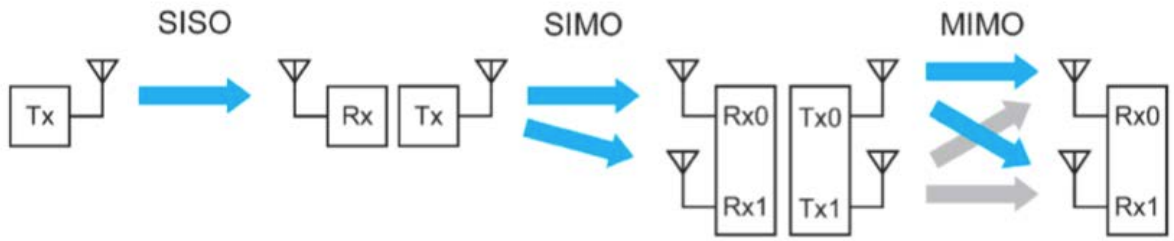

Figure G.1. SISO, SIMO and MIMO radio transmission (extracted from [Jaci09]

In order to predict the improvement in capacity provided by MIMO over SISO based in simulation results, the RMG Model [KuCo07] was implemented. The description of this model is presented below, based in [KuCo07] and [Bati08] and relies on simulation results from a MIMO radio channel simulator that takes into account the Geometrically Based Single Bounce (GBSB) channel mode.

The RMG is defined as the ratio between the MIMO and SISO capacities of a radio link, as shows (G.1), and in order to use the low-complexity of the model, the distribution of the RMG is modelled with an inverse Sigmoid function, also known as logistic function or S-shape function, which is completely modelled by its mean and variance.

$$G_{M/S} = \frac{C_{MIMO}}{C_{SISO}} \tag{G.1}$$

The general sigmoid function is given by:

$$\delta(x, \mu, s) = \frac{1}{1+e^{-\frac{x-\mu}{s}}} \tag{G.2}$$

where:

- μ is the mean value of the distribution;
- s determines the slope which is related to σ^2 by:

$$\sigma^2 = \frac{\pi^2}{3} s^2 \tag{G.3}$$

- σ^2 is the variance.

Both the mean value and the variance depend on the number of transmitter and receiver antennas, but the mean value also depends on the distance between transmitter and receiver. Focusing on obtaining a model that gives a realistic statistical RMG as a result, the inverse of the distribution is given by:

$$g(u, \mu_{RMG}, \sigma_{RMG}) = \mu_{RMG}(d, N_T, N_R) - \frac{\sqrt{3\sigma_{RMG}{}^2(d,N_t,N_R)}}{\pi} \ln \frac{1-u}{u} \quad \text{(G.4)}$$

where:

- u is the random value with a Uniform distribution, i.e., $u = U[0,1]$;
- d is the distance between BS and MT;
- $\sigma_{RMG}{}^2(d, N_t, N_R)$ is the variance depending on the cell type, N_T and N_R;
- $\mu_{RMG}(d, N_T, N_R)$ is the average RMG depending on the cell type, N_T and N_R;
- N_T is the number of transmitter antennas;
- N_R is the number of receiving antennas.

The simulation parameters of the default RMG model are presented in Table G.1, the values for the variance needed for this thesis are presented in Table G.2 and the mean results of the RMG model are presented in Table G.3. Other values for other MIMO configurations are in [KuCo07]. In Figure G.2, one can see the modelled values of the RMG plotted for various antenna configurations and its variation with distance.

Table G.1. Simulation parameters of the default RMG model (extracted from [KuCo07]).

Carrier Frequency [GHz]	2		
Bandwidth [MHz]	5		
Time resolution (receiver filter) [ns]	200		
Antenna spacing	λ		
Noise floor	-150		
SNR [dB]	10		
Cluster Density [10^{-4} m^2]	Pico	Micro	Macro
	8.9	2.2	2.2
Avg. number of scatterers per cluster	10		
$\boldsymbol{N_T}$	[2; 16]		
$\boldsymbol{N_R}$	[2; 16]		
Number of runs	100		
Distance [m]	Pico	Micro	Macro
	[10; 60]	[100; 600]	[1200; 2400]

Table G.2. Variance for different number of transmitter and receiver antennas (extracted from [Duar08]).

$\sigma_{RMG}{}^2(10^{-3})$		[10; 60] m		[100; 600] m		[1200; 2400] m	
N_R		2	4	2	4	2	4
N_T	**2**	18.5	10.4	24.0	15.9	1.9	1.8
	4	11.8	45.5	15.9	71.4	0.8	1.1

Table G.3. Average RMG value for systems with two transmitter and receiver antennas (extracted from [Duar08]).

$N_{R/T}$	μ_{RMG}
2	1.54

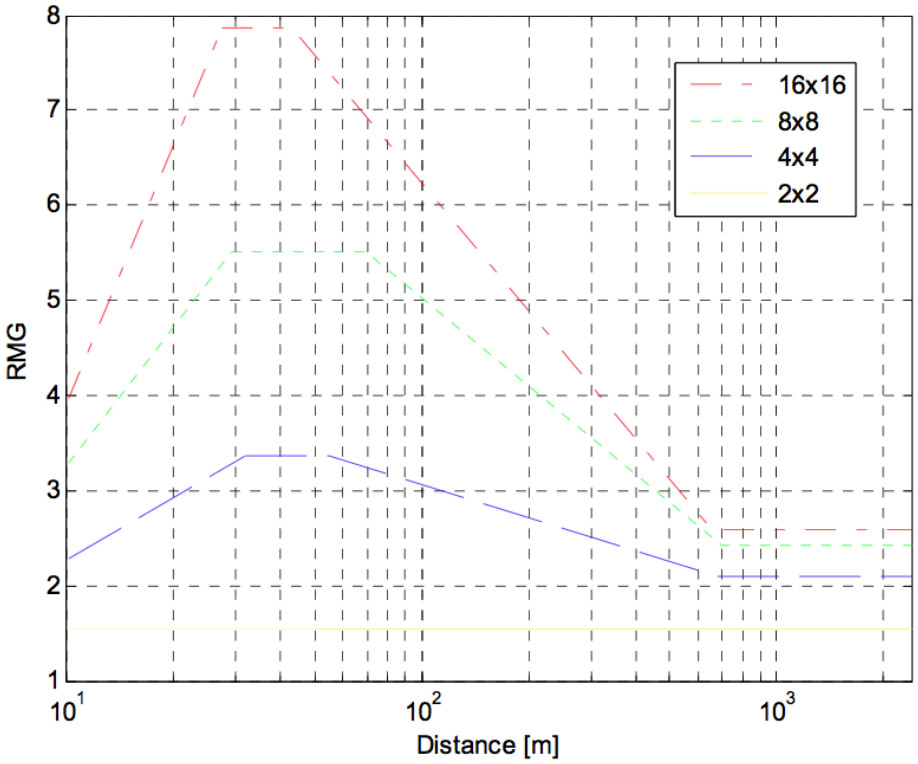

Figure G.2. Distribution of the RMG for multiple antenna configurations (extracted from [Bati08]).

Annex H

Antennas’ Radiation Pattern

This annex describes the antennas used through the simulations.

The antennas used in the simulator are the Kathrein 80010675 [Kath12] model, whose horizontal and vertical radiation patterns are presented in Figure H.1, the latter being illustrated with a 90° offset. Horizontal and vertical radiation pattern present a half power beamwidth of 66.17º and 3.32º respectively.

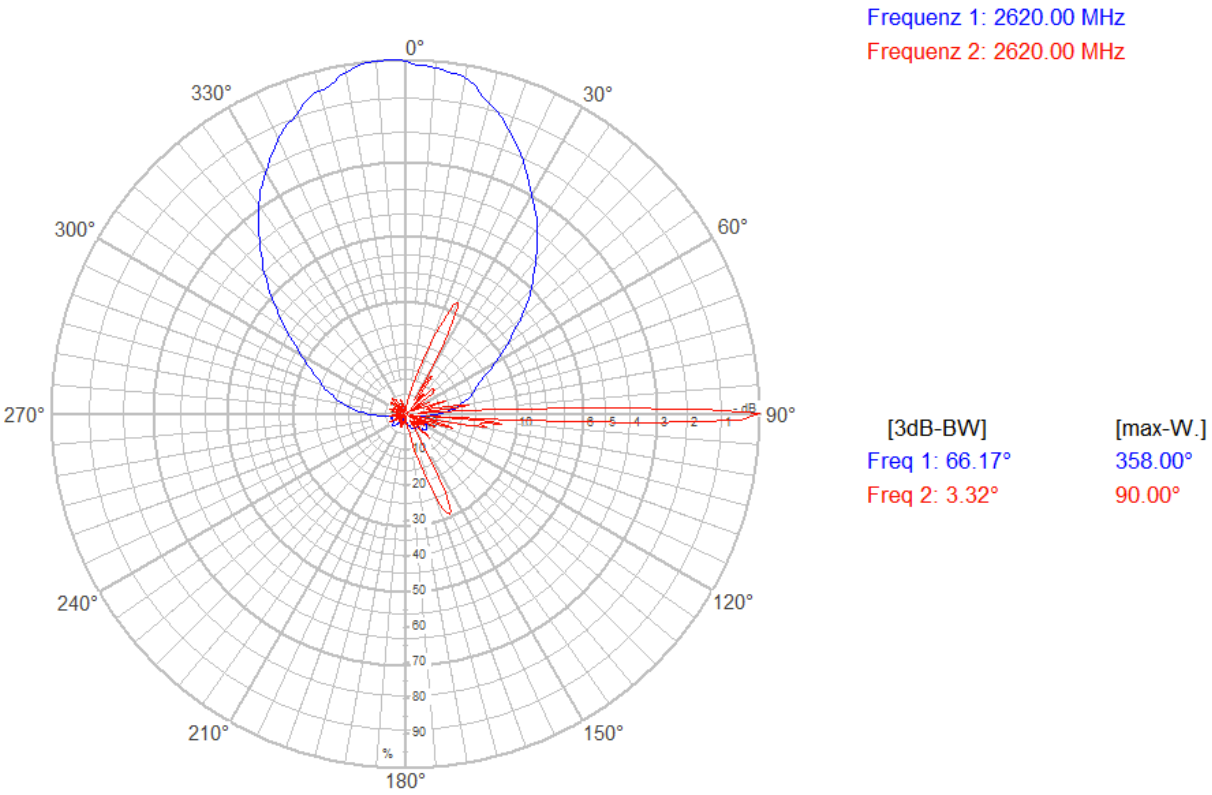

Figure H.1. Horizontal (blue) and vertical (red) radiation pattern of the used antennas [Kath12].

Annex I

BSs and users distribution along the network

This annex describes the heterogeneity of the network in terms of location and density of BSs and users along the city of Lisbon.

The simulations performed in this thesis do not address a homogenous and ideal network with fixed distance between BSs, but a real network with huge differences in terms of location and density of the BSs. In the same terms, users distribution is done according to the density of population assigned by district.

Figure I.1 shows the distribution of BSs, the blue zone, almost imperceptible with blue patterns, represent the centre of Lisbon, whereas the yellow zone with green patterns represent the outer zone. One can observe from Figure I.1 that the centre, compared to the outer zone, has a more constant density of users along the region as well as a higher density. Also one can see that the outer zone has a more heterogeneous distribution of BSs, the higher density zone being the Northeast zone of Parque das Nações, which is a recent financial services district and the lower density zones being the Airport of Portela at North and the Forest Park of Monsanto at West.

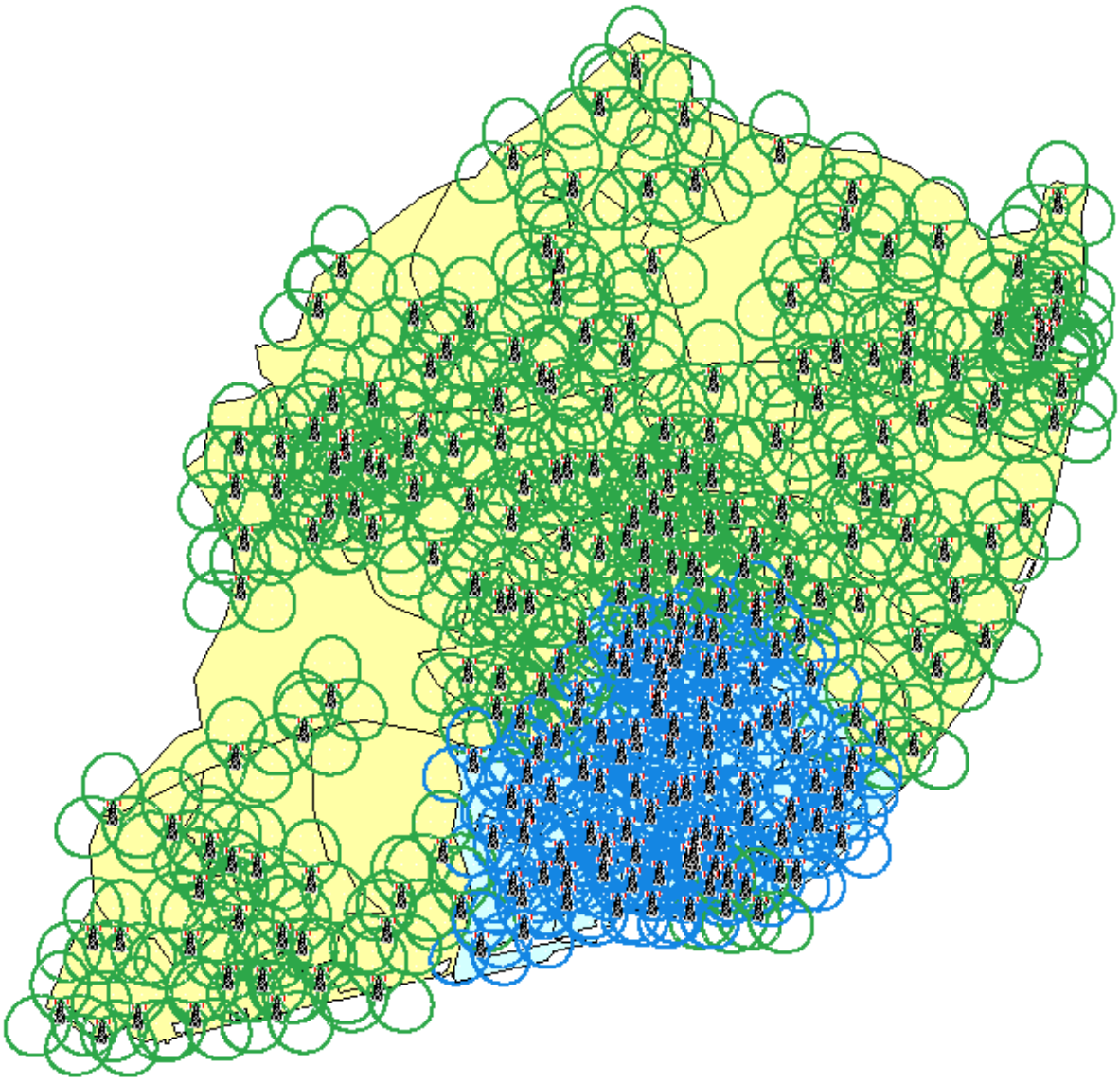

Figure I.1. Network of BSs in the city of Lisbon.

From Figure I.2, one can see that the users density is higher in the blue zone, i.e., centre of Lisbon and in the outer zone just above the north centre. As one could expect, the location and density of BSs almost overlaps the location and density of users, in order to provide them coverage as far as services access is concerned and capacity in terms of being able to assure the quality of their data services.

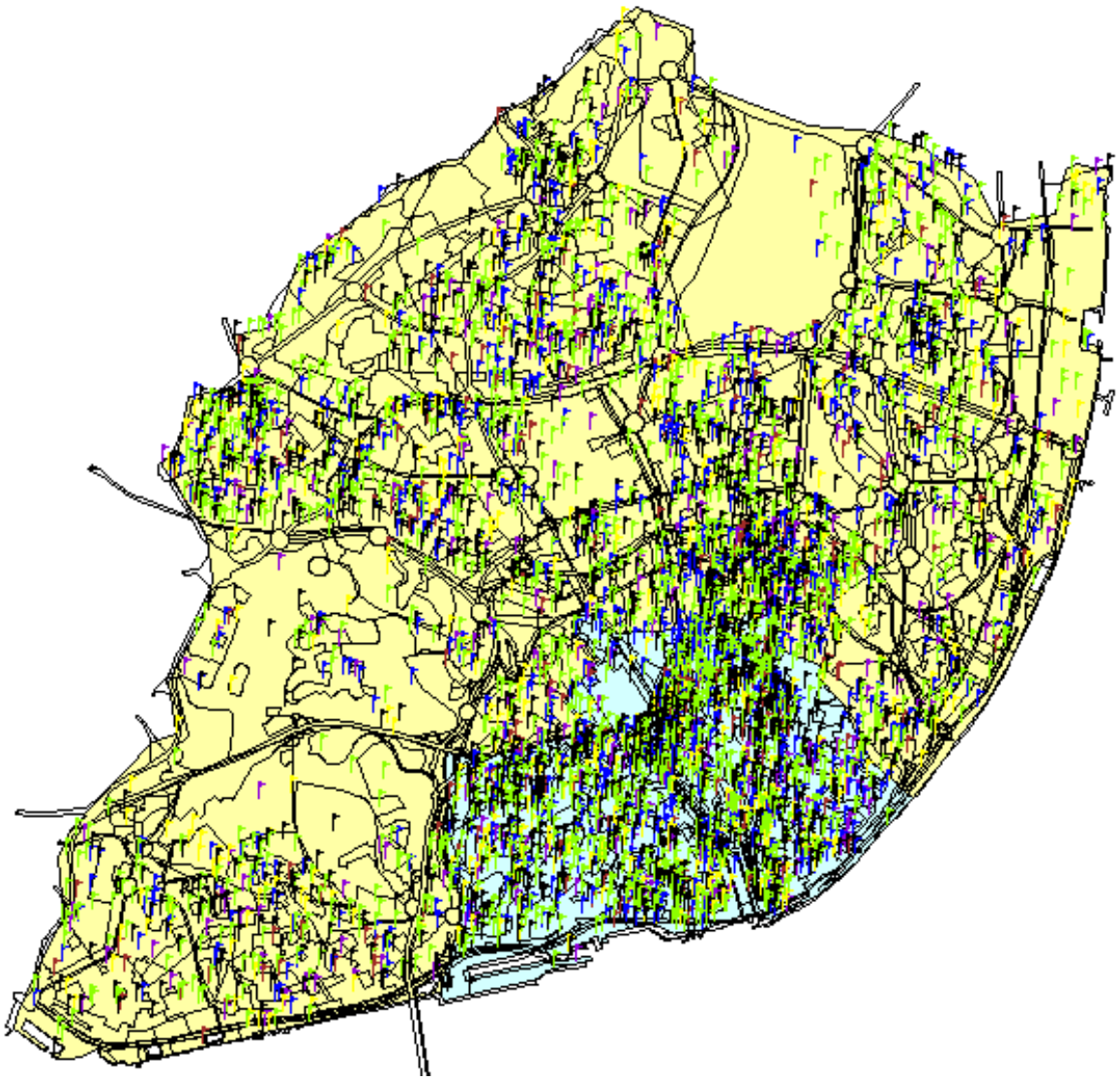

Figure I.2. Distribution of users long the districts of Lisbon.

Annex J

Measurements results

This annex shows graphically the variation of the radio channel condition and throughput obtained in the measurements route.

One can see the frequency band used along the Lisbon Network route in Figure J.1, which varied between the 800 to the 2600 MHz band, identified by the blue and green colours, respectively. The 2600 MHz band usage was clearly dominant, and in fact this band is the responsible for providing the LTE service, while the 800 MHz one is used to reinforce the overall coverage of the city.

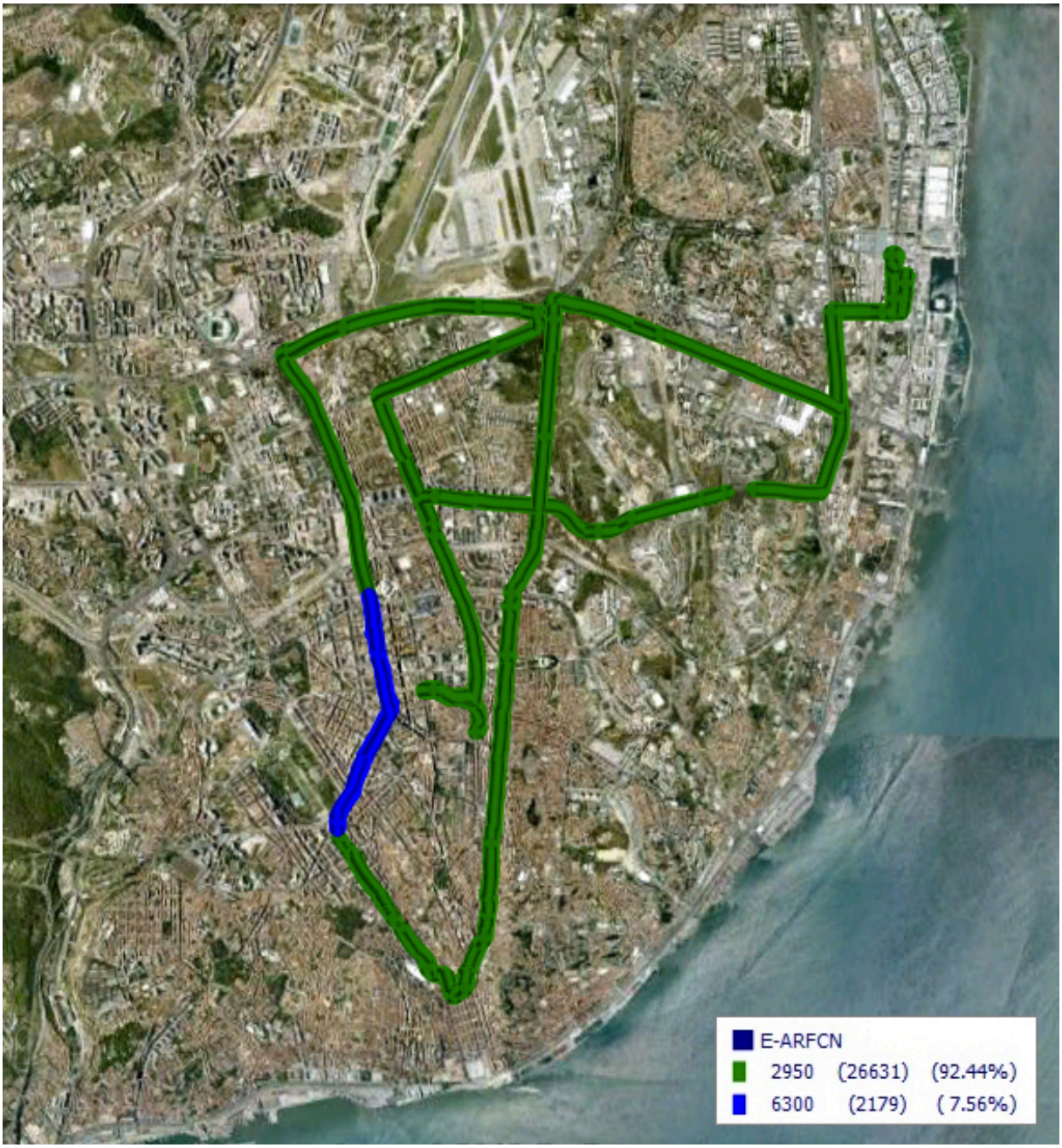

Figure J.1. 2600 MHz (green) and 800 MHz (blue) E-ARFCN used along the network.

The average RSRP per location is shown in Figure J.2 and one can see the different neighbourhoods characterisation regarding signal coverage and identify simultaneously the most and least favourable places to the LTE service. During the measurements campaign, one could see that the avenues highlighted by the red colour presented in the upper part of the Lisbon map corresponded to places further away to BSs while others happened occurred when travelling along tunnels.

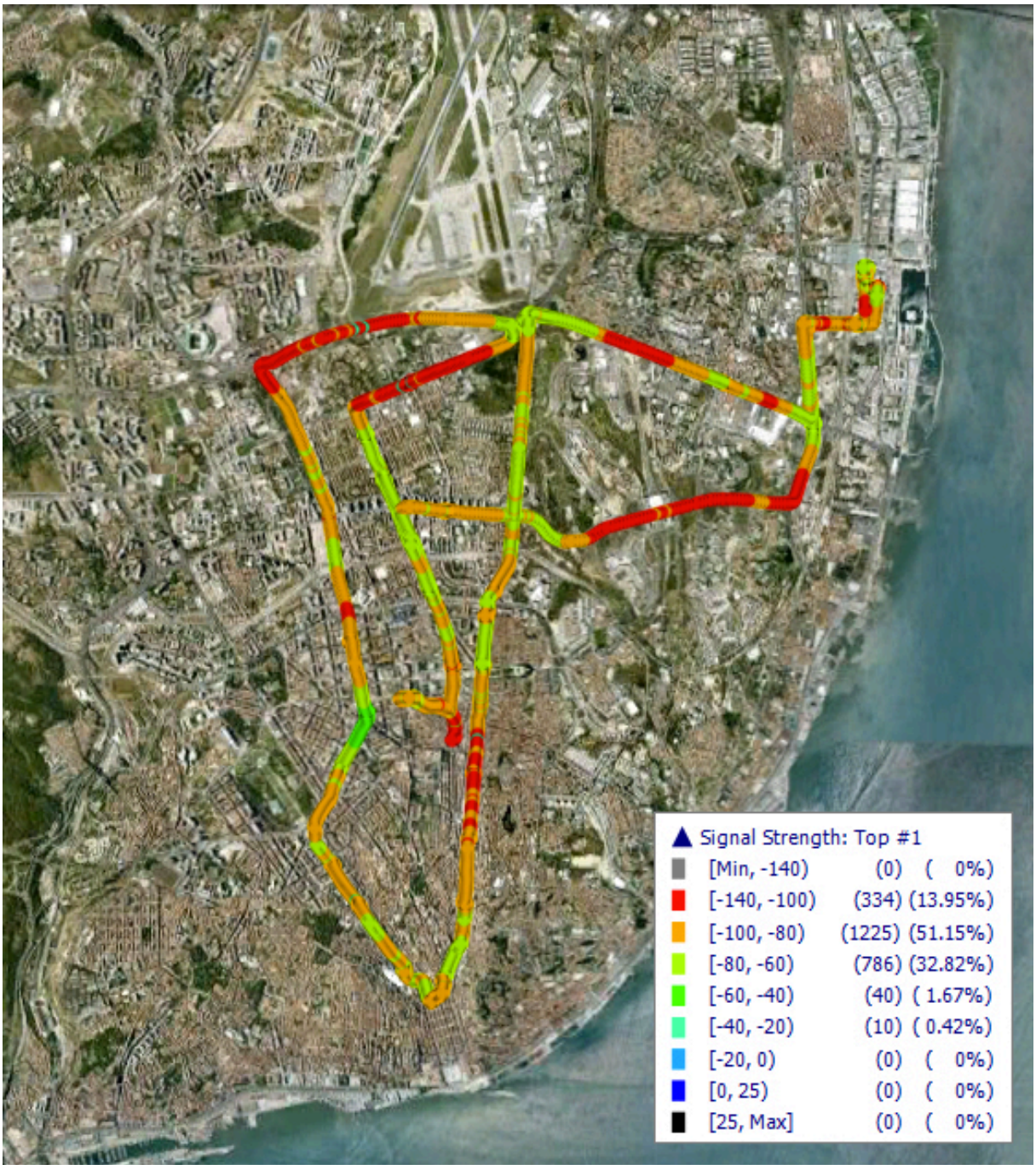

Figure J.2. RSRP along the network.

In Figure J.3, RS SNR is illustrated for the performed route and one can see a more homogeneous distribution of values, compared to the ones presented for the RSRP in Figure J.2. One can highlight the most favourable radio channel case being a large traffic circle known as Rotunda do Relógio, immediately below the airport and the least favourable radio channel case being the avenue highlighted by the red colour, which corresponds to a very low dense populated area of Lisbon.

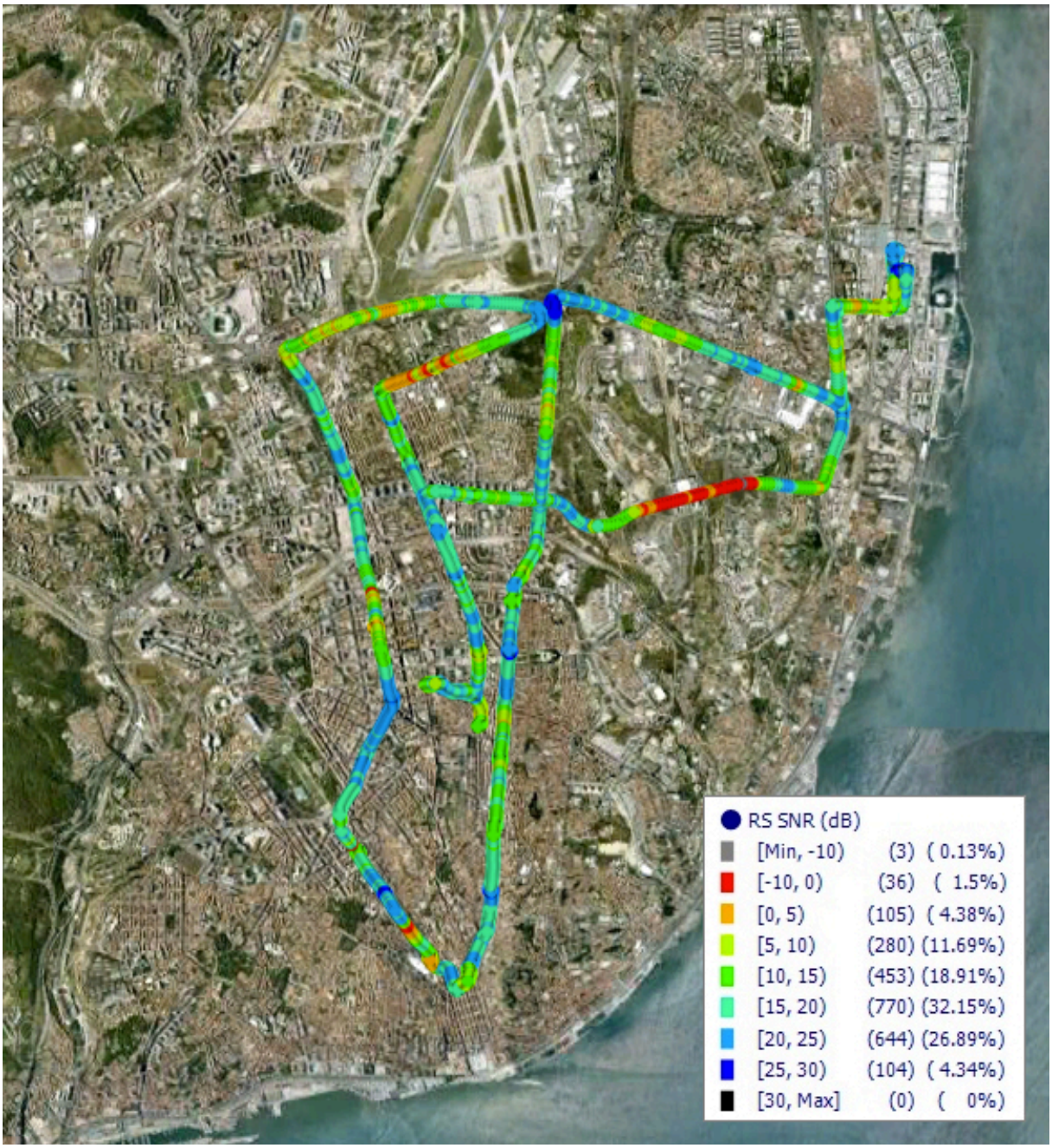

Figure J.3. RS SNR along the network.

In Figure J.4, one can obtain geographically the highest interference power reaching the MT and see that besides the interval of power from -120 dBm to -80 dBm, there is clearly a higher interference zone located in the down left part of the route, highlighted by the green colour, that corresponds to the neighbourhood where the 800 MHz frequency band was used, as one can see from Figure J.1.

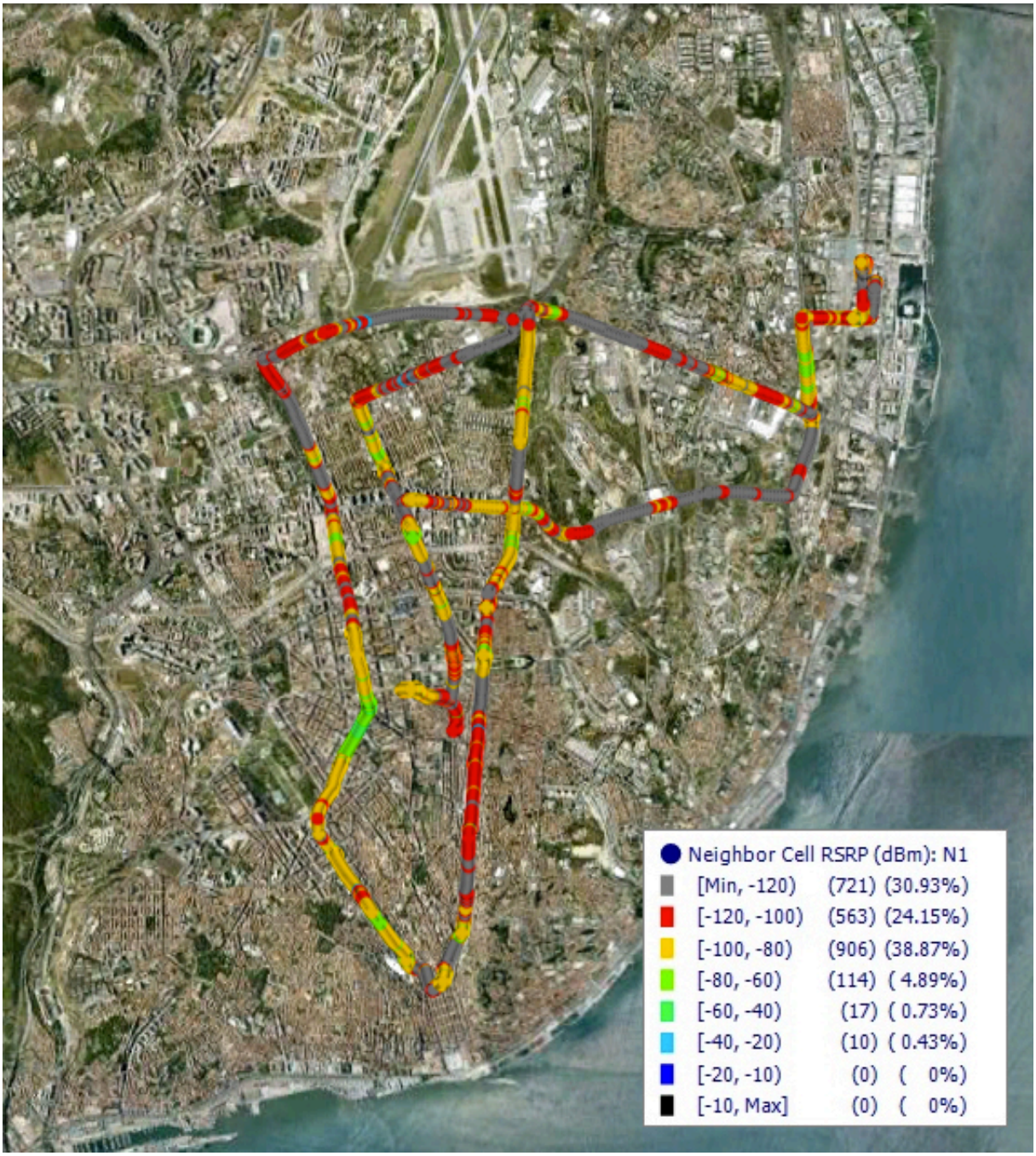

Figure J.4. Highest neighbour cell RSRP along the network.

CQI along the network is illustrated in Figure J.5 and the most outstanding aspect that one can observe from such results is the heterogeneity and rapid variation of the radio channel condition when travelling along an urban network, as one could expect.

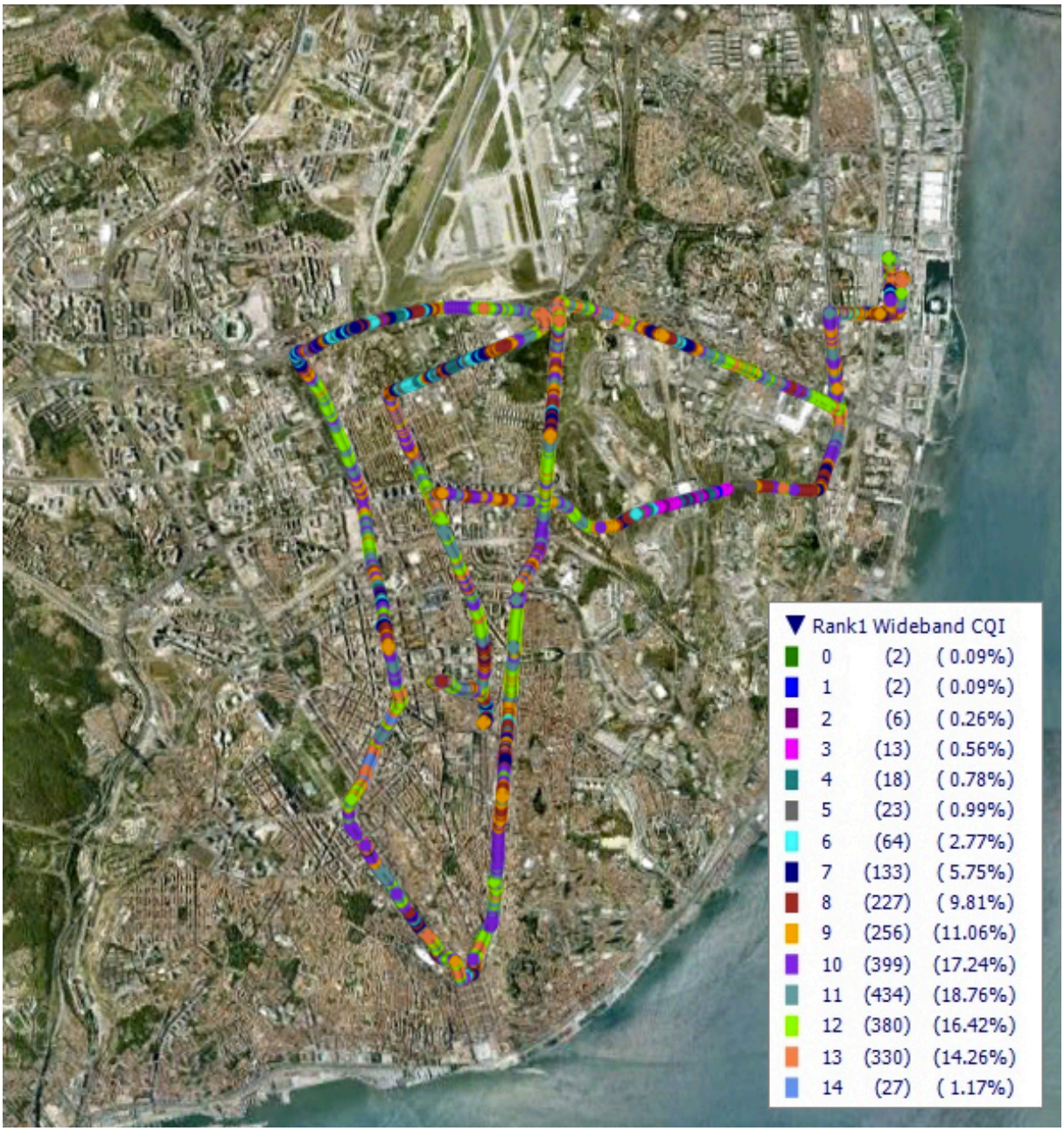

Figure J.5. CQI along the network.

The obtained throughput regarding the PDSCH is shown in Figure J.6 and one can see that the majority of the throughput peaks correspond to the most favourable radio condition cases, with some exceptions such as the neighbourhood where the 800 MHz frequency band was used, because of the 50 RBs usage limitation.

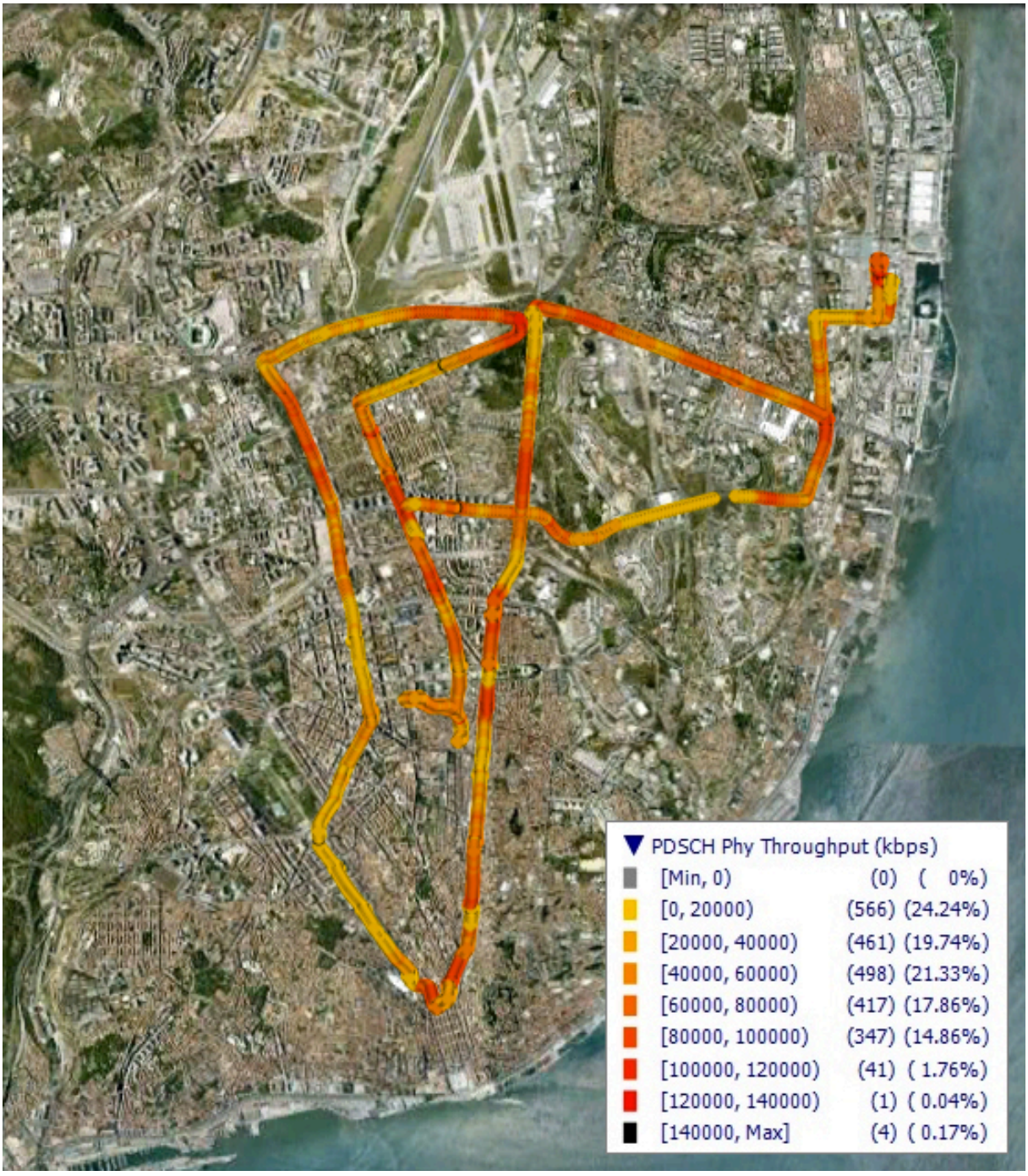

Figure J.6. Throughput along the network.

RBs usage along the network is illustrated in Figure J.7 and one can immediately see that most of the time, almost all RBs were used in the LTE DL connection. The other evident case is the 50 RBs usage limit for the 800 MHz frequency band, which occurred in the neighbourhood highlighted by the green colour, which identifies a RBs usage between 40 and 60 RBs. Low RBs usage are identified by the red colour and are most of the times associated to connection losses and handovers processes.

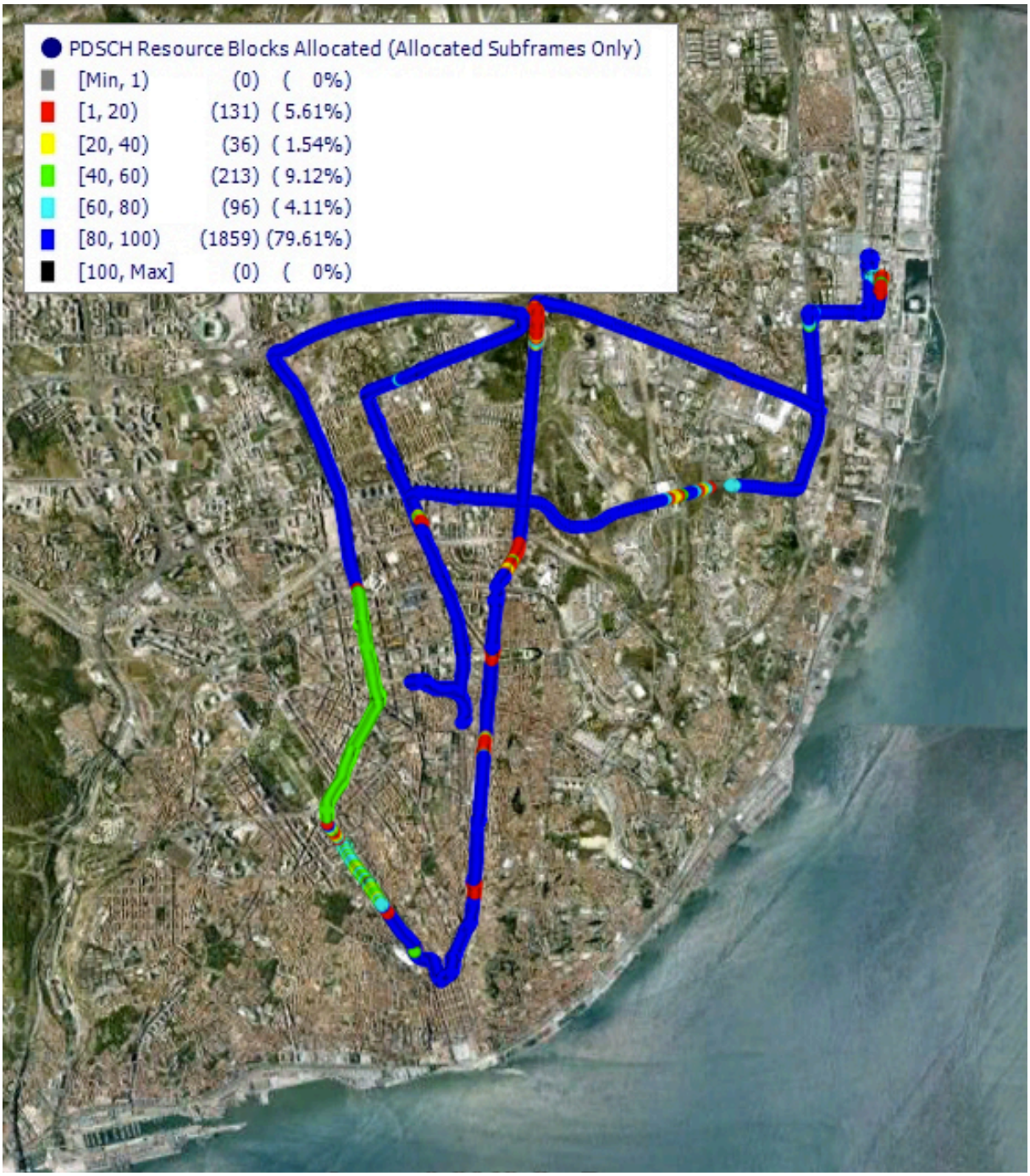

Figure J.7. Number of used RBs along the network.

The MT speed is shown in Figure J.8 and one can see that the majority of the route was performed with speeds between 0 km/s and 40 km/h and the higher speeds are associated to the vehicles-dedicated streets, such as the longer green lines represented in the upper part of the route.

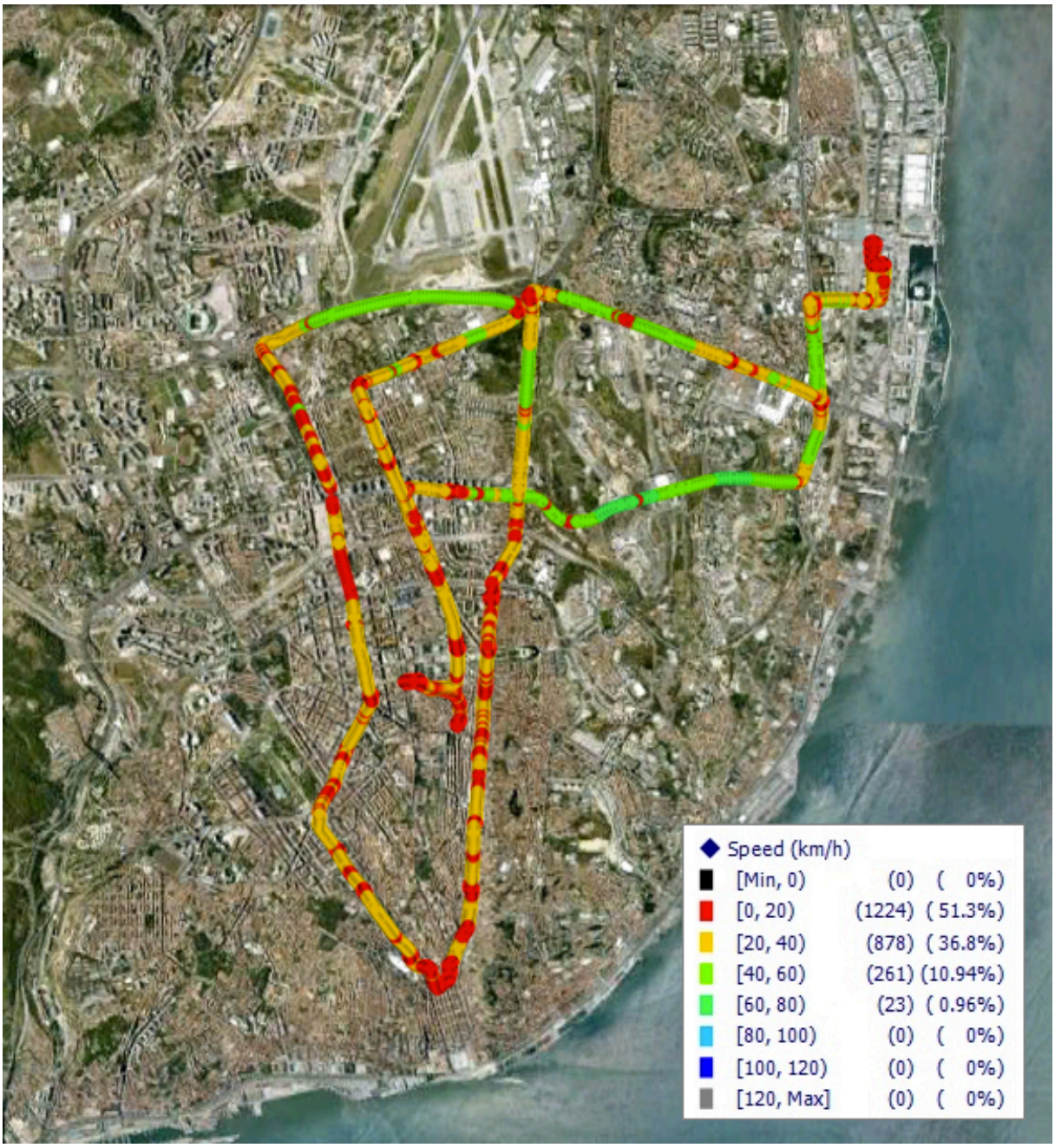

Figure J.8. MT speed along the network.

The handover events along the sectors and BSs are represented in Figure J.9 by a hand symbol, along with the RSRP but with lower granularity compared to Figure J.2. One can see that there are generally more handovers events for the poorer radio condition cases, identified by the red and orange colours than for the better radio channel condition ones, illustrated by the green and yellow colours.

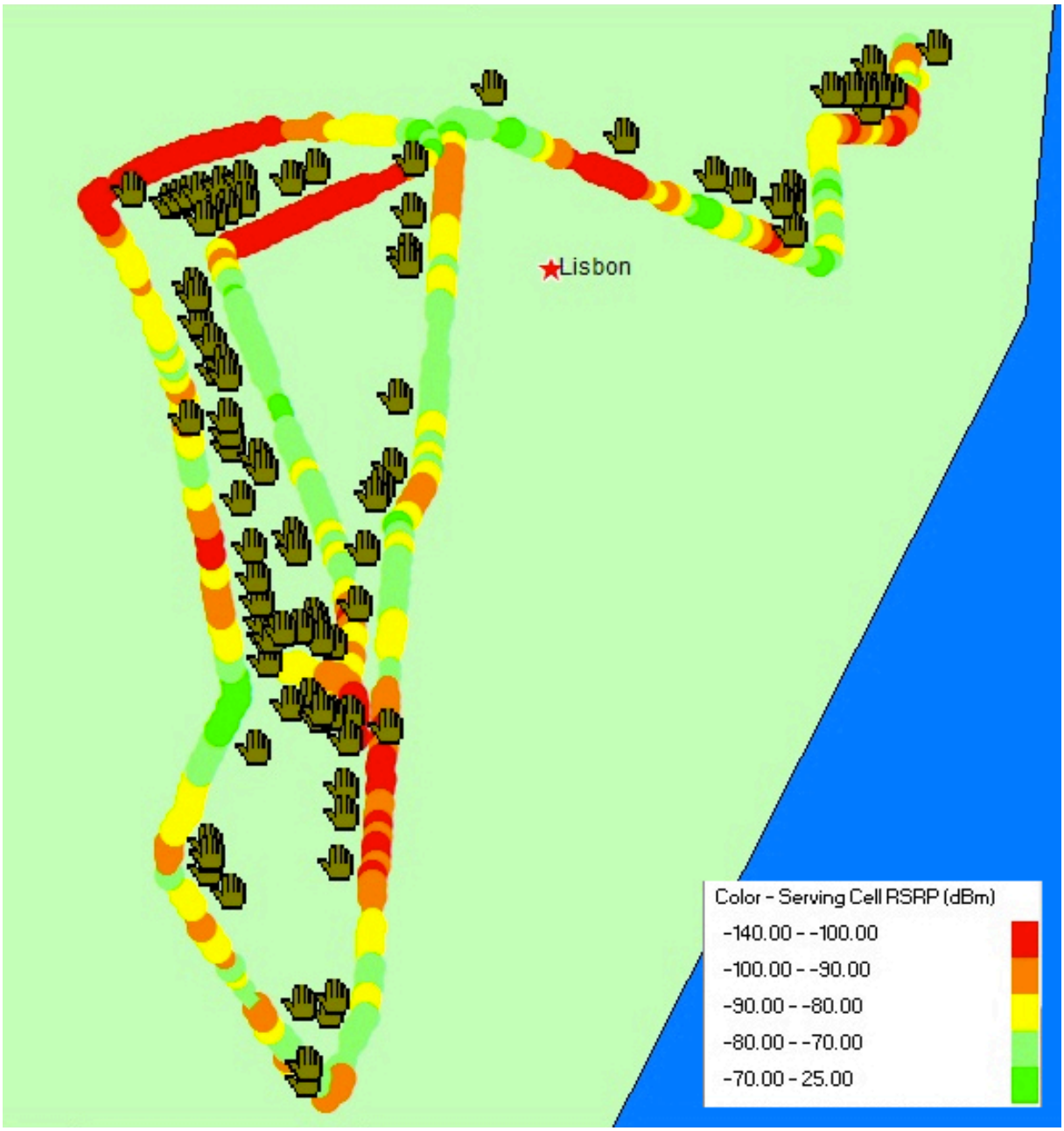

Figure J.9. Performed handovers along the network, each hand symbol representing one between sectors or cells.

References

[3GPP07] 3GPP, Technical Specification Group - Radio Access Network Working, *Collection of PDSCH results*, Report R4-072218, Jeju, Korea, Nov. 2007.

[3GPP08a] 3GPP, Technical Specification Group - Radio Access Network Working, *PDSCH Demodulation Ideal Results*, Report R4-080194, Sorrento, Italy, Feb. 2008.

[3GPP08b] 3GPP, Technical Specification Group - Radio Access Network Working, *PDSCH 2x2 MCW Ideal Simulation Results*, Report R4-081792, Jeju, Korea, Aug. 2008.

[3GPP08c] 3GPP, Technical Specification Group - Radio Access Network Working, *LTE UE PDSCH demodulation results with impairments for MIMO-FDD case*, Report R4-081439, Munich, Germany, Jun. 2008.

[3GPP08d] 3GPP, Technical Specification Group - Radio Access Network Working, *PDSCH MIMO FDD results*, Report R4-081129, Kansas City, USA, May 2008.

[3GPP10] 3GPP, *LTE; Evolved Universal Terrestrial Radio Access (E-UTRA); Physical channels and modulation (Release 9)*, ETSI TS, No. 36.211, Ver. 9.1.0, Apr. 2010 (http://www.3gpp.org).

[3GPP11a] 3GPP, *LTE; Evolved Universal Terrestrial Radio Access (E-UTRA) and Evolved Universal Terrestrial Radio Access Network (E-UTRAN); Overall description; Stage 2,* ETSI TS, No. 36.300, Ver. 9.7.0, Apr. 2011 (http://www.3gpp.org).

[3GPP11b] 3GPP, *LTE; E-UTRA; UE radio transmission and reception (Release 9)*, ETSI TS, No. 36.101, Ver. 9.8.0, Jun. 2011 (http://www.3gpp.org).

[3GPP11c] 3GPP, *LTE; Requirements for further advancements for E-UTRA (LTE Advanced) (Release 10)*, ETSI TR, No. 36.913, Ver. 10.0.0, Apr. 2011 (http://www.3gpp.org).

[3GPP11d] 3GPP, *Digital cellular telecommunications system (Phase 2+); Universal Mobile Telecommunications System (UMTS); LTE; Services and service capabilities*, ETSI TS, No. 22.105, Ver. 10.0.0, May 2011 (http://www.3gpp.org).

[3GPP11e] 3GPP, *Digital cellular telecommunications system (Phase 2+); Universal Mobile Telecommunications System (UMTS); LTE; Quality of Service (QoS) concept and architecture*, ETSI TS, No. 23.107, Ver. 10.1.0, Jun. 2011 (http://www.3gpp.org).

[3GPP11f] 3GPP, *Digital cellular communications system (Phase 2+); Universal Mobile Telecommunication System (UMTS); LTE; Policy and charging control architecture*, ETSI

TS, No. 23.203, Ver. 10.4.0, Jun 2011 (http://www.3gpp.org).

[3GPP11g] 3GPP, *LTE; Evolved Universal Terrestrial Radio Access (E-UTRA); Physical layer procedures*, ETSI TS, No. 36.213, Ver. 10.3.0, Oct. 2011.

[Agil09] Agilent Technologies, *Agilent 3GPP Long Term Evolution: System Overview, Product Development, and Test Challenges*, Application Note, USA, 2009 (http://cp.literature.agilent.com/litweb/pdf/5989-8139EN.pdf).

[ANAC11] ANACOM, *Project of Regulation for the Auction of the Attribution of the Frequencies Usage Licenses for the bands 450 MHz, 800 MHz, 900 MHz, 1800 MHz, 2.1 GHz and 2.6 GHz (in Portuguese)*, Jul. 2011 (http://www.anacom.pt).

[ANAC12] http://www.anacom.pt/render.jsp?contentId=1105917, Jan. 2012.

[Asco12] http://www.ascom.com/en/tems-investigation-3.htm, June 2012.

[Bati08] Batista,T., *Capacity Increase in UMTS/HSPA+ Through the Use of MIMO Systems*, M.Sc. Thesis, Instituto Superior Técnico, Lisbon, Portugal, Jul. 2008.

[BQCR08] Boussif, M., Quintero, N., Calabrese, F., Rosa, C., et al., "Interference Based Power Control Performance in LTE Uplink", *IEEE International Symposium on Wireless Communication Systems*, Oct. 2008, pp. 698-702.

[Busi12] http://www.businessinsider.com/the-future-of-mobile-deck-2012-3?op=1, Sep. 2012.

[Card06] Cardeiro,J., *Optimisation of Base Station Location in UMTS-FDD for Realistic Traffic Distribution*, M.Sc. Thesis, Instituto Superior Técnico, Lisbon, Portugal, Mar. 2006.

[Carr11] Carreira, P., Data Rate Performance Gains in UMTS Evolution to LTE at the Cellular Level, M.Sc. Thesis, Instituto Superior Técnico, Lisbon, Portugal, Oct. 2011.

[CEGH02] Catreux,S., Erceg,V., Gesbert,D., Heath,R., "Adaptive Modulation and MIMO Coding for Broadband Wireless Data Networks", *IEEE Communications Magazine*, Vol. 40, No. 6, June 2002, pp.108-115.

[Cisc12] Cisco VNI Forecast, *Cisco Visual Networking Index: Global Mobile Data Traffic Forecast Update, 2011-2016*, Feb. 2012 (http://www.cisco.com/en/US/solutions/collateral/ns341/ns525/ns537/ns705/ns827/white_paper_c11-520862.pdf).

[Corr09] Correia, L., *Mobile Communications Systems, Lecture Notes*, Instituto Superior Técnico, Lisbon, Portugal, 2009.

[DaPS11] Dahlman, E., Parkvall, S., Sköld, J., *4G LTE/LTE-Advanced for Mobile Broadband*, Academic Press, Oxford, United Kingdom, 2011.

[Duar08] Duarte, S., *Analysis of Technologies for Long Term Evolution in UMTS*, M.Sc. Thesis, Instituto Superior Técnico, Lisbon, Portugal, Sep. 2008.

[Jaci09] Jacinto, N., *Performance Gains Evaluation from UMTS/HSPA+ to LTE at the Radio Network Level*, M.Sc. Thesis, Instituto Superior Técnico, Lisbon, Portugal, Nov. 2009.

[Kath12] http://www.kathrein.com/svg/download/9363879b.pdf, Jun. 2012.

[KhPr08] Khan, D. A., Priyanto, B. E., “Performance Evaluation of Frequency Hopping Schemes in UTRA-LTE Uplink”, *2008 Annual IEEE Student Paper Conference*, Feb. 2008, pp. 1-5.

[KuCo07] Kuipers,M., Correia, L.M., "Modelling the Relative MIMO Gain", in *Proc. of PIMRC’08 - IEEE Personal, Indoor and Mobile Radio Communications*, Cannes, France, Sep. 2008.

[HoTo09] Holma, H., Toskala,A., *LTE for UMTS - OFDMA and SC-FDMA Based Radio Access*, Wiley, Chichester, United Kingdom, 2009.

[HPYW10] Han, B., Peng, M., Yang, C., Wang, W., “Interference Margin Analysis for OFDMA Cellular Networks Planning”, *2010 IEEE 21st International Symposium on Personal Indoor and Mobile Radio Communications (PIMRC)*, Sep. 2010, pp. 2360-2364.

[Kath12] http://www.kathrein.de/svg/download/9363879b.pdf, July 2012.

[Khan09] Khan, Farooq, *LTE for 4G Mobile Broadband*, Cambridge University Press, New York, 2009.

[LaCo06] Ladeira, D., Costa, P., Optimal planning of UMTS cellular networks for HSDPA data-based services (in Portuguese), M.Sc. Thesis, Instituto Superior Técnico, Lisbon, Portugal, Mar. 2006.

[Lope08] Lopes,J., *Performance of UMTS/HSDPA/HSUPA at the Cellular Level,* M.Sc. Thesis, Instituto Superior Técnico, Lisbon, Portugal, Mar. 2008.

[Marq08] Marques,A., *Modelling of building height interference dependence in UMTS,* M.Sc. Thesis, IST-UTL, Lisbon, Portugal, Sep. 2008.

[Mora10] Morais, M., *Probability and Statistics – Course Notes* (In Portuguese), Technical University of Lisbon, Lisbon, Portugal, 2010 (http://www.math.ist.utl.pt/~mjmorais/2010-09-12-NotasApoioPE-EdRevista-SeccaoFolhas.pdf).

[Øste11] Østerbø, O., “Scheduling and Capacity Estimation in LTE”, *2011 23rd International Teletraffic Congress (ITC)*, Sep. 2011, pp. 63-70.

[PPAH10] Puttonen, J., Puupponen, H., Aho, K., Henttonen, T., Moisio, M., “Impact of Control Channel Limitations on the LTE VoIP Capacity”, *2010 Ninth International Conference on Networks (ICN)*, Apr. 2010, pp. 77-82.

[RaYW09] Rahman, M., Yanikomeroglu, H., Wong, W., “Interference Avoidance with Dynamic Inter-Cell Coordination for Downlink LTE System”, *Wireless Communication and Networking Conference*, Apr. 2009, pp. 1-6.

[Salv08] Salvado, L., *UMTS/HSDPA comparison with WiMAX/IEEE 802.16e in mobility scenarios*, M.Sc. Thesis, Instituto Superior Técnico, Lisbon, Portugal, Fev. 2008.

[ScZW08] Schoenen, R., Zirwas, W., Walke, B. H., “Capacity and Coverage Analysis of a 3GPP-LTE Multihop Deployment Scenario”, *IEEE International Conference on Communications*

Workshops, May 2008, pp. 31-36.

[SeCa04] Sebastião,D. and Cardeiro,J., *Modelation and Traffic Dimensioning in the UMTS Radio Interface* (in Portuguese), Graduation Thesis, Instituto Superior Técnico, Lisbon, Portugal, Oct. 2004.

[SeTB09] Sesia, S., Toufik, I., Baker, M., *LTE The UMTS Long Term Evolution*, Wiley, Chichester, United Kingdom, 2009.

[SHWH11] Stäbler, O., Hoppe, R., Wölfle, G., Hager, T., Herrmann, T., "Consideration of MIMO in the Planning of LTE Networks in Urban and Indoor Scenarios", *Proceedings of the 5th European Conference on Antennas and Propagation (EUCAP)*, April 2011, pp. 2187-2191.

[Wire11] http://wirelesshabitat.eu/archives/104, Sep. 2012.